Mineral Res. Expl. Bul., 122, 1-21, 2000

# DEPOSITIONAL ENVIRONMENTS AND SEQUENCE STRATIGRAPHY OF GLAUCONITES OF WESTERN BLACK SEA REGION

Baki VAROL**; A. Mete ÖZGÜNER*; Erdal KOŞUN**; Şefik İMAMĞOLU*; Mahmut DANIŞ* and Tahir KARAKULLUKÇU*

ABSTRACT.- Glauconitic sediments which are subject to this study, have been deposited with different age and facies characteristics around Devrek-Zonguldak and Kastamonu regions. Glauconies within Lower Cretaceous sequence of Western Black sea region, developed in siliciclastic units which had been deposited in outer shelf by transgressive conditions. Typical occurrences, are found in Sapca formation of Zonguldak region. Glauconitic sandstones have preferably been accumulated in sand bars during sea level changes controlled by eustatic and tectonic factors. These sediments are characterised by large and small scale cross beddings, sheet sands with parallel lamination, and bioturbation. Glaucony grains within the sandstones have autochthon and allocton characteristics according to their depositional environments. The movements within the environment of glaucony formation had been accomplished by long and short distance displacements. In consequence limestone, quartz, feldspar and mafic rock grains which had been subjected to different degrees of glauconitisation were concentrated in off shore sand bars. The glauconies have been cemented by argillaceous matrix that shows different degree of glauconitisation or rarely cemented by carbonate within the silicislastics. The glauconitisation in Kastamonu region is observed within Lower Eocene units. This mineralisation had been developed in carbonate facies which differs from Zonguldak region. The areas where Lower Eocene limestones of reefal characteristics laterally pass to open sea facies, have prepared suitable environmental conditions for the glaucony formations. Fossil, intraclast and pellet type carbonate grains in this level have been glauconitised by different degrees and exhibit hard ground and complete authocthon properties. Glaucony occurrences of the region have widely been controlled by sea level changes. Autochthon glauconies of silisiclastics of Zonguldak region which had especially been formed in periods of maximum transgression, were transported to the lower system tracts by regression of the sea. Glaucony formation of Kastamonu region occurred in hard grounds which marked upper surface of reefs when they had been drowned by rapid rising of sea level.

## INTRODUCTION

Glauconitic facies which are characterised by green grains of sand-gravel size within sedimentary sequences, have been formed in recent continental shelfs with their common occurrence within 50° S - 65° N latitudes. Although this mineral is not considered as an exact depth indicator, it occurs most widespreadly within outer shelf-upper slope environment and in 200-300 m water depth (Hein and others, 1974). Despite its preference to source grains of fossiliferous carbonate, intraclast and pellet, glaucony mineral with marine affinities can also form by diagenic change of silicate minerals such as mica, quartz, volcanic glass and pyroxene, (Ojakankasr and Keller, 1964; Triplehorn, 1966; Odin and Matter, 1981). Potassium necessity of glaucony formation is provided from sea water (Odin and Matter, 1981). For this reason, continual sea water exposure of the hard grounds, facilitate ionic exchanges leading to glaucony formation. Similarly, suitable conditions of glauconite formation are prepared at the sea floor ekposure during short sedimentational hiatuses (Clari and others, 1995; Varol and Şerifi, 1995).

In recent years glaucony is commonly used as an index mineral in sequence stratigraphy. It especially gets concentrated during the periods of sedimentary hiatuses of rapid sea level rises or at maximum flooding surfaces (Amorossi, 1995).

This study, has target to describe glauconies which have been formed within different facies (silisiclastic and carbonate) and different time intervals (Lower Cretaceous/Lower Eocene) from petrographic, environmental and sequence stratigraphic point of view.

## GEOLOGICAL BACKGROUND

Stratigraphy comprising the glaucony bearing units within Zonguldak-Devrek area (Fig.1a) has previously been established and the formation names have been obtained from this early studies (Yergök and others 1987). Paleozoic units within our geological map area have been mentioned as basement rocks. The glaucony occurs within Kilimli, Sapca and Cemaller formations of Aptian-Cenomanian age. Among them the oldest glaucony occurrences are seen in Kilimli formation (Aptian) and the youngest glaucony occurrences are observed in the Cemaller formation (Cenomanian). These time overlapping formations one over each other

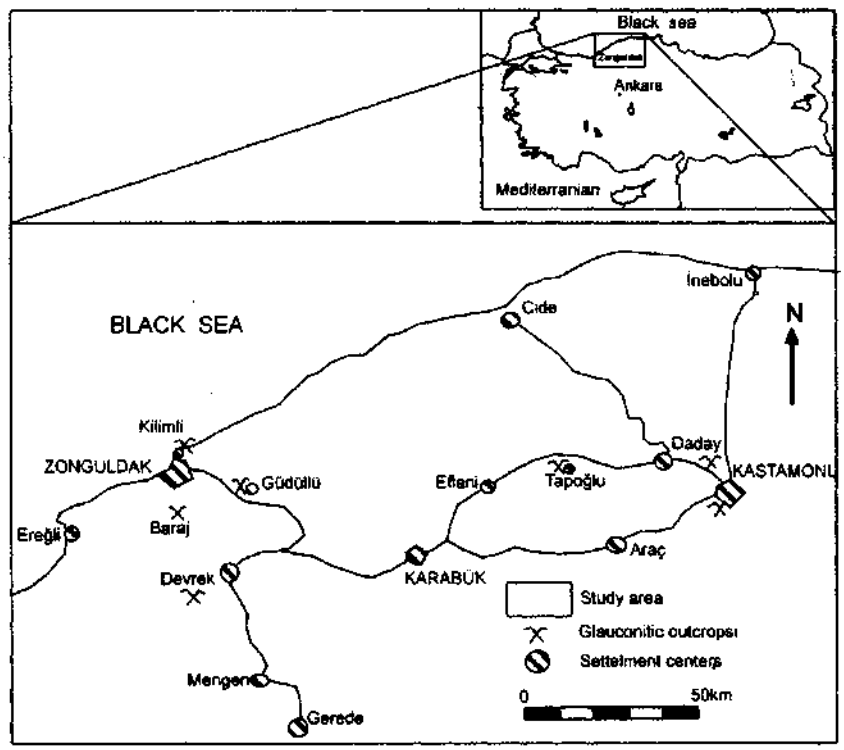


Fig. 1a- Location map of the study area.

resulted from the geodynamic evolution which caused age differences of glauconitisation. Kilimli formation formed only at the present Black sea coast in the north, but younger Sapca and Cemaller formations have been deposited in further south and became thickened by control of the southward transgression. Silurian-Devonian and Upper Jurrasic units maked up uneven basement topography. This topography which constitutes transgressional surface of Lower Cretaceous, tectonically and gradually rises towards south. In this frame; Aptian-Cenomanian glauconitic units indicate the mentioned north-southward age rejuvanation (Fig. 1b).

Glauconitic occurrences of Tertiary basin in Kastamonu region (Fig. 1a) have Lower Eocene age and are included in İnözü formation. Tertiary sequence of the region starts with Paleocene alluvial and submarine fan deposits and they are overlied by carbonates, upper surface of which is glauconitic. Fossil content of the carbonates indicate Lower Eocene age (Barkut and others, 1990). 3-8 m thick uppermost level of these carbonates with shallow marine and sparcely reefal characteristics contain glaucony grains. Alternation of pelagic limestone-tuffite levels of Budamis. formation start above it. Glauconies diminish and finally disappear upwards in a few metres from the base of the pelagic unit.

## MATERIAL AND METHOD

This study has been carried out in two parts which consist of field and laboratory studies. Outcrops of the glauconitic units have been mapped by using 1:25000 scale topographic maps of Zonguldak F 27-b1, b2, c2, Kastamonu F 31-b1, b4 and F 30-a2 sheets. 6 stratigraphic sections with 58-150 m thickness have been measured under the names of Zonguldak-Kilimli, Devrek, Kozlu barajı, Güdüllü-Sofular, Kastamonu merkez and Tapoğlu mah. Stratigraphic locations of the glauconitic levels have been marked on them. The sequences have been interpreted from the sequence stratigraphic point of view.

Mineralogy and petrography of the glauconitic material have been studied under polarisation microscopes, x-ray diffractometer and electron microscope. However, the laboratory studies, have been carried out by petrographic-mineralogic determinations glaucony has been recognised by its green colour in single nicol and by medium relief and again more green colour properties in cross nicol. In addition, it has also been recognised by 9.92 Ao, 4.97 Ao, 4.52 Ao, 2.58 Ao peaks in X-Ray studies belonging to (001), (002), (020), (130) faces. Terminologically, while its grain or facies

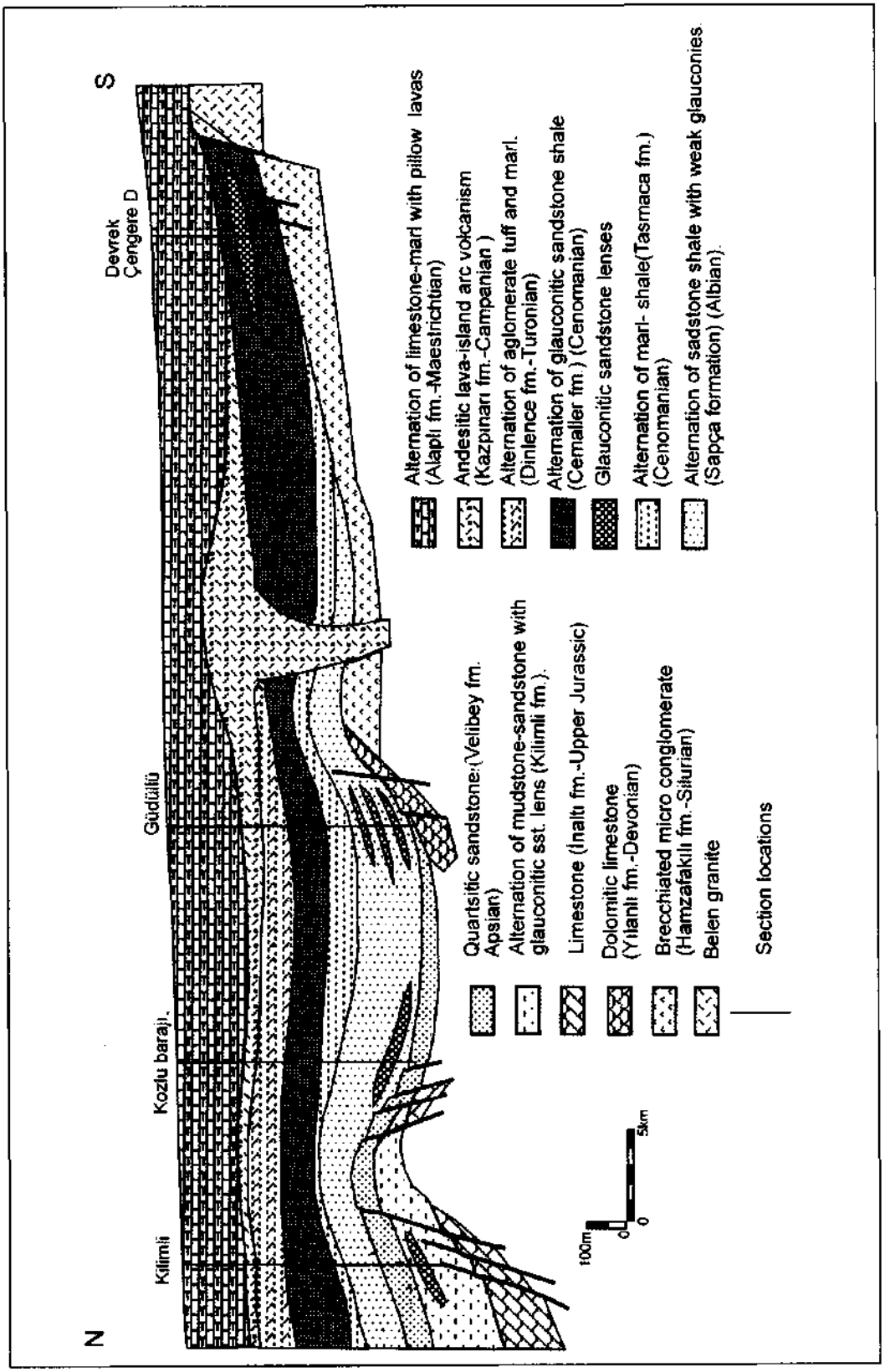


Fig. 1b- Schematic section showing stratigraphic relations of glauconitic sandstone lenses during Cretaceous in Zonguldak region.

properties are questioned; word glaucony (glaucony grain, sandstone with glauconies) and while its mineralogical properties are pointed, word glauconite (glauconitised grain) have been utilised (Odin and Matter, 1981). As to the intensity of glauconitisation; its colour index has been used (Table 1). Accordingly, dark green coloured grains are separated as strongly glauconitised grains while light green coloured grains are distinguished as weakly glauconitised particles. Glaucony grains have been separated

**Table 1- Comparison of chemical and other descriptive properties of Kastamonu-Zonguldak glauconies with mean standart values for glauconies.**

| | | MEAN CHEMICAL COMPOSITION OF GLAUCONIES | | | | | | | |
|---|---|---|---|---|---|---|---|---|---|
| Sample No | Sample Location | % MgO | % $Al_2O_3$ | % $SiO_2$ | % $K_2O$ | % $Fe_2O_3$ | %FeO/ $TiO_2$ | Glaucony colour | Probable source rock by means of S.E.M measurements |
| Mean | WORLD | 2.6-4.6 | 5-8 | 47.5-50 | 3-8.5 | 19-27 | 1-3.2/ 0.1-0.2 | Lightgreen Darkgreen | Mostly limestone and various rocks |
| GL-1 | KASTAMONU | 4.29 | 11.24 | 57.28 | 6.78 | 20.41 | -- | Darkgreen | Limestone grain |
| GL-2 | " | 4.74 | 11.64 | 51.58 | 6.75 | 25.28 | -- | Darkgreen | Limestone grain |
| GL-5 | " | 2.84 | 7.35 | 39.94 | 7.84 | 42.03 | -- | Darkgreen | Goethite grain |
| GL-7 | " | 4.23 | 12.94 | 58.27 | 6.19 | 18.37 | -- | Darkgreen | Fossil crust |
| GL-9 | " | 3.30 | 14.91 | 60.94 | 7.19 | 13.67 | -- | Darkgreen | Reef crust |
| GL-10 | " | 2.84 | 13.88 | 67.55 | 5.97 | 9.76 | -- | Green | İlitic clay pellet |
| | | | | | | | | | |
| GL-13 | ZONGULDAK | 1.22 | 11.04 | 79.86 | 2.2 | 3.86 | -/1.82 | Lightgreen | Quartz grain |
| GL-14 | " | 4.10 | 17.87 | 56.33 | 6.38 | 15.32 | -- | Darkgreen | Pellet |
| GL-16 | " | 1.95 | 26.37 | 59.04 | 5.91 | 5.80 | -/0.93 | Lightgreen | İntraclast |
| GL-18 | " | -- | 1927 | 66.27 | 13.18 | 0.55 | -/0.73 | Lightgreen | Potash feldspar |

by acid treatment of the samples and some of them have been chosen under binocular. Electron microscope (Jeol. JSM 840 model) image analyses of six different types of glaucony grains with fossil, fossil cast, intraclast, pellet, rock fragment and mineral shapes have been carried out. Their chemical compositions have been determined by FDS (Tracor TN- 5502 model) with % 90 accuracy.

## GLAUCONITIC SEQUENCES

Four glauconitic sequences between Zonguldak-Devrek area and 2 glauconitic sequences within Kastamonu region have been examined and sampled. Their typical sections and definitions have been given below according to their locations.

### Zonguldak-Devrek section.

The section has been measured from the road cut passing through Yörükoğlu village. Glauconitic levels of this location are situated in silisiclastic units. Thickness of traceable glauconitic sandstones of the area changes between 70-110 m and can show mapable outcrops. Glauconitic levels with SW-NE trends between Yörükoğlu-Keloğlu villages, approximately constitute 4 km long lens shaped body (Fig. 2a).

The best observable location of this glauconitic lens within Cemaller formation is Keloğlu village. The total thickness in that location is 110 m. This sequence begins with silty-argillaceous level which sits disconformably over Silurian rocks and is 174 m thick with 5 % or less over all glaucony content. Overlying sandy, silty and in places with carbonate levels are in the form of 7-18 m thick packages showing alternate levels with 7-35 % glaucony grains. In the uppermost part, it ends with a level with 5 % glaucony content or less. Maximum glaucony occurrence is located within 8 m thick sandstone lens at the 43,5 th m of this sequence (Fig. 2b).

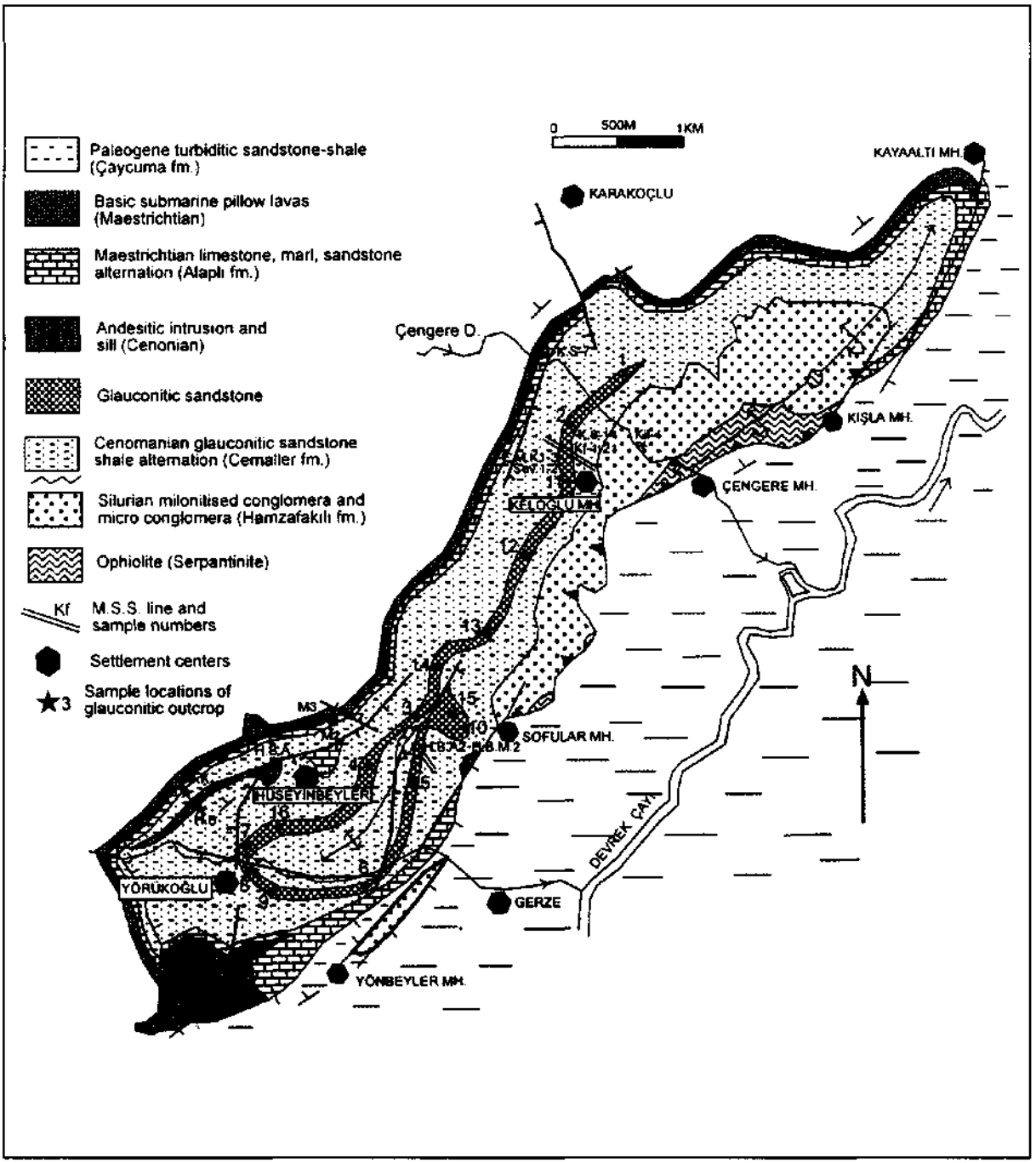


Fig. 2a- Geological map of glauconitic sandstones of Zonguldak-Devrek region.

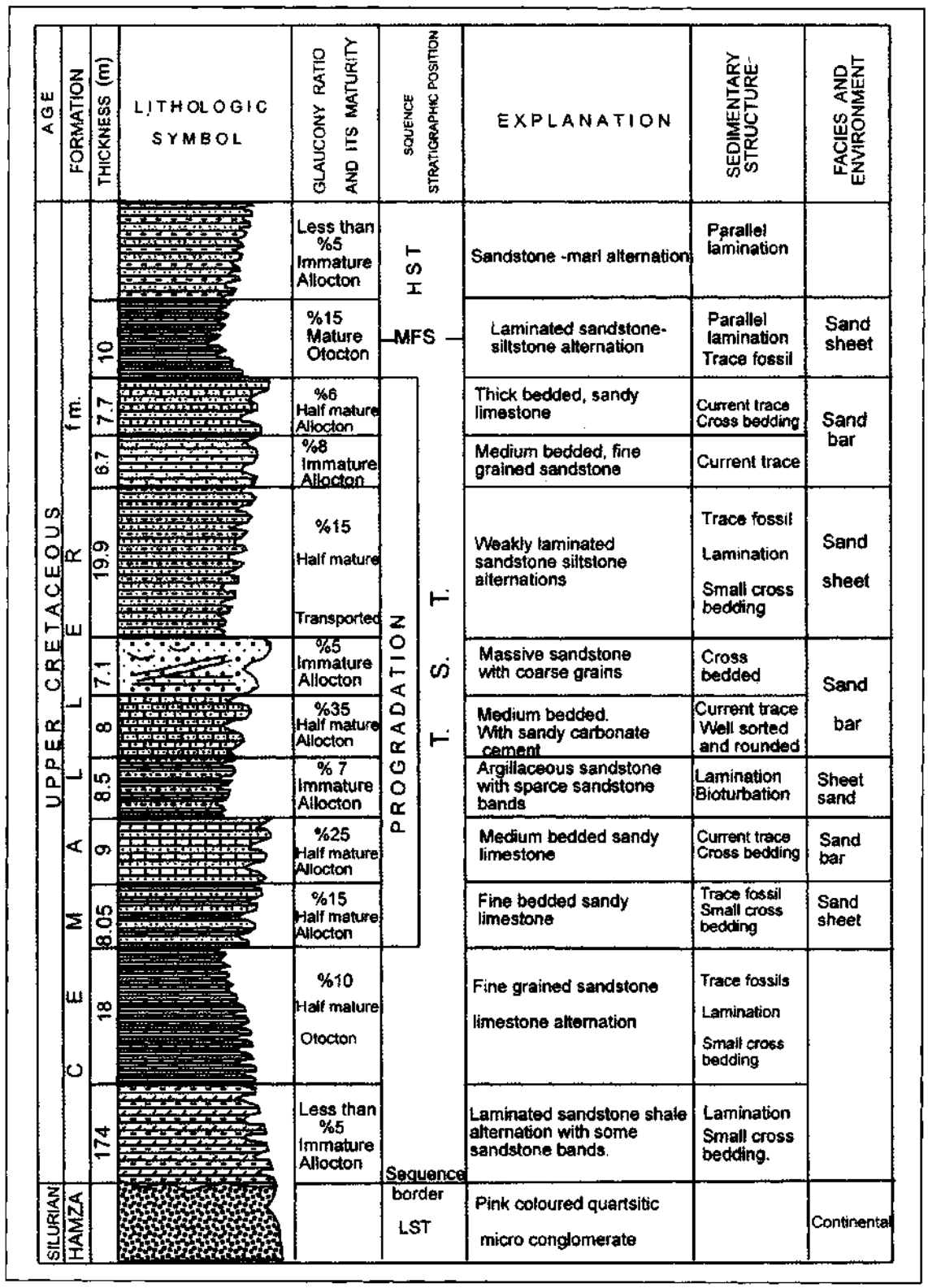


Fig. 2b- Vertical section of glauconitic unit of Zonguldak-Devrek region.

### Zonguldak-Kozlu dam section

The section was measured from the road cut passing beside the Kozlu dam. Glauconitic levels of this region is located within 50-60 m thick sandstone sequence. Glauconies are scarcely observed only in uppermost part of underlying Velibey formation which has widespread outcrops in the region. They get prominent concentration within overlying Sapca formation of silisiclastics sandstone-claystone alternation. Glauconitic sandstones in Sapça formation (Albian) are observable in an outcrop of 500 m lateral extention that has been bordered by two faults. In addition, glauconitic sandstone lenses of a few metres dimension are found in limited outcrops in Gaca stream valley (Fig. 3a).

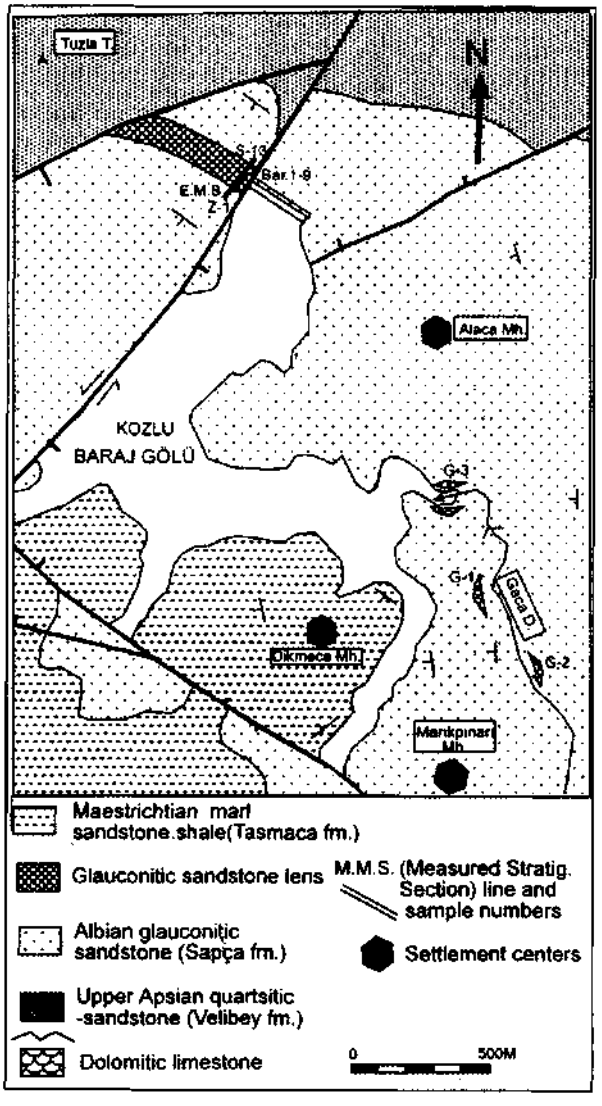


Fig. 3a- Geological map of glauconitic sandstones of Zonguldak-Kozlu dam region.

Levels with 12-19 % glauconitised grains are found within 56 m thick section that has been measured nearby Kozlu dam. This sequence is overlain by 100-200 m thick argillaceous silty, sandy levels that contain scarce glaucony minerals (Fig. 3b).

### Zonguldak-Kilimli section

Glaucony occurrences of Kilimli region are observable in a restricted area of 1/2 $km^2$. Greater part of the outcrop is situated under the sea. In the hand specimens ratio of glaucony grains doesn't exceed % 10-15 (Fig. 4a). Measured 64 m thickness constitutes the upper levels of Kilimli formation. Continuous alternations of mudstone, siltstone, marl are overlain by a channel fill coarse conglomerates. Their gravels are made up of glauconitic sandstone, but the matrix was subjected to scarce glauconitisation. Glauconies are concentraled in quartzitic sandstones at upper levels which also contain black plant fragments and fossil shells (Fig. 4b).

### Zonguldak-Güdüllü section

The sequence has been measured between Dedehasan çukuru Location and Güdüllü village. The first glauconitic unit in the region is located on the 10 m thick sandstone overlying the basement. In this region quartsitic Velibey formation is also seen to be deposited in places with time overlapping transgression. Since the glauconitic sandstone, siltstone, marl lenses of mapable size are cropping out in three different levels, they are named as G1, G2 and G3 (Fig. 5a).

Glaucony quantities and thicknesses of these levels are changing in different places and they are richest in the valley situated north of Taşlıgüney hill (Fig. 5a). The lower level has thickness changing between 4,5-18 m. Its averege glaucony ratio is 15 %. The middle level with 8-23 m thickness contains 12-22 % of glaucony, thickness of the upper level varies between 4,5-7,5 m and contains 7-13 % glaucony grains. The ends of these levels get thinner and become lens shaped. They are separated by siltstone sandstone, marl intercalations with weak glaucony content (5 % and less). Laminae made entirely of glaucony grains can be observable within the glauconitic sandstone lenses (Fig. 5b).

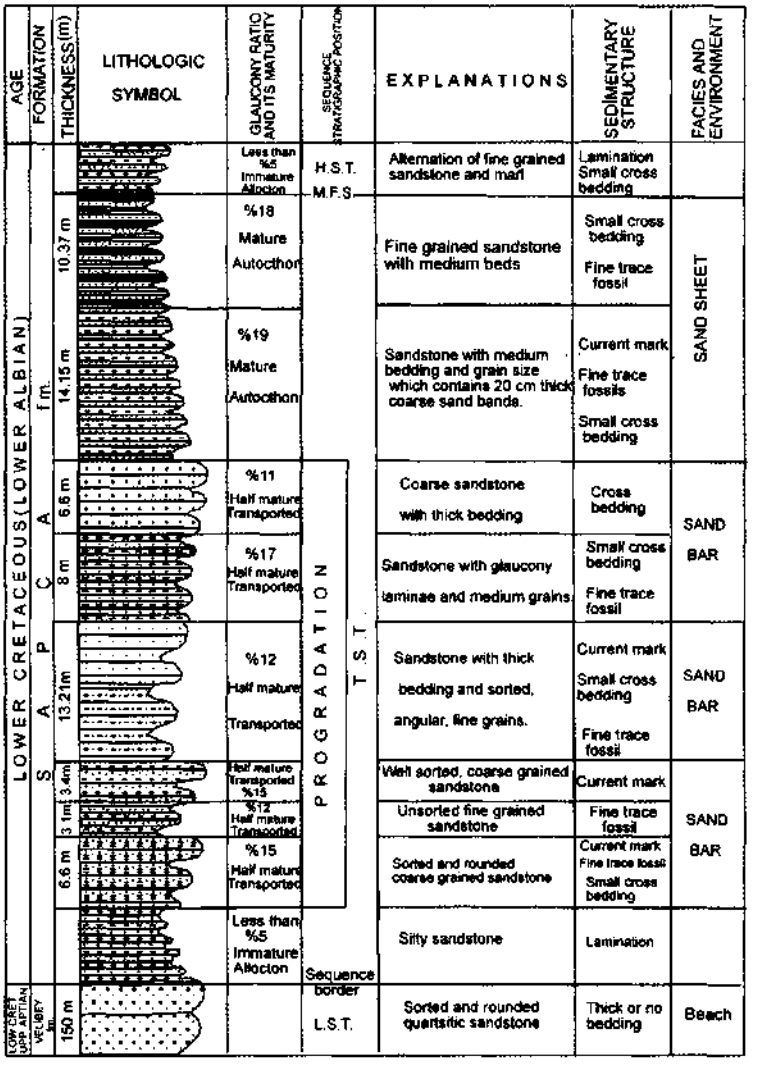


Fig. 3b- Vertical section of glauconitic unit of Zonguldak-Kozlu dam region.

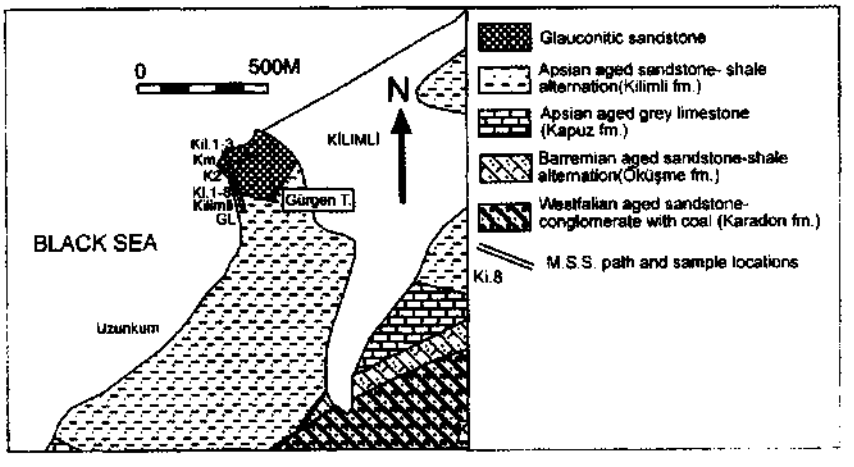


Fig. 4a- Geological map of glauconitic sandstones of Zonguldak-Kilimli region.

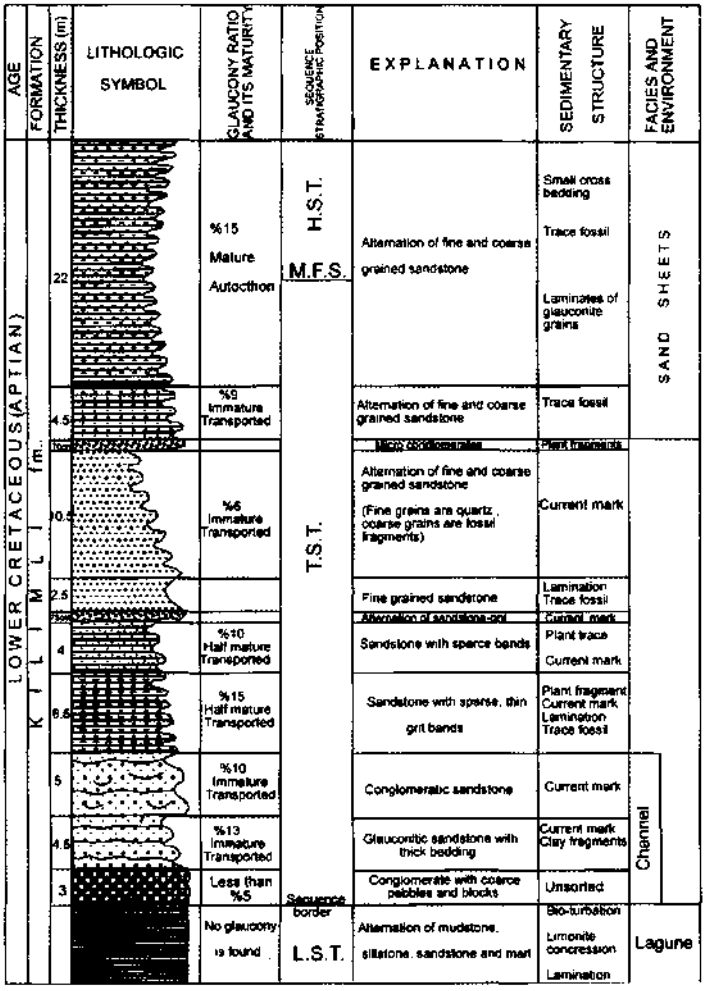


Fig. 4b- Vertical section of glauconitic unit of Zonguldak-Kilimli region.

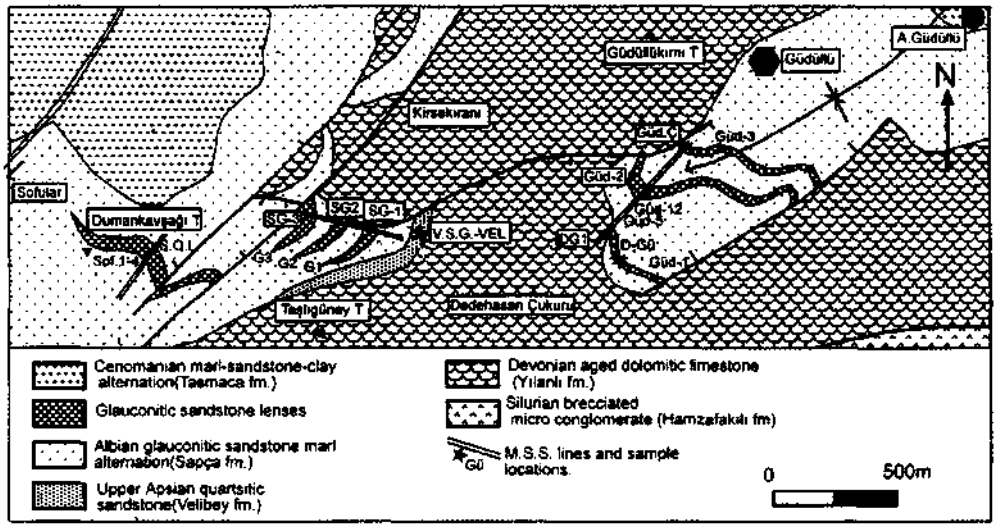


Fig. 5a- Geological map of glauconitic sandstones of Zonguldak-Güdüllü region.

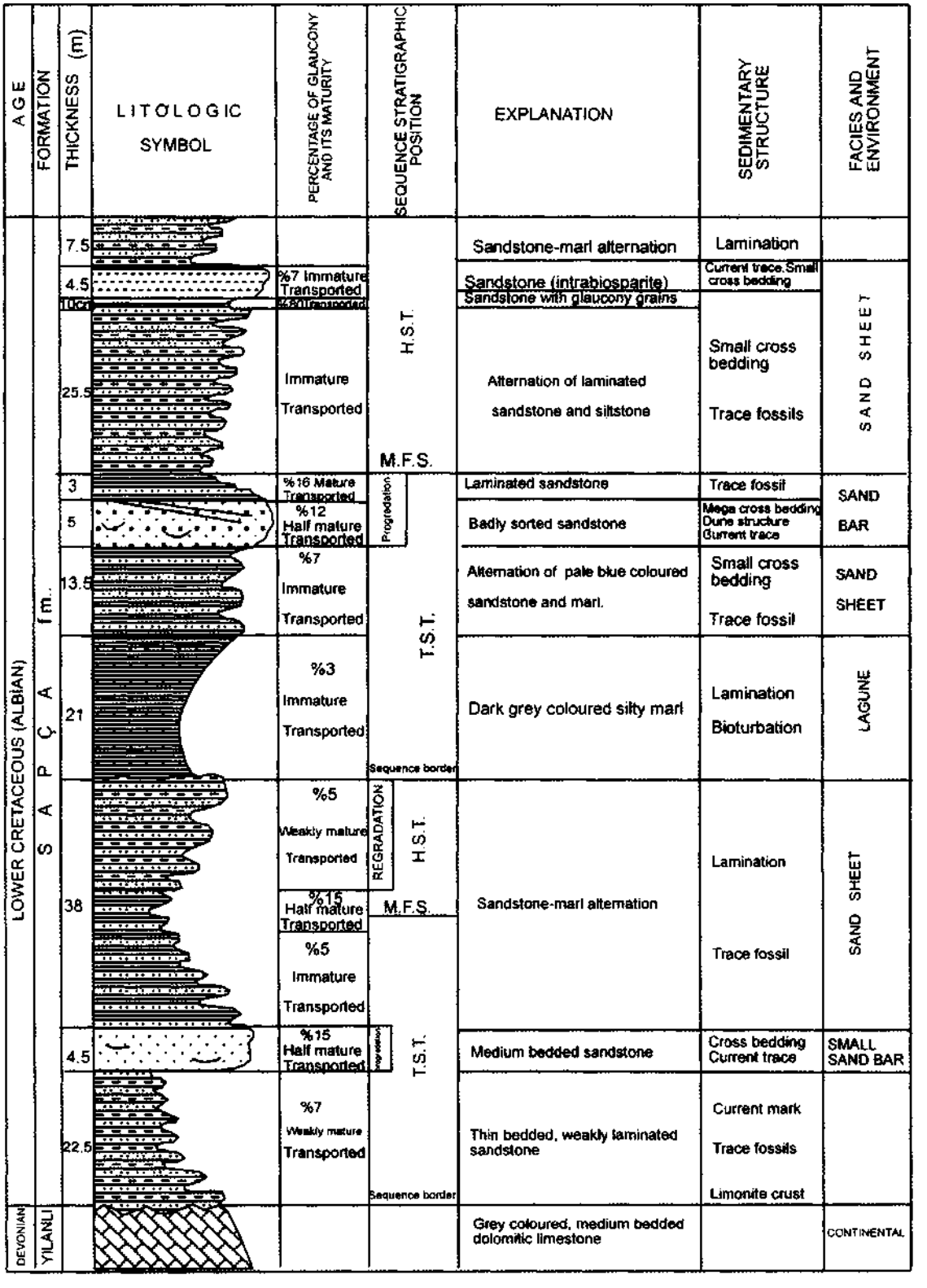


Fig. 5b- Vertical section of glauconitic unit of Zonguldak-Güdüllü region.

Kastamonu section

Here, Paleocene aged deltaic conglomerates discordantly overly Triassic schists. 3-8 m thick glauconitic level constitute the uppermost part of Lower Eocene reefal limestones (İnozü formation) which overly the mentioned Paleocene deltaic conglomerates. Glauconitic lenses occurring at the same stratigraphic level are concordantly overlain by pelagic marls and tuffites which has small amount of glaucony.

One glauconitic lens with 1,5 km outcrop length and NW - SE direction is situated in the west of Kastamonu. Another glauconitic limestone lens outcrop further south in Kızıllar Tepe and is 500 m long and has N-S orientation (Fig. 6a and Fig. 6b). Basal parts of these glauconitic lenses have hardground characteristics and partly brecciated limestone properties. These surfaces contain trace fossils and aboundant glaucony grains within solution cavities and average glaucony ratio of the overlying level is 15-20 % and has completely been generated from replacement of carbonate grains.

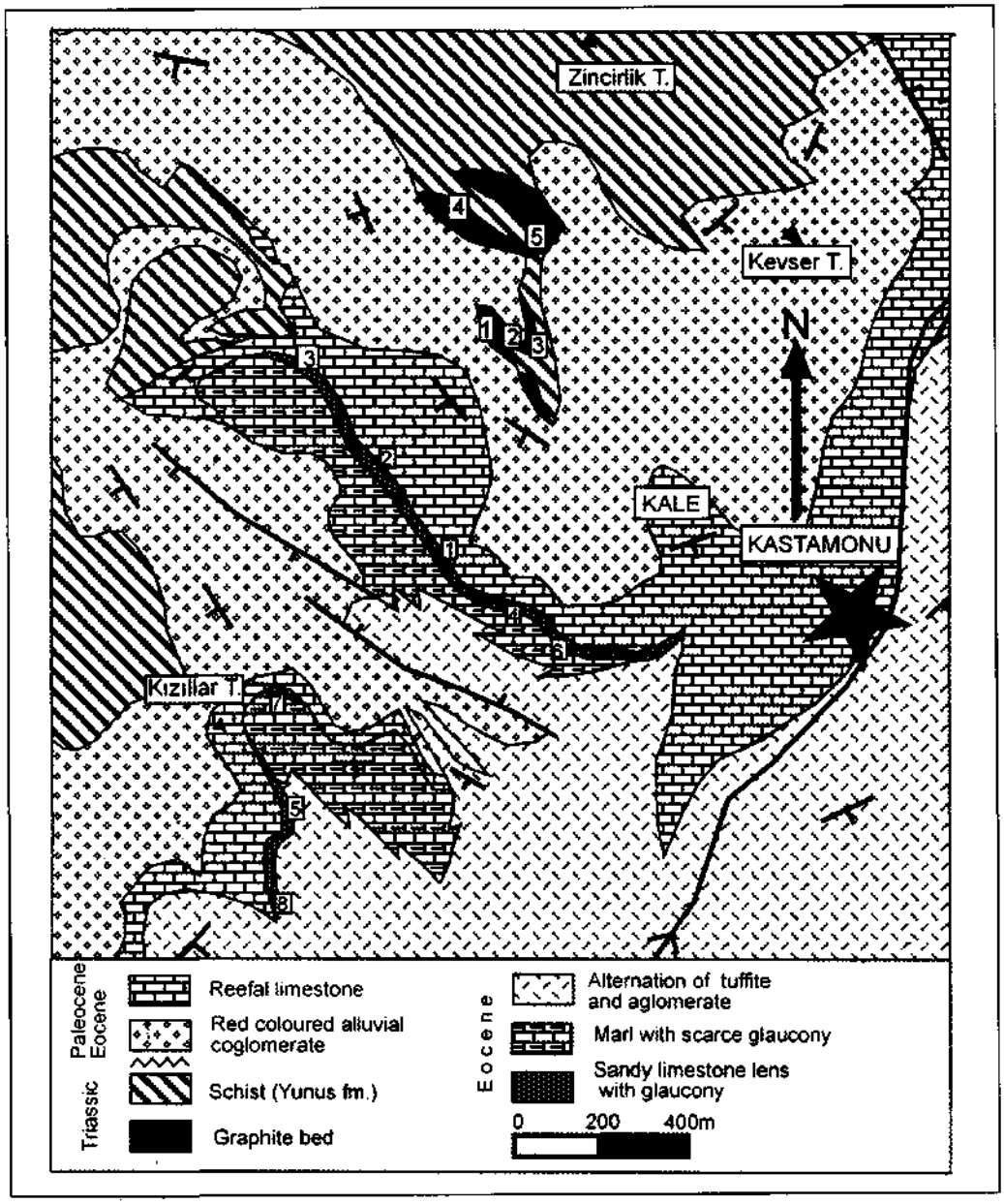


Fig. 6a- Geological map of glauconitic unit of Kastamonu region.

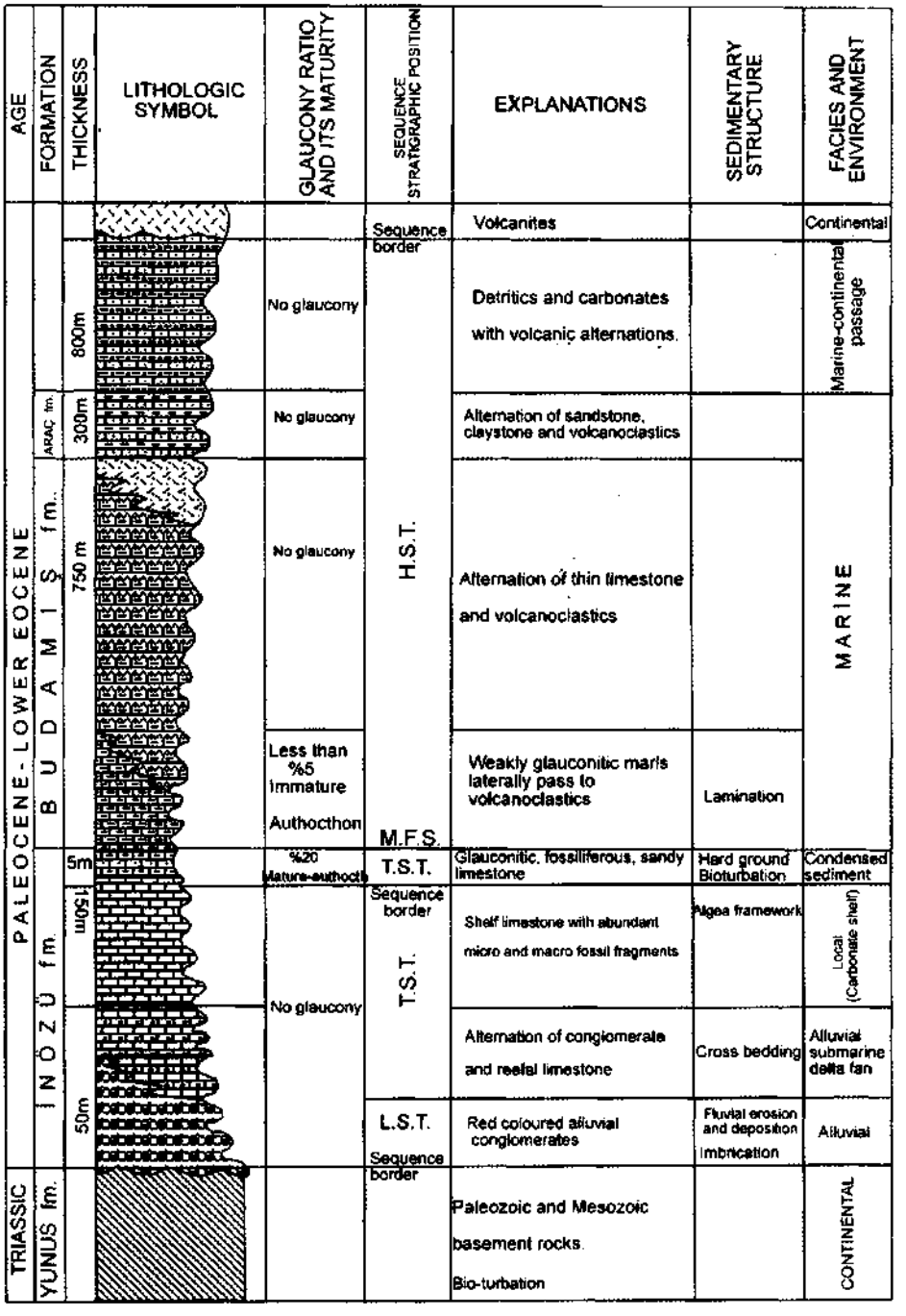


Fig. 6b- Vertical section of glauconitic unit of Kastamonu region.

Kastamonu-Tapoğlu section

The section has been measured at the south of Tapoğlu village. Here the sequence begins with delta conglomerates which discordantly overlies. Triassic basement schists. All are concordantly overlain by reefal limestones (Safranbolu formation). The glauconitic lens with 3,5 km length here follows uppermost border of the reefal limestone. To the south of the study area it thins out and dissappears within pelagic marls and silty limestone levels. Glauconies which are only found in the basal level of the pelagics gradually decrease and diminish upwards (Fig. 7 a, b).

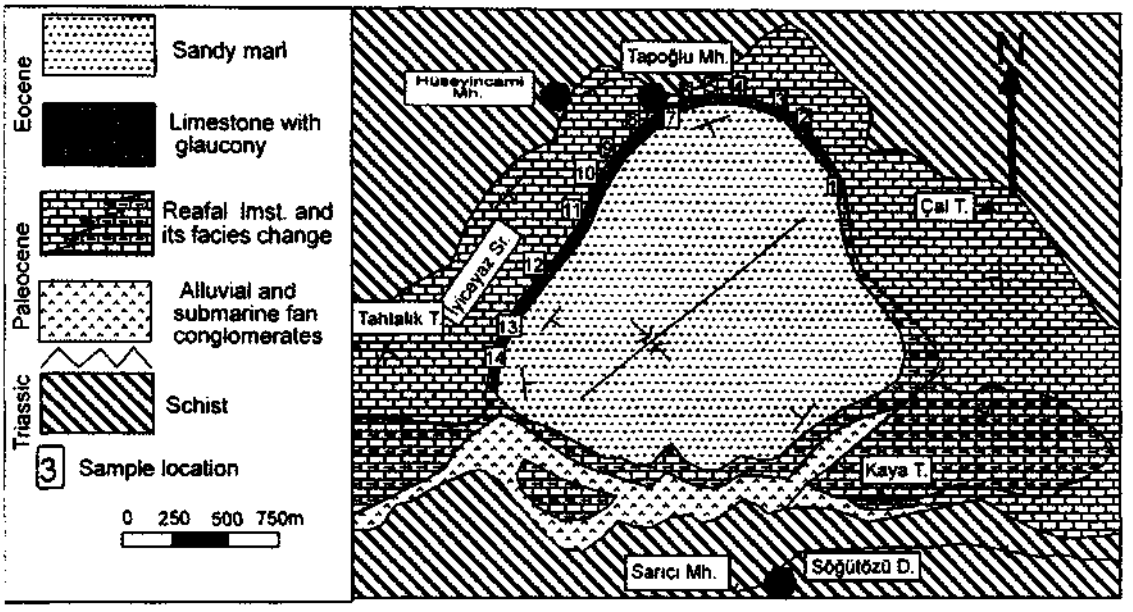


Fig. 7a- Geological map of glauconitic unit of Kastamonu-Daday-Tapoğlu Mahallesi.

## PETROGRAPHY

Detailed studies on petrographic characteristics of glaucony minerals have been carried out and published by many workers (Odin and Matter, 1981; Amireh and others, 1988; Varol and Şerifi, 1995). Various petrographic types and their developing conditions have been explained on micro and macro environmental scale. In this article, only basic petrographic types have been selected and their chemical compositions and their images under normal and electron microscope have been correlated and discussed. Maturity index, related to their green colour (Odin and Matter, 1981) has been applied and the parameters such as immature, moderately mature and mature have also been utilised in all samples of the stratigraphic sections (Table 2). In addition; potassium oxide increase that is proportional to the increase of green colour which reflects the maturity of glauconitic mineralisation and behaviour of other elements, have been tested in such a way as shown in Table 2.

**Table 2- Genetic classification of glauconies and related facies (after Odin and Matter, 1981).**

| FACIES | TEXTURE | AUTHIGENIC MINERAL (001) | AUTHIGENIC MINERAL $K_2O$ | ENVIRONMENT | | |
|---|---|---|---|---|---|---|
| GLAUCONY | GREEN — highly evolved | glauconitic mica | | Glaucony mineral | No deposition $10^5$---$10^6$ yıl | Open sea |
| | GREEN — evolved | 10A° | ---%8 | | | |
| | GRANULAR — weakly evolved | | ---%6 | EVOLUTION | | |
| | GRANULAR — nascent | 14A° glauconitic smectite | ---%4 | | No deposition $10^3$---$10^4$ yıl | |
| | FİLM green | glauconitic minerals | | Various minerals | Break in sedimentation | |

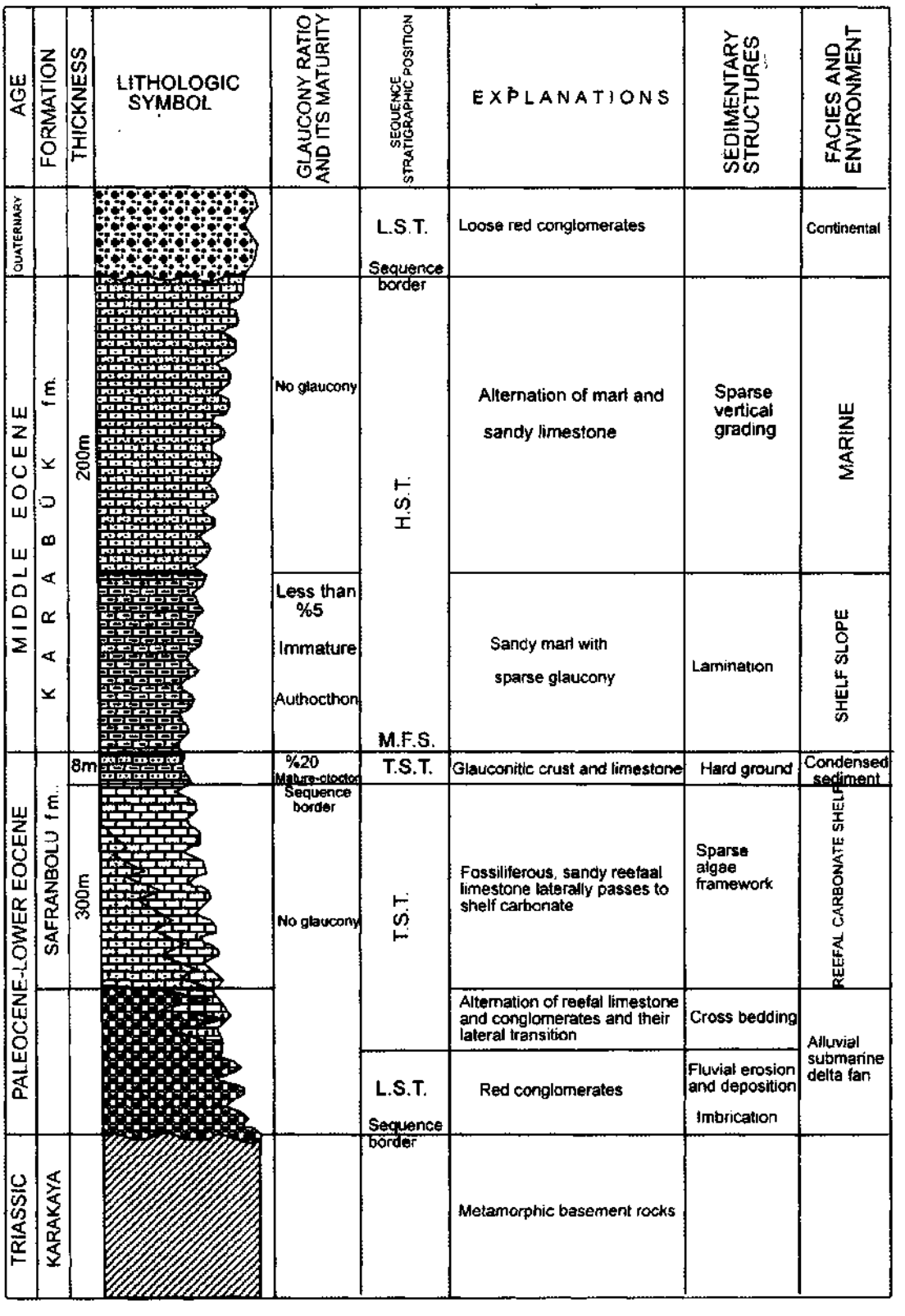


Fig. 7b- Vertical section of glauconitic unit of Kastamonu-Daday-Tapoğlu Mahallesi.

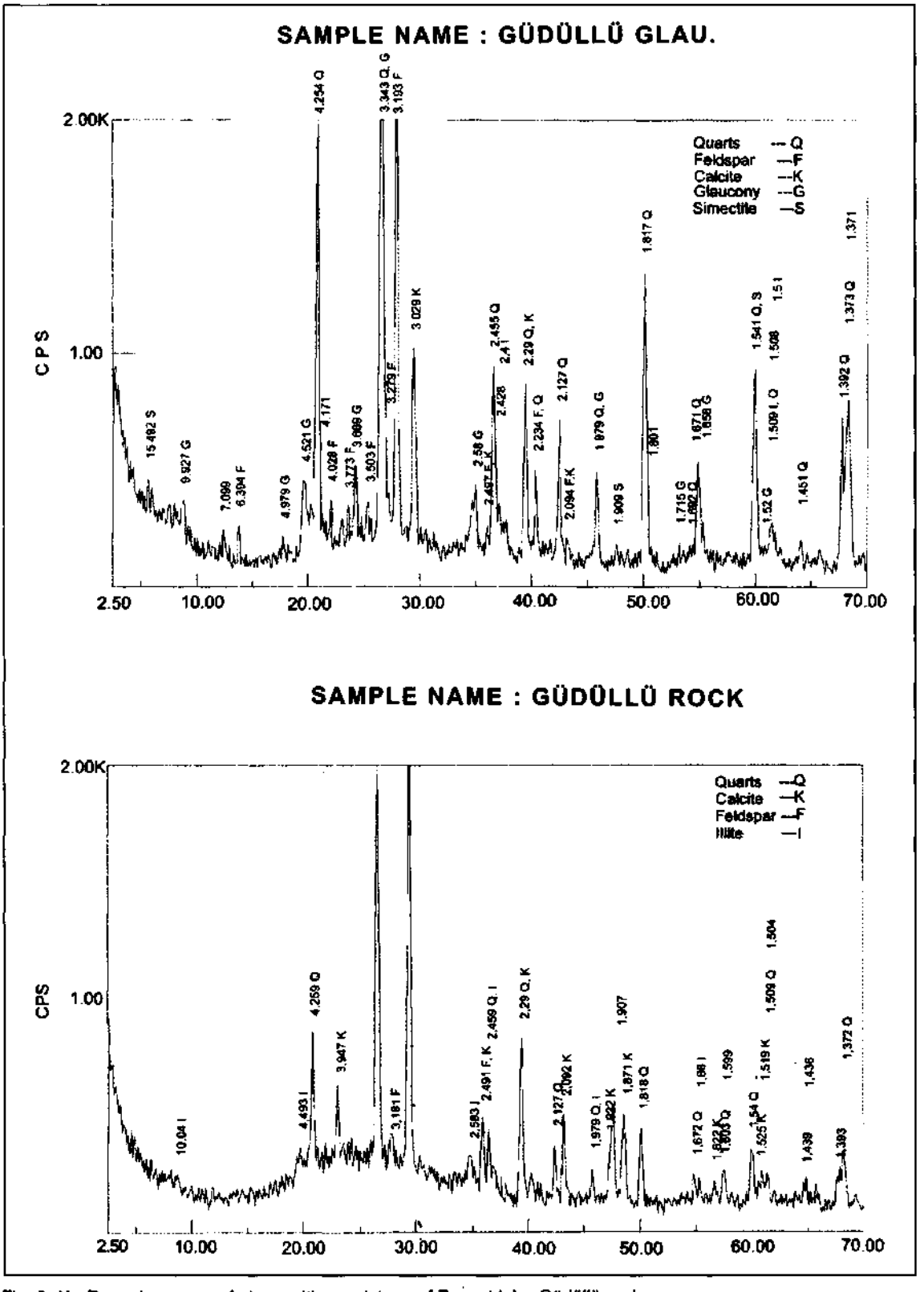


Fig. 8- X - Ray micrograpy of glauconitic sandstone of Zonguldak - Güdüllü region.

Under the light of these data; the grains which contain $K_2O$ upto 4 % and with light green-colourless appearence have been classified as immature, the grains that contain $K_2O$ between of 4-6 % and with green colour have been grouped as moderately mature and grains which contain $K_2O$ between 6-8 % and with dark green colour have been classified as mature.

Glaucony grains which fit into the above groupings have silicate and carbonate origins. Glaucony grains with silicate origin dominate Albian-Cenomanian silisiclastic levels of Zonguldak region. The silisiclastic level is basically made of 75 % quartz, 15 % feldspar and 10 % volcanic rock fragments. Evolutions of glaucony mineralisation of this kind of grains have been discussed by various researchers (Wermund, 1961; Odin, 1972; Hein and others, 1974). In our samples, especially quartz grains have been glauconitised at different intensities (Huges and Whitehead, 1987; Ojakangasr and Keller, 1964). Among these, immature glaucony grains have very faint green colour with $K_2O$ ratio up to 4 %. In electron microscope images the fractures can easily be seen on the weakly glauconitised quartz grains (Plate I, fig. A). However in quartz grains with increased intensity of glauconitisation; crystal surfaces have been covered with a crystal plate like growths (2-4 micron) which reflects glauconitisation texture (Plate I, fig. B and fig. C). In addition to these, some grains with poor glaucony mineralisation have very high potassium oxide (12-13 %) and aluminium oxides. These anomalies have probably been produced by alkaline feldspar grains. Petrographically determined alkaline feldspars which show poor glaucanitisation have chemical analyses with high $K_2O$ and $Al_2O_3$ values since they greatly conserve their chemical compositions (Plate I, fig. D).

Glauconies which have been evolved from carbonate grains, characterise Lower Eocene sequence of Kastamonu region. These have been formed by replacement of carbonate grains such as bioclast, intraclast, pellet or by filling of fossil cavities. In comparison with those of Zonguldak silisiclastics they constitute glaucony grains of higher degree maturity (mean $K_2O$ contend is between 5-7 %). Other kinds, have filled fossil lobes or microcavities of crusts of these organisms. In electron microscope views these glaucony infillings show small spheric patterns (Plate II, fig. A and fig. B).

Common property of glaucony mineralisation as result of replacement of carbonate grains such as intraclast and bioclast is the formation of fructured structure. These fractures have deep penetrations and in places they break the grains completely (Plate II, fig. C and fig. D). Many researchers have attributed these fractures to series of events occurred during glaucony mineralisation. According to Mc Rae (1972) and Odin and Matter (1981); during evolution of maturity stages from simectitic glauconite which represents first phase of glauconitisation, to glauconitic mica which represents final product, volumetric shrinkage developes by expelling the crystal water that is the cause of these fractures. Actually the grains which had experienced this kind of glauconitisation have dark green colour (highest degree of colour index) and well developed lamellar structure (5-6 micron) of glauconitic texture (Plate II, fig. E). On the other hand, abundant carbonate remains have been observed within poorly mineralised and light green-white coloured grains.

## DEPOSITIONAL PROPERTIES

Descriptive depositional properties of Albian-Cenomanian glauconitic silisiclastic units of the Zonguldak-Devrek area:

*1) Bedding.-* Bedding characteristics and types within glauconitic sequences have shown conspicuous differences from one stratigraphic section to another. Similarly bedding thickness changes from 10 cm to 100 cm. However, bedding and lithologic characteristics at lower and upper boundaries of glauconitic sandstone levels in all sequences are rather similar to each other. They are generally represented by fine grained sediments which consist of fine bedded, laminated marl, mudstone and siltstone. Glauconitic levels which could be followed in lateral and vertical extent have lens geometry. Among these the maximum lateral extent is seen in Devrek area where the lens is 4-6 km long then the glauconitic levels laterally pass into sandstones without glaucony and disappear.

Conspicous differences in the bedding properties are seen in Kilimli region. Here, at the bottom glauconitic sandstone sequence begins with the level of glauconitic channel fill conglomerates and gets thinner upwards. On the other hand, upward thickening sequences without channel fills have been observed in the other locations in the Zonguldak region. Generally upward thickening sequence is characteristic of glauconitic sandstones (Mc Cubin, 1982).

Cross beddings of glauconitic sandstones are conspicuous in places. Beside large scale cross bedding types small scale ones are also frequently observed. The greatest cross beddings within the region have lower angle and has 10m approximate set

thickness (Devrek-Gerzedere and Kozlu dam Gacadere) (Plate III, fig. A). Their paleocurrent directions are seen to be towards the inner basin. Parallel beded glauconitic sandstones which overlie cross beded glauconitic sandstones have widespread inner lamination.

Glauconitic sheet sands which overlies cross-bedded levels in Güdüllü region has widespread extention in the area (Plate III, fig. B). All these bedding properties, support that the glauconies concentrated either in paleo offshore sand bars or in sand sheets (Jeray kievicz and Wojeweda, 1986 and Surly and Noe-Nygaard, 1991). Hydrodynamic conditions of their deposition will be explained in sequence stratigraphy.

*2) Biogenic Structures.-* Abundance and importance of biogenic structures and trace fossils in relation with glaucony genesis have been explained by several investigators (Bromley, 1975). These biogenic activities increase during hiatuses of sedimentation. In glauconitic levels of the study area the following kinds have been observed.

Horizontal biogenic traces, are seen within laminated glauconitic mudstone, siltstone, claystone alternations of sheet sand struptures, which had been deposited in outer shelf of Zonguldak region. Horizontal biogeic traces have also been developed, within glauconitic carbonate lenses and especially in their basal hard grounds. These traces are about 1 cm wide.

Horizontal bioturbation activities that indicate decrease in sedimentation rate is commonly seen in fine grained silisiclastic levels where authigenic glauconite precipitation had been concentrated. In addition, there is a comparable increase of fossil shell fragments within these levels (Plate III, fig. C). U shape and vertical biogenic traces are more prominant in allocton glauconitic coarse grained silisiclastics which indicate rapid deposition on near shores. Abundant biogenic traces with 0,3 cm widths are observable at bedding surfaces of glauconitic sandstones of Kozlu dam. This type of fine but intense biogenic activities indicate partly stagnant environmental conditions (Rhoads, 1976).

*3) Lamination.-* It can be seen in most part of glauconitic levels within the silisiclastic levels. Glauconies have been concentrated in laminae planes and reach 15-20 % abundance. Parallel and cross laminations are typical especially in sand sheet levels. This lamination has been, formed by lining of fine and medium size grains of the glauconitic sands and also by vertical micro grading of the particals. Cross and parallel laminated levels dominate and alternate in most part of the sequence in Güdüllü (Plate III, fig. B). Black plant fragments are also seen within glauconitic laminates of Kilimli region (Plate IV, fig. A).

Alternations of mudstone and siltstone laminates of thin bedded levels underlying and overlying the glauconitic sand bars are readily seen. Their glaucony content is about 5 %.

Laminated claystone-siltstone levels with scarce glaucony occur as intercalated packets in glauconitic sandstone lenses in Devrek. Cementations of Kozlu dam and Kilimli glauconitic sandstones are stronger since carbonate content of laminated levels of glauconitic sandstones is higher. Here, carbonate cement together with glauconitised grains have again been glauconitised at different degrees.

*4) Hardground.-* It has been accepted by many investigators that submarine hard grounds constitute suitable environmental conditions for glaucony, phosphate and mangan mineralisations (Clari PA. and others, 1995). While sea bottom begins to be hardened during sedimentational hiatuses, the necessary elements for glaucony formation is either provided from the sea water or from the clays. According to Odin and Matter, 1981; minimum time required for the extraction of potassium from sea water which is necessary for glauconite mineralisation is 1000 - 10000 years. In other words for glaucony formation at least such a minimum period of sedimentational hiatus is necessary.

Hardground surfaces are absent in Zonguldak region within Albian-Cenomaian glauconitic silisiclastic levels. However, levels with concentration of biogenic activity material and early diagenetic glauconitised cements, may indicate short periods of sedimentational hiatuses.

Typical hardgrounds with glauconitic mineralisation have been observed in Lower Eocene limestones of Kastamonu region. The percentage of glaucony grains (40-60 %) within hard grounds at the upper surface of reefal limestones has high order. This amount falls to 5 % in the immediately overlying pelagics and in a few metres upwards glauconies dissappear completely. These mineralised hardgrounds contain a lot of biogenic traces, caverns and cavities of solution surfaces and neptunian dykes which vertically or diagonally cut the bedding plane as pointed out by Tucker and others, 1992. Glaucony grains have been drived from altered intraclasts, bioclasts and pellets within the

hardground and have filled all the cavities above the hard ground. Therefore glaucony mineralisation in hardgrounds is a kind of cavity filling rather than widespread precipitation.

## SEQUENCE STRATIGRAPHY OF GLAUCONITIC SECTIONS IN KİLİMLİ, KOZLU, GÜDÜLLÜ, DEVREK, KASTAMONU AREAS

Amorossi (1995), has stressed the importance of distribution pattern of glaucony concentrated levels, maturity of the glauconies (that is $K_2O$ percentage or intensity of their green colour) and genetically their allocton or autocthon characteristics from point of view of interpreting the sequence stratigraphy of silisiclastics. He explained that more concentrations of authocthon glaucony grains have been found in condensed levels, on the maximum flooding surfaces (M.F.S.) in transgressive system tract levels and in lower levels of high system tract (H.S.T.). In the upper levels of T.S.T. abundance and maturity of the glauconies increase while in that of H.S.T. they decrease. From point of view of glaucony concentration and maturity, condense level and maximum flooding surface (M.F.S.) are far more richer in comparison with the levels below and above. Allocton, outer sequence (detrital) glauconies are found in lower system tracts (L.S.T.) where the general level of the sea is lower. These are also seen in T.S.T. and H.S.T. systems. Detrital glauconies generally show less concentration and less maturity than their authocthon equivalents.

### Sequence stratigraphy of Kilimli region

The sequence in this outcrop is thinning upwards which is reverse to the normal thickening upward sequence of glauconitic sand bars. However in the erosional channel of sand bars thinning upward sequence is normal (Moslow, 1983). Erosional channel that had been carved during a sand bar formation took place at the base of the sequence which sits on sandstone, mudstone, siltstone alternation with limonite concretions and trace fossils in this location.

Non-existence of clay within the lower part of the glauconitic sequence is an indication of dominant role of waves. The section indicates that erosional process of the channel didn't stop within the sand bar but continued and cut down into the underlying sediments. This also indicates that the sand bar sequence is transgressive (Moslow, 1983). Waves and storms cut some fragments from sand bar and deposited them at the base of the channel.

Base of the channel represents lower boundary of the transgressive sequence. Glauconies occurring in the lower part are light green coloured, immature or moderately mature and had been transported. Dark green coloured and fractured, authigenic glauconies are seen to have been deposited at the maximum flooding surface (MFS) where upward thinning of the sequence ends. The glauconies deposited at this level are both more mature and have higher concentration (Fig. 4b).

The glaucony grains within 6,5 m thick part of the transgressive sequence with 15 % concentration (Fig. 4b) were probably transported by waves and tide currents so that their percentage selectively increased. They are less mature than the glauconies of the maximum flooding surface.

### Sequence stratigraphy of Kozlu dam section

Base of the sequence concordantly overlie the Velibey formation beach sandstones and contains small amount of immature, light green glauconies. It is observable that maturity and percentage of glaucony grains increase and gain authocthon character upwards in the sequence towards maximum flooding surface (M.F.S.). The glauconies at the M.F.S. surface are dark green and fractured. In further upward levels towards H.S.T. it is clearly observable that glaucony percentage and maturity decrease (Fig. 3b).

Thick bedded glauconitic sandstone lens shows thickening upward and contains bands with coarse quartz grains, transported glauconies and tiny bioturbation traces. This section is thought to be prograding within whole general transgressive sequence. The overlying fine grained section contains micro cross bedding, trace fossils and scarce authocthon, mature glauconies both in the cement and also in the grains and probably represents washover part of the sand bar (Moslow, 1983).

### Sequence stratigraphy of Güdüllü section

Two different depositional systems have occurred within the sequence. First transgressive sequence discordantly overlies Devonian dolomitic limestones and contains moderately mature glaucony grains with ratio of 15 %. Rising of the sea level continued up to maximum flooding surface (M.F.S.). 4,5 m thick glauconitic sandstone lens with 15 % allocton glaucony grains has progradated. H.S.T. sequence occupies the upward levels which have been

influenced by regression and their glaucony contend decreases. It is deduced that the sea level became lower down to the base of the lagoon sequence which consists of dark grey, silty, laminated marls with trace fossils. Base of the lagune sequence marks both the end of the first sequence and begining of the second sequence. Even the new sequence started transgressively and continued with sandstone levels having 7 % immature glaucony grains which was subsequently transported towards the open sea probably by tectonic uprising and was deposited within off shore sand bar with low angle mega cross beddings (Plate IV, fig. B) (Jeraykievicz and Wojeweda, 1986; Surlyk and Noe-Nygaard, 1991). Sheet sand levels which immediately overlie the lens contains 15 % mature glauconies and represent M.F.S. level. In the further up levels glaucony ratio and maturity decrease and H.S.T. of the second depositional sequence develop (Fig. 5b).

**Sequence stratigraphy of Devrek section**

Glauconitic sandstone sequence of the area began by transgression of Upper Cenonian sea over the shelf. The transgression ended when it reached the maximum flooding surface where off shore sand bar formed. This level has a washover platform fades which contains parallel lamination and well sorted, authocthon, increased quantities of glaucony grains (Fig. 2b). Towards the upper levels; glaucony ratio decreases, the shelf gets shallower character and high system tract (H.S.T.) sequence is represented.

Glauconitic sandstones show 20°-25° mega cross bedding at the road cut of Gerze Dere valley (Plate III, fig. A). The current direction is approximately parallel to the shore. High glaucony contents reaching to 25 %-35 % occur in middle part of sand bar sequence which consist of transported glaucony grains. Clay patches which contain tiny quartz and glaucony grains can be seen in these levels. In addition, alternations of thin beds of bad sorted angular quartz grains and well sorted, rounded quartz grains are also observable. These structures representing agitation and quiet periods, can also indicate selective transportation of glaucony grains by currents.

Horizontal trace fossils which are frequently seen within the sequence, developed during the calm periods of transgression, no deposition took place. However vertical and U shape fossil traces eitrter developed in rapid depositional or during the lowering periods of sea level.

**Sequence stratigraphy of Kastamonu section**

Discordant basal contact of Paleocene delta conglomerates constitutes the lower boundary of the sequence while the upper surface of the overlying reefal limestone which is base of the hard ground forms the upper boundary of the sequence. Alluvial conglomerate part at the base of the sequence represents low system tract (L.S.T.) and the upper reefal limestone part to the glauconitic hard ground constitutes transgressive system tract (T.S.T.).

Reefal carbonate production developed parallel with the transgression. In consequence of sudden faulting the reefal limestone sunk down under the photic zone and drowned under the pelagic sediments. Hence a new stratigraphic sequence started. Glaucony formation period in the hiatus of the sedimentation just after the faulting, represents transgressional system of the second sequence (Wolfgang, 1991; Clari and others, 1995). Upper boundary of the hard ground indicates beginning of the sedimentary deposition and upper boundary of the glauconitic level constitutes maximum flooding surface (M.F.S.). Remaining part of the above sequence which was deposited up to the Tertiary basin closure which represents high system tract (H.S.T.). This upmost discordant surface signifies the upper border (SB) of the second sequence (Fig. 6b).

Marl and tuffite sedimentation over the glauconitic limestone lens marks the end of sedimentation hiatus, then glauconite deposition couldn't be possible. Hence, the thickness of glauconitic limestone lens couldn't develope more than 8 m. Glaucony deposition, transportation and redeposition which all caused the development of thick glauconitic sequences in Zonguldak silisiclastics can not be seen in the Kastamonu carbonates.

## CONCLUSIONS

Glaucony occurrences in Zonguldak-Devrek region have Albian-Cenomanian age and deposited in open shelf environment of silisiclastics. Different ages of glauconitisation, are related to time overlapping transgresions from north to south within the mentioned period. These depositional systems where off shore conditions dominated, have generally been deposited in the form of sand bars and sand sheets. Glaucony grains which were transported within active shore environment from time to time, were deposited in silisiclastics that show microcross lamination, microlamination and vertical grading. Transportation of glaucony grains,

must have probably been accomplished in shoaling periods related to sea level changes. General transgressive development of the region was cut by regresive interphases. Black plant fragments which are seen in glauconitic occurrences also support this shoaling and sea level changes. Carbonate deposition occurred in local areas where silisiclastic movements couldn't reach. These relative sea-level changes have repeated the development of glauconitic levels as characteristic sequences.

All glauconitic off shore sand bars which were situated in different locations within Cretaceous open shelf basin of Zonguldak region, constitute upward thickening packets within transgressive system sequences. In the main bodies of sand bars, immature, moderately mature, mature and transported or semi-transported glauconies have been found. Mature and autochthon glauconitic levels, are situated immediately over the sand bars and indicate that the water depth increased in such a way that a new sand bar could not be formed.

However, Lower Eocene reefal limestone also occurs in a transgressive system in Kastamonu region. This system, begins with delta and submarine fans and continues with reefal limestones by the time until open sea conditions get realised. 5-8 m thick glauconitic limestone lens with hard ground basement that is composed of abundant glauconies, benthic and pelagic fossils, represents maximum transgressional period in the region. Synsedimentary fractures developed on the upper surface of the reefal mass indicate that the mass must have suddenly gone down under water and drawned during this maximum transgression. In addition, these reefal limestones and overlying pelagics and transition zone of the reef derived bioclastic, glauconitic sandy limestone between them support sea level changes during glaucony formation and during subsequent period.

## ACKNOWLEDGEMENTS

This study was carried out within the Western Black sea Phosphorite Exploration Projects 97-12A, 98-11F of MTA in 1997-1998. We thank to the MTA authorities for the support we received.

Suggestions made by the Publication Department of M.T.A. and by the referees towards improving the text are acknowledged.

Dr. Selahaddin Kadir who kindly did some X-ray work on the samples.

Last but not the least we are gratefull to Dr. Tandoğan Engin of MTA who improved the English of the text.

*Manuscript received November 8, 1999.*

## REFERENCES

Amireh, B.S.;Jarrar, G.; Henjes-Kunst, F. and Schneider, W.,1988, K-Ar dating, X-ray diffractometry, optical and scanning electron microscopy of glauconies from the early Cretaceous Kurnup Group of Jordan: Geological Journal, Vol.33, pp.49-65.

Amorosi, A., 1995, Glaucony and Sequence Startigraphy: A conceptual Framework of Distribution in Siliciclastic Sequences. Journal of Sedimentary Research Vol. B65 No.4 November, 1995, pp.419-425

Barkut, M.Y.; Bilginer, E; and Pehlivan, Şükrü, 1990, Kastamonu Araç ve güneyinin jeolojisi: MTA Rap.; No.9079 (unpublished), Ankara.

Bromley, R.G., 1975, Trace Fossils at Omission Surfaces: Frey R.W., ed., The Study of Trace Fossils, Springer-Verlag, Berlin, pp.399-428.

Clari, P.A.; Dela Pierre, F. and Martire, L. 1995, Discontinuities in carbonate successions: identification, interpretation and classification of some Italian examples: Sedimentary Geology, Vol.100, pp.97-121.

Hein, J.R.; Allwardt A.O. and Griggs G.B., 1974, The Occurrence of Glauconite in Monterey Bay, California. Diversity, origins and Sedimentary Environmental Significance. J. Sedim. Petrol. Vol.44, pp.562-571.

Huges, A.D. and Whitehead, D., 1987, Glauconitization of detrital silica substrates in the Barton Formation (Upper Eosen) of the Hampshire Basin, Southern England, Sedimentology 1987, Vol.34 pp.825-835.

Jeraykievicz and Wojeweda, 1986, Offshore bars v.s lowstand shoreface deposits in the Cretaceous Interior Seaway of North America (Sedimentrary Environment and Fades, Edited by Reading H.G.1996, pp.277-280).

Mc Cubbin, D.G., 1982, Barrier-Island and Strand-Plain Fades (Sandstone Depositional Environments Edited by Scholle PA. and Spearing D. 1982). AAPG Memoir, Vol.31.1982.

Mc Rea, S.G., 1972, Glauconite Earth ScienceRev.8, pp.397-440.

Moslow, T.F., 1983, Depositional Models of Shelf and Shoreline Sandstones Continuing Education Course Note Series-27, AAPG Full Education Conference.

Odin, G.S., 1972 a, Observations nouvelles sur la structure de la glauconie en accordeon: description du processus de genese par neoformation. Sedimentology, Vol. 19, pp.285-294.

_____and Matter, A., 1981, De Glauconiarium Origine. Sedimentology 1981. Vol.28, pp. 611-641.

Ojakangasr, R.W. and Keller W.D., 1964, Glauconitisation of rhyolite sand grains. Journal of Sedimentary Petrology Vol.34 No.1 pp.84-90.

Rhoads, D.C., 1975, The Paleoecological and Environmental Significance of Trace Fossils: Frey R.W., 1975, ed The Study of Trace Fossils. Springer Verlag, Berlin.

Surlyk and Noe-Nygaard, 1991, Shallow marine sand deposition in an elongate, intracratonic rift basin: Upper Jurassic-Lower Cretaceous of East Greenland (Sedimentary Environment and Fades. Edited by Reading H.G. , 1996, pp.273-277).

Tucker, M.E.; Wright, V.P.: and Dickson, J.A.D., 1992, Carbonate Sedimentology, Blackwell Scientific Publications.

Triplehorn, D.M., 1966, Morphology, internal structure and origin of glauconite pellets. Sedimentology, Vol.6. pp.247-266.

Varol B. and Şerifi C., 1995, Üst Kretase Glokonilerinin (Kilis, G.D. Türkiye) Sedimenter Petrografisi ve Çökel Ortamları: Tr. J. of Earth Sciences 4 (1995), Tubitak, 13-26.

Wermund, E. G., 1961, Glauconite in Early Tertiary Sediments of Gulf Coastal Province.Bull. Am. Ass. Petrol. Geol. Vol.45, pp.1667-1696.

Wolfgang, S., 1991, Depositional bias and environmental change-important factors in sequence startigraphy. Sedimentary Geology, 70(1991), 109-130.

Yergök, A.F; Akman, Ü; iplikçi, E; Karabıyık; Keskin i; Mengi, H; Umut, M; Armağan F; Erdoğan, K; Kaymakçı, H; and Çetin A.F., 1987, Batı Karadeniz Bölgesinin Jeolojisi: MTA Rap.,No., 8273 (unpublished), Ankara.

PLATES

**PLATE-I**

Fig. A- Partly preserved fractures on the surface of glauconitised quartz grains (S.E.M. view).

Fig. B- Glauconitised intraclast grain (S.E.M. view) (Zonguldak region).

Fig. C- Mature glauconitisation of argillaceous pellet with rosette structure (S.E.M. view) (Zonguldak region).

Fig. D- Immature glauconitisation of alkaline feldspar grain (S.E.M. view) (Zonguldak region).

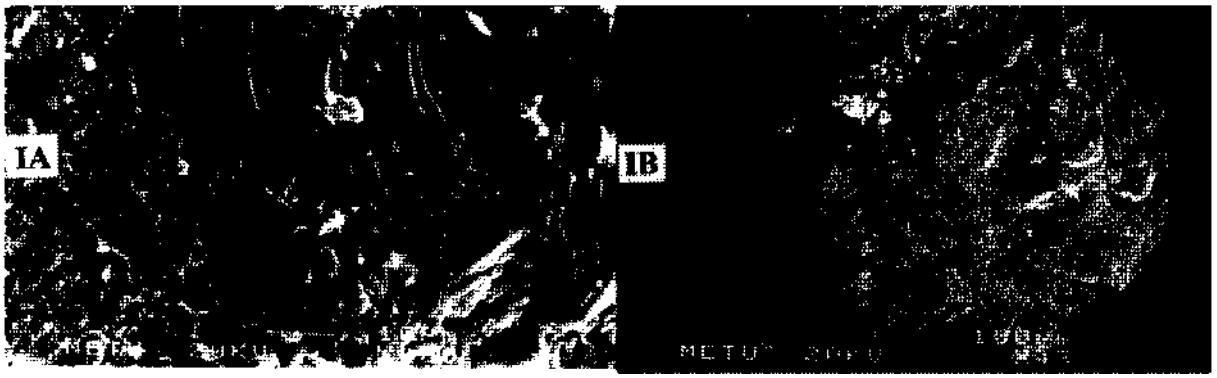
IA
IB

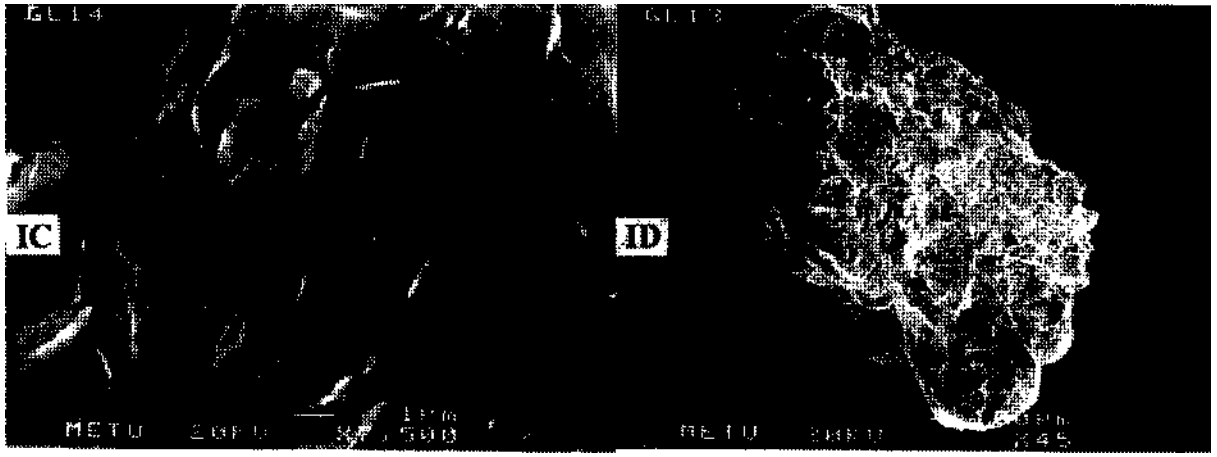
IC
ID

**PLATE-II**

Fig. A- Authigenic glauconies developed within the crust of coral organism (S.E.M. view). Glauconies filled all micro cavities on the crust (Kastamonu region).

Fig. B- Enlarged view of Fig. A (S.E.M. view).

Fig. C- Completely glauconitised reef fragment. Dark green coloured mature glaucony with high $K_2O$ ratio (Kastamonu region).

Fig. D- Micro fractures on glauconitised surface. These may have developed with volume change which caused by expulsion of water during transformation from simectitic to illitic sturcture (S.E.M. view).

Fig. E- S.E.M. view of well developed glaucony crystals within a micro fracture in Fig. D. Micro cavity and fractures in glauconitic areas.

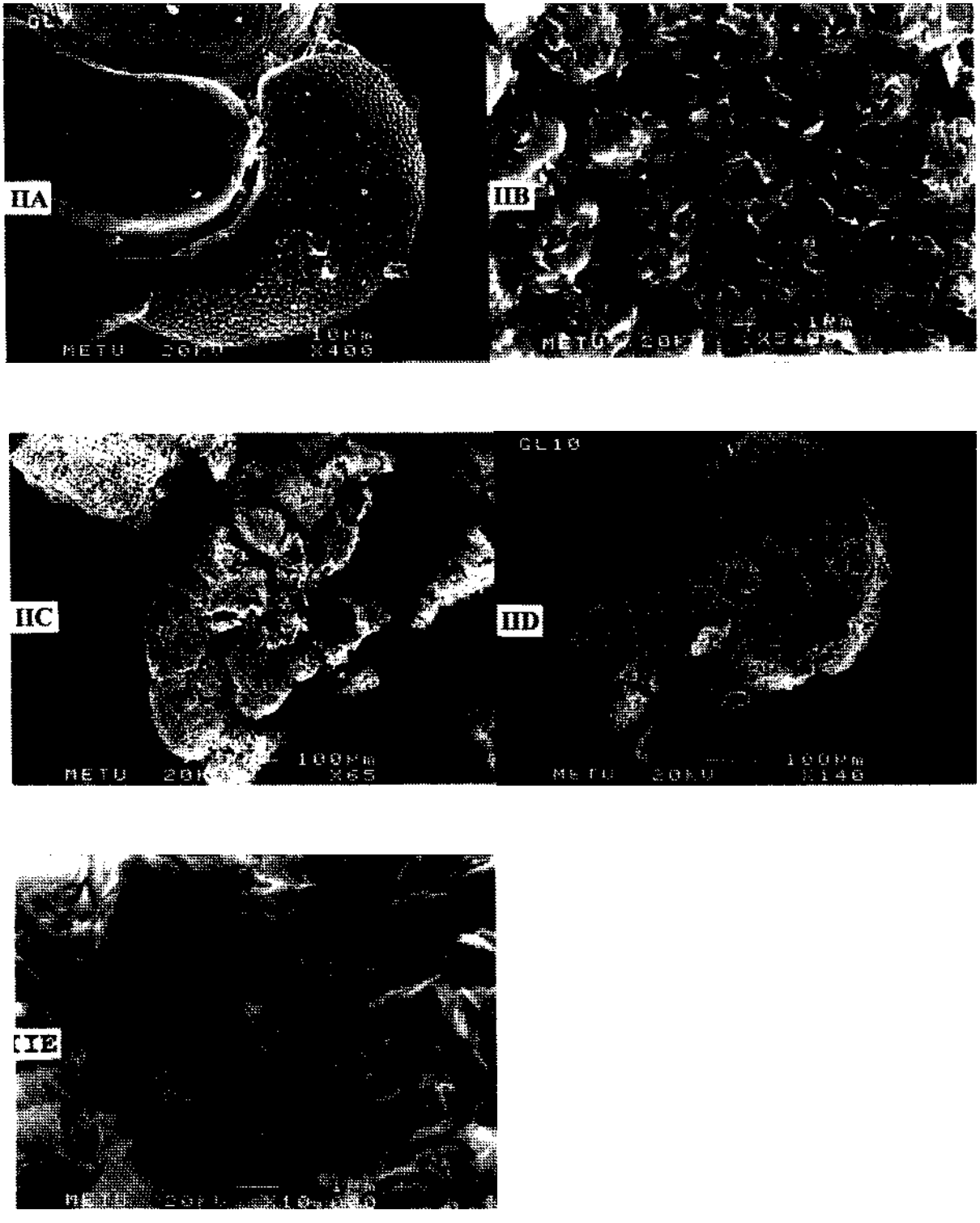
IIA
IIB
IIC
IID
IIE

PLATE-III

Fig. A- Mega cross beddings in glauconitic sand bars (Zonguldak-Devrek-Yörükoğlu Mahallesi, Gerze dere valley road cut).

Fig. B- Low angle small cross beddings in the sheet sand beds.

Fig. C- Glauconitic hardgrounds with glaucony filled trace fossils (Kastamonu region).

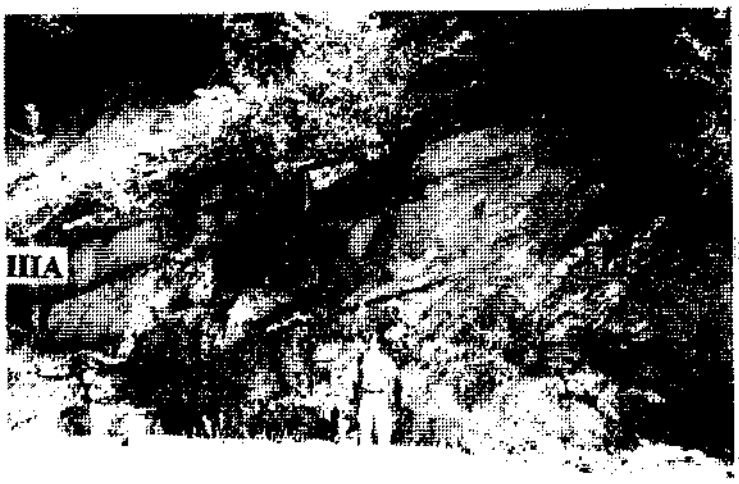
IIIA


IIIB


IIIC

**PLATE-IV**

Fig. A- Alternation of glaucony and quartz sand laminates. Carbonised plant remain painted the laminate black at the lower left corner of the photograph (Kilimli region).

Fig. B- Glauconitic sand bar and low angle cross bedding (Zonguldak-Güdüllüköy road cut, 300 m far from Güdüllü village).

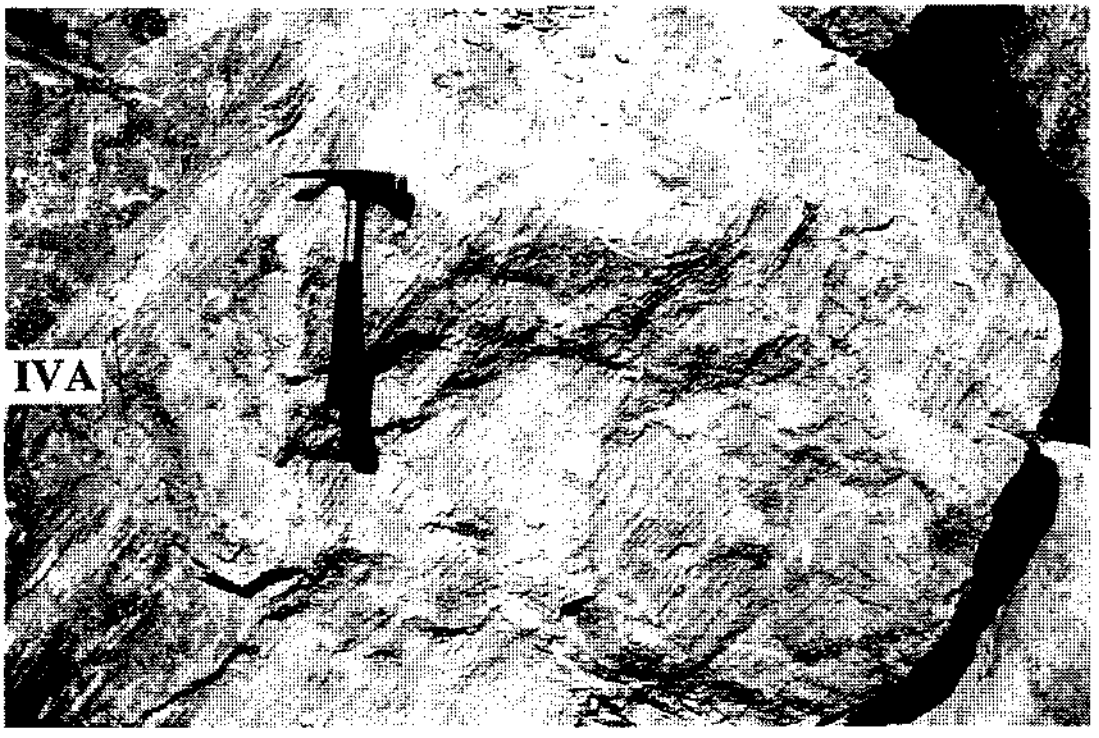
IVA


IVB

Mineral Res. Expl. Bul., 122, 23-30, 2000

# GEOLOGY AND ORIGIN OF THE ALBITE DEPOSITE OF THE ÇİNE SUBMASSIF, SOUTHERN MENDERES MASSIF (SW-TURKEY)

AN UYGUN* and Ahmet GÜMÜŞÇÜ**

ABSTRACT.- Around 250 albite occurrences are recorded in the Cine Submassif that represents the southern part of the Menderes Massif, from where annually 1.7 million tons of Na-feldspar is produced. The study area is covered by the widespread exposures of the Pan-African Precambrian core-complex of the southern Menderes Massif. The albite deposits are mainly within the meta-pegmatites, located along NNW-SSE trending tectonic zones. In this study, the effects of the Alpine metamorphic and metasomatic events on the albitization process are discussed, and the importance of the younger intrusives within the Cine Submassif are emphasized. Moreover, the geometry, dimensions and petrologic properties of the albite deposits are explained and the quality of the various market products is documented.

## INTRODUCTION

It is noticeable that large production of albite at the southern part of the Menderes Massif has been obtained during the last ten years. This is also indicated by the fact that Turkey is now one of the leading feldspar producing countries in the world. Although the albite occurrences have been known since 1950, the earliest production towards the end of 1960's was mainly for the glass industry. Albite mining developed and production has increased in Çine-Milas-Söke-Yatağan-Karpuzlu regions since 1980's.

It is known that around 250 feldspar deposits are present in the region known as Cine Submassif. About 100 of these deposits are located within the area of which the authors company has the mining license. Since 1987, with the foundation of the company's production site in Milas, albite production capacity of 850 000 (650 000 tones of raw ore, 25 000 tones of grinded ore and 225 000 tones of flotation product) tones per year (t/y) has been achieved with the mining activities in the 15 quarries in the study area.

The presented results of this study includes the recent investigations of the authors in the recent years and include; remote sensing studies by satellite images, photogeology, fieldwork, prospecting, detailed geological mapping, drilling, trenching, and a series of geochemical work including technological studies. In this study, the authors aim to share their data and experiences with studies interested on regional and local geology related to. the albite exploration and production, and discuss the origin, geometry and mineralogy of the albite deposits, and the effects of these criteria on the quality of the products.

## GEOLOGY OF THE ALBITE DEPOSITS

The Menderes Massif in the western Anatolia is situated between Lycian Nappes in the south and the Neotethyan İzmir-Ankara belt in the north. The geological studies of the area since 1950's have been summarized by Candan and Dora (1998) in detail. According to these authors, Menderes Massif is mainly composed of a Pan-African basement called as the "core" and an overlying "cover" series of Early Paleozoic-Paleogene age. The "core" units are mainly composed of silisiclastic metasedimentary rocks, leptitic gneisses and migmatites of felsic volcanic origin, and metagranites and metagabbros which cut through these rocks. Within the metasedimentary cover units, carbonates are dominant at the top and silisiclastics at the bottom (Candan and Dora, 1998).

By the studies of Satır and Friedrichsen (1986), Hetzel and Reischmann (1996), and Candan and Dora (1998) the polymetamorphic history of the Menderes Massif can be summarized in two main periods;

a) A high temperature granulite - high pressure eclogite fades metamorphic event based on zircon age (~550 my) from Precambrian core,

b) A high pressure epidote / blueschist / eclogite facies metamorphic event based on Tertiary mica (43-37 my) ages.

The part of the Menderes Massif situated to the south of the Büyük Menderes Graben is known as the Cine Submassif. Albite deposits are especially widespread in the southern part of the Cine Submassif (Fig. 1). The rich albite deposits in the region were assigned for the first time by Graciansky (1965), who indicated the Karadere Belt of the present study as an

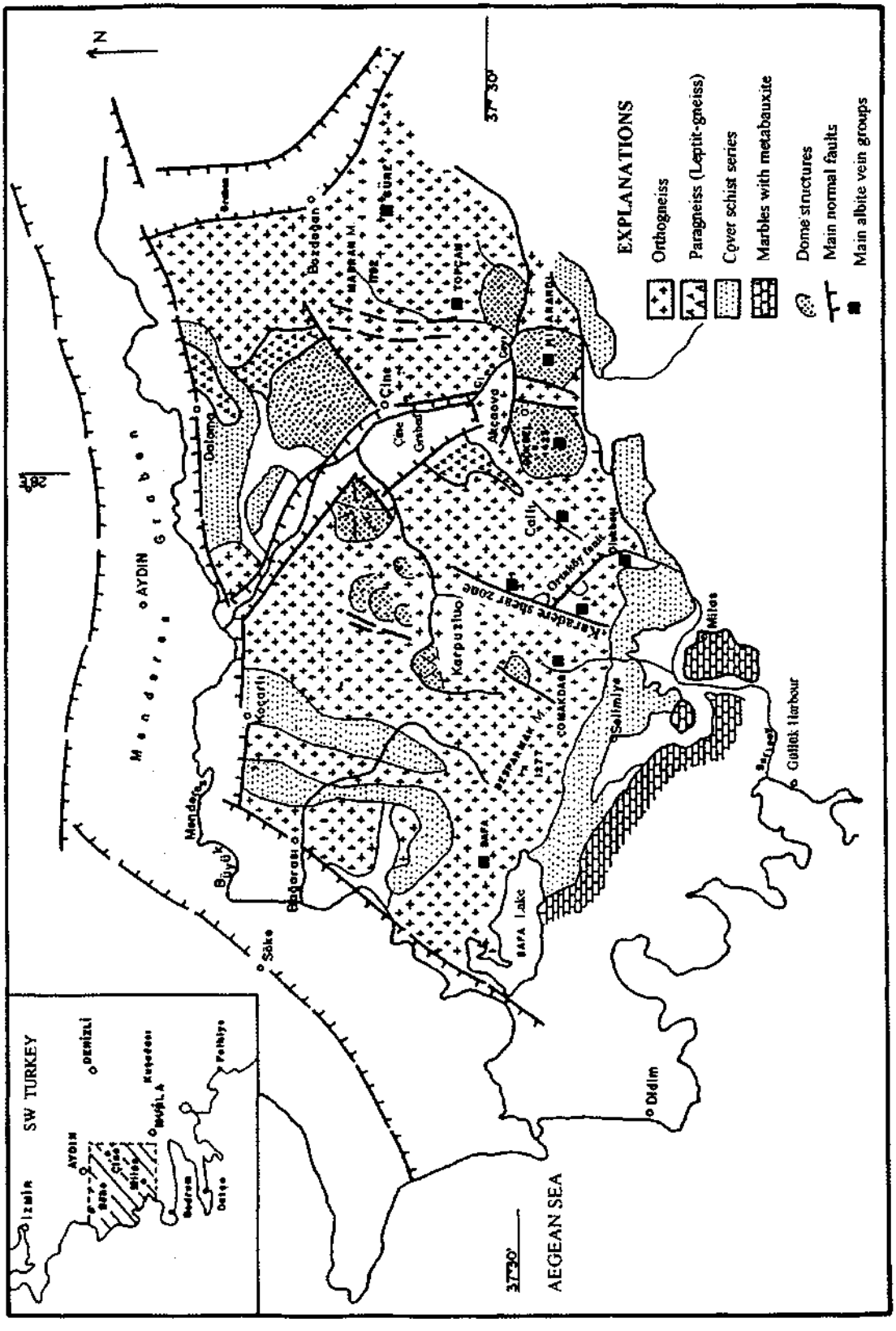


Fig. 1- Geological sketch-map of the Çine Submassif (Menderes Massif-SW-Turkey). The contacts of some units are from Candan and Dora (1998).

assemblage of "partly kaolinized, fine grained albite gneiss with muscovite". Beside the Çine Submassif, albite deposits are also known around Nazilli-Beydağ and Buldan in the north. However, they are not important in terms of their reserves and quality. Çine Submassif is composed of both coarse-grained augen gneisses and fine grained micarich gneisses. The augen gneisses with typical augen-shaped K-feldspar porphyroblasts display a well-developed granite morphology and are interpreted as metagranites due to their petrographic properties. The studies carried out on the satellite images of the Çine Submassif, that is generally indicated as a core complex by Bozkurt et al., (1993) clearly show the presence of at least 10 intrusives or dome-shaped structures (Fig. 1). The petrographic properties of these intrusive and dome structures can vary from one case to the other, e.g. the Gökbel Pluton to the west of Hisarardı that has different properties in terms of color and texture is characterized by K-feldspar veins with tourmaline and quartz rather than albite.

The albite occurrences that are concentrated at the southern part of the Çine Submassif are collected from west to east under the groups of Bafa-Çomakdağ-Karadere-Olukbaşı-Çallı-Gökbel-Hisarardı-Karpuzlu-Topçam-Güre, respectively, by conformity with their alignment along NNE-SSW trending main tectonic lines that are dominant in the region (Fig. 1). The Karadere Group, the largest one in the study area, is located on a 20 km long, N10°E trending shear zone, extending from north of Milas to east of Karpuzlu and includes important albite occurrences such as Kutay, Alakaya, Sarıkaya, Yassıtaş, Yumrutaş., Söbçayırı, Sarıkısık, Sarpdere, and Gökkaya deposits (Fig. 2).

The structural unconformity between the roughly E-W trending tectonic elements of the "cover schists" in the south and NNE-SSW trending ones of the."core" in the Çine Submassif is variably interpreted as disconformity (Şengör et al., 1984), a shear zone (Bozkurt et al., 1993), an intrusive contact (Erdoğan and Güngör, 1996) or a detachment fault. According to the authors' field observations, it is important to note that the albite occurrences are restricted only to the "core", although locally, both marginal mylonitic zones and intrusive contacts are observed between the "core" and "cover" units. Although local tectonic control may cause deformation of albite veins within shear planes or transversal/oblique fracture systems that are more or less perpendicular to main alignment or even formation of S-type folds at the margins of the mega-shear zones,it is certain that albite occurrences are mostly of intrusive character and align parallel to the dominating NNE-SSW structural trend in the study area.

The geological map of the Karadere region, prepared by the field studies and aerial photographs, includes all the important quarries and is presented in Figure 3. Distribution of the albite deposits in this part is also well conformable with NNE-SSW trending orientation of the main tectonic elements.

The albite deposits in the outcrops and within the quarries are observed as vein-type elongated masses. The width of the veins can vary from 2-3 m to 30-40 m. Although the length of the albite-veins are controlled by some faults and some gneissic enclaves, it reaches up to 600 m in Söbçayırı quarry and 1000 m as in Karadere vein. The margins of the deposits are generally marked by meta-granitic wall rocks with high angle contacts.

Except the NNE-SSW trending main albite veins, deposits nearly vertical or oblique to these veins are also present. For example, Asar tepe and Kocayer deposits are situated within a nearly E-W oriented fault system.

Locally, the albite bearing veins may have long extensions along their dip directions. For example, in the Söbçayırı quarry, the difference between basal elevation and the ore at the top of the quarry is 120 m. Moreover, a drill hole at the base of the quarry intercepted 85 m albite ore, indicating that the veins may have extensions down to 200 m.

In terms of reserve, the main albite deposits (e.g. Çukuroluk and Yanıktepe quarries in Çallı group) are formed within the void-spaces at the junctions of two main fault systems. Other albite deposits (e.g. Erendede quarry) seem to be small-scaled laccoliths or fillings along the axial closure of a recumbent anticline are also present.

All these observations, suggest that the aplite and pegmatites of the Pan-African granitic complex in Çine submassif were replaced by the present "albitites" as a result of anatexis, rejuvenation and metasomatism processes in the period of alpine deformation and metamorphism.

## MINERALOGY OF THE ALBITE DEPOSITS

"Each feldspar is different, if it is not, it is not a feldspar"

Mineralogical differences in the albitites of the Çine Submassif can be well explained with the above phrase of F. Laves which is at the beginning of the chapter on "Feldspars" in Tröger (1969).

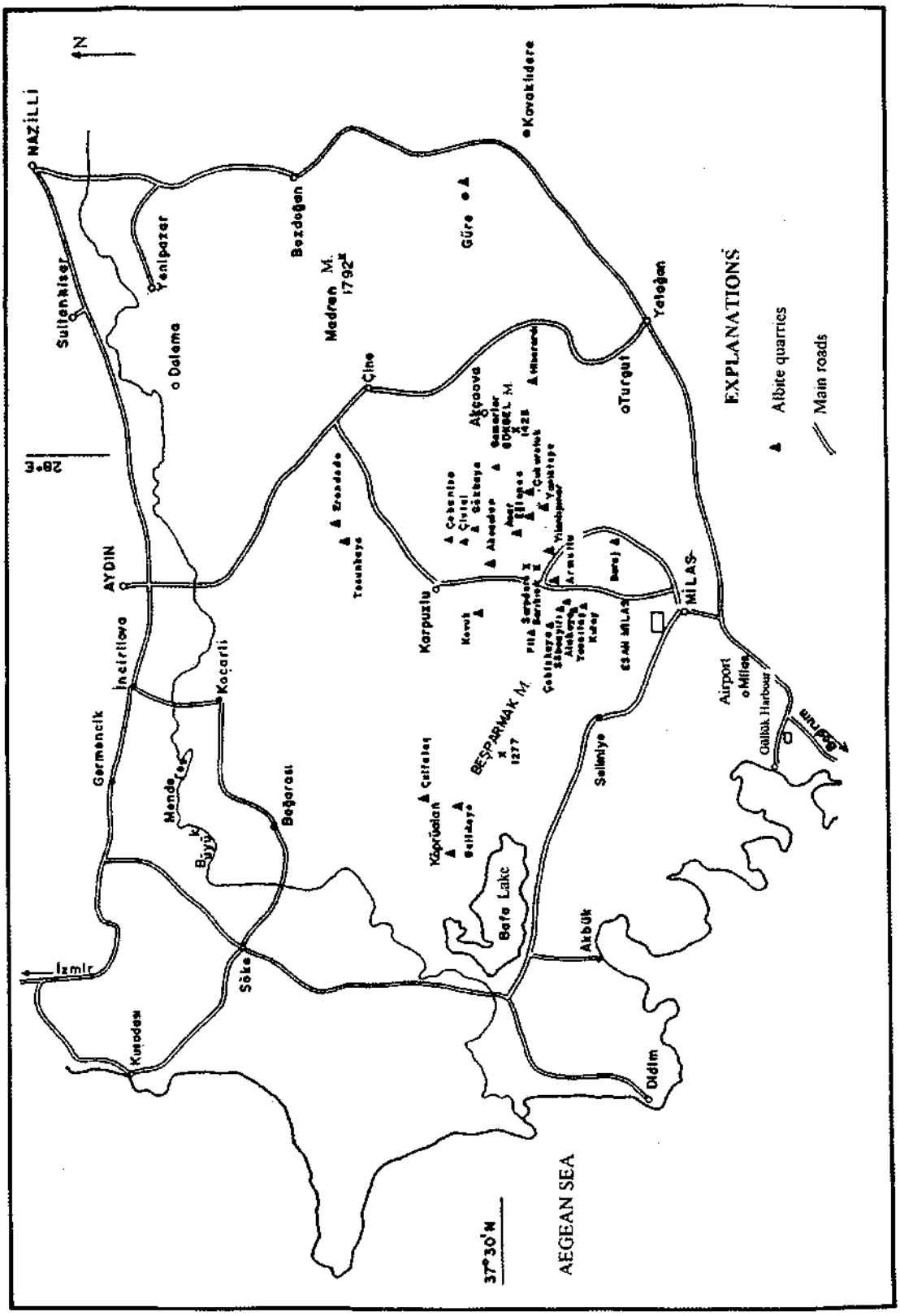


Fig. 2- Distribution of the albite deposits of Esan in the Milas-Çine region (SW-Turkey).

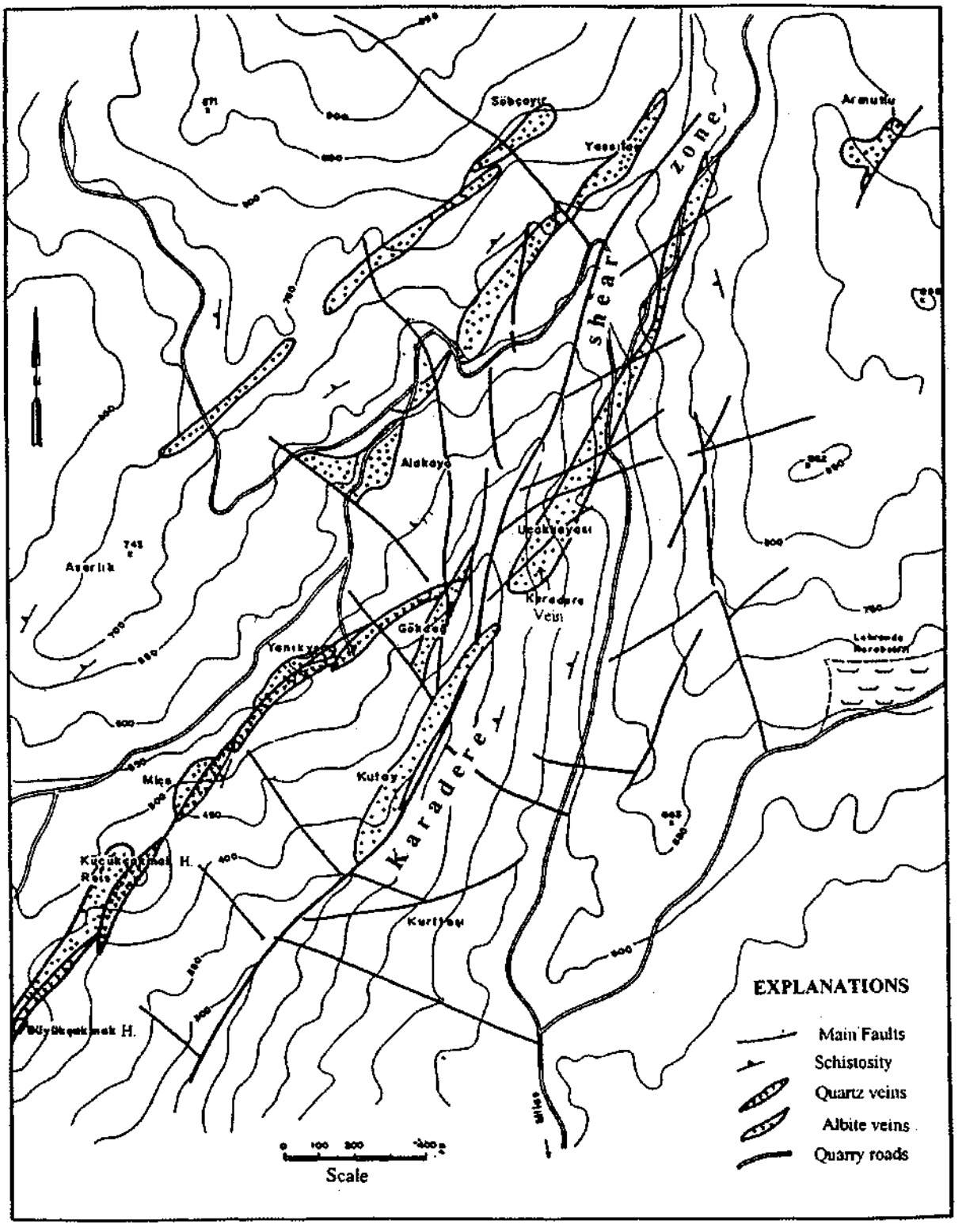


Fig. 3- Geological sketch-map of the Karadere shear zone and the distribution of the albite deposits.

Field observations, microscope studies, XRD and chemical analysis carried out on the aibitites shows that the main mineral phases are albite and quartz. The $Na_2O$ content of the bulk rock samples varies between 7-11 % in some, of the albite veins, whereas the modal analysis of the samples display maximum albite contents about 70 %, and quartz 25 %.

Albitites typically display blastomylonitic textures. Two different generations of albite are observed; a- coarse grained (~1 mm) the first generation albites representing relict magmatic phenocrystals with deformed and broken polysynthetic twining, and b- finer grained (100-300 m) second generation albites that are developed as a mosaic along the margins of primary phenocrystalls and have no twinning. In addition to the primary coarse quartz grains (0.5 mm average length), there are finer grained elongated fresh quartz grains of second generation, that surround the primary albite phenocrystalls (mortar texture) together with secondary albite, or fill up the fractures and hail the fractured portions of the porphyroclasts.

The other main mineral in the samples is perthitic alkali feldspar. It also resembles the primary magmatic porphyroclasts, is relatively coarse-grained (above 1 mm) and can be found as in the form of microperthite or filmperthite, rarely leuco- or cryptocrystalline perthite. Locally preserved microclines are also noticed from the samples taken from the Erendede quarry. In some samples, the amount of the perthitic alkali feldspar can reach up to 40 % of the whole rock. Consequently, the $K_2O$ ratio in these rock samples is relatively high. For example, in the Söke-Yeşilköy-Köprüalan quarry, the $K_2O$ amount of the bulk sample changes between 0.4 - 7.0 % and a special product (code E-22) with an average of 3 % $K_2O$ and 8 % $Na_2O$ is obtained from this deposit. In also Ballıkaya deposits, where perthite crystals reaching to 1.5 cm are observed the $K_2O$ or $Na_2O$ contents reach up to 5-7 %.

In terms of CaO content, the highest value detected is 2.13 % in an albite vein at Eğlencederesi. However, this value does not exceed the albite-oligoclase boundary in modal analysis.

Apart form these three main minerals, other phases observed under the microscope are mica (muscovite, biotite), rutile, titanite, zircon, apatite and rarely chlorite. Although, tourmaline, garnet and epidote are present in the wall rock, but they are not present in the albite veins.

Biotites are present in the form of yellowish-brown colored sheets, sometimes with rutile or zircon inclusions. The first phase biotites (niagmatic) are intensely deformed, recrystallized and chloritized at grain boundaries. As it directly controls the color of the product, the presence of biotite is a normally a negative factor for the quality of the albite. However, it could easily be removed by magnetic separation and flotation. It's presence may even turn to an advantage, as most of the rutile (another negative agent for the color of the product) is enclosed in biotite (e.g. aibitites of the Asar tepe quarry) and can be also easily removed from the system during mineral separation and flotation.

Muscovite is generally secondary and is in the form of thin, long lepidoblasts, that are formed along shear or schistosity planes. Very small (< 50 m) muscovite crystals are sometimes scattered within the cleavage planes of some of the albite grains (e.g. Kocayer and Eğlencederesi veins) and indicates the presence of two different albite generations in the rock. According to Göncüoğlu (1997, written communication) the "ghost" orientation that is also discerned in muscovites as in the second generation albites and quartz show that the deformation continued during recrystallization process. Moreover, the presence of shear planes that cut this "ghost" orientation is indicative for another late-stage brittle deformation phase postponing the main deformation/recrystallization event. The occurrence of muscovite can be partly related to the removal of K from K-feldspars during metasomatism.

Secondary chlorite rarely develops after biotite. However, the formation of secondary Mg-chlorite may have a positive effect for the albite products, as it can the originally unsuitable colors during the smelting. This is the case with the Güre albite deposits to the east of Cine. The presence of secondary Mg-chlorite within albites of Sardine Island of Italy is also described by Bornioli et al., (1995).

The most important components determining the commercial quality of albite are Ti minerals that directly effecting the firing color. The $TiO_2$ content within the "extra albite" is less than 0.13 %, and it is more than 0.25 % within the ordinary products that are qualified as "standard albite". The studied albites used for the flotation process contain $TiO_2$ values that range between 0.13 and 0.25 % and they are processed according to the grain size of the Ti-mineral (300 or 500 m ).

The Ti-minerals in the samples are mostly rutile, and sometimes titanite. Generally, the length of the prismatic rutile crystals ranges between 0.1 - 0.3 mm

and rarely exceeds 0.8 mm. Rutile, together with apatite, is mainly concentrated in the recrystallized part of the rock and is found together with fine grained albite and quartz between coarser porphyroclasts. As in the samples from the Erendede quarry, rutile grains sometimes do not negatively effect the smelting color very much, as they are found as tiny inclusions within the quartz grains. On the other hand, rutile together with zircon and apatite is concentrated along the gneiss and the albite vein boundaries (e.g. Armutdüzü, Sarıkısık, and Sarpdere to the north of Armutdüzü quarries), and in zones within the albitites, where the $TiO_2$ content reaches up to 7-8 %. These concentrations may be due to pegmatitic zonation or can also be evaluated as relicts of the metasomatism process. However, according to the recent observations these zones may also represent partly assimilated meta-sandstone enclaves with high heavy mineral contents. Transformation to titanite by metasomatism or formation of leucoxens as a result of alteration of rutile can be observed locally, however, in contrast to rutile, these secondary minerals do not effect the firing color of the product.

In addition to the primary rutile of pegmatitic - pneumatolytic (?) origin, zircon is in the form of very fine grains (> 0.1 mm), and apatite is in the form of hypidiomorphic crystals of 0.1 - 0.5 mm. The apatite content may locally exceed 3% (e.g. Yanıktepe quarry). Göncüoğlu (1997, written communication) differentiated two different zircon generations in the samples from Yassıtaş vein: An earlier, rounded and metamict one of xenolitic origin and a later idiomorphic, and transparent one directly crystallized from a melt.

In the Eğlencederesi vein, the occurrence with about 1 % calcite is the only accessory carbonate mineralization observed in albite deposits in the region. The other observed accessory minerals are arsenopyrite, pyrite, and hematite in the Armutludüzü quarry. This secondary mineralization contains up to 5 ppm gold.

## CHEMICAL PROPERTIES OF THE ALBITE PRODUCTS

In the previous chapters, it was mentioned that albite exploited from the quarries were divided in to 3 main types as "standard" "extra" and "floated". Apart form the main minerals, accessories such as perthite, titanite and their grain size are very important for the quality of the product and for its usage.

For this purpose, some standards including 9 product types have been developed for albite ores produced at Milas-Çine region by Esan. Chemical constituents for these albite products are summarized as follows:

The products of E-series are raw ores, and are named as E-10 standart, E21-medium, E-30 super, E40 super extra. E-22 is a product that contains perthitic feldspars with both alkalies. GG and FG are floated, 300 m sized ores, and are called as "glass" and "transparent frit" quality, respectively. SG and CG are the E-10 and E-30 qualities, grinded to 63 m.

**Table 1- Chemical properties of the albite products.**

| | E-10 | E-21 | E-22 | E-30 | E-40 | GG | FG | SG | CG |
|---|---|---|---|---|---|---|---|---|---|
| $SiO_2$ | 70.41 | 70.74 | 68.40 | 70.15 | 70.32 | 70.86 | 70.60 | 70.74 | 70.15 |
| $Al_2O_3$ | 17.75 | 17.92 | 18.35 | 17.90 | 18.10 | 17.90 | 18.30 | 17.92 | 17.90 |
| $Fe_2O_3$ | 0.14 | 0.08 | 0.08 | 0.08 | 0.07 | 0.04 | 0.04 | 0.08 | 0.08 |
| $TiO_2$ | 0.30 | 0.16 | 0.30 | 0.12 | 0.10 | 0.05 | 0.06 | 0.26 | 0.12 |
| CaO | 0.75 | 0.50 | 0.39 | 0.90 | 0.50 | 0.25 | 0.30 | 0.50 | 0.90 |
| MgO | 0.15 | 0.20 | 0.31 | 0.10 | 0.20 | 0.30 | 0.10 | 0.20 | 0.10 |
| $K_2O$ | 0.40 | 0.40 | 3.32 | 0.40 | 0.40 | 0.30 | 0.30 | 0.40 | 0.40 |
| $Na_2O$ | 9.50 | 9.50 | 8.18 | 9.75 | 9.82 | 10.00 | 10.00 | 9.50 | 9.75 |
| AK | 0.60 | 0.50 | 0.50 | 0.60 | 0.50 | 0.30 | 0.30 | 0.50 | 0.60 |

## RESULTS

The Çine Submassif is a Pan-African-Precambrian ortho/paragneiss complex, and includes 10 concentric or radial intrusive dome structures that can be differentiated on the satellite images. According to the field and petrological data it is suggested that the albite deposits along NNE-SSW trending tectonic zones in the Çine Submassif are primary aplites and pegmatites of the granitic core rocks. However, generation of the albites is not a simple process and it must include different stages such as anatexis, rejuvenation and metasomatism related with the main metamorphic event during the alpine deformation.

Mineralogically the albite deposits also include two different generations of albite and quartz. Especially, the primary (magmatic) perthitic feldspars were deformed and altered during metamorphism and metasomatism, respectively. The formation of secondary albite and quartz hailed the deformational fabrics. In the albites of Sardine Island of Italy, it is known that K-feldspars and plagioclases are replaced by hydrothermal albite and quartz during metasomatism (Benedusi and Bornioli, 1997).

That no albite occurrences are reported from the northern part of the Menderes Massif but only in the south may depend on the alkaline character of the orthogneisses in the Çine Submassif as well as on a late alkaline-metasomatism related to the alpine rejuvenation of the core rocks. Some other veins within the same tectonic system (at Gökbeldağ and around Madrandağ regions) with small size K-feldspars with tourmaline and long quartz grains may be interpreted as hydrothermal in origin.

In addition to the petrological studies of the albites and different intrusive bodies in the Çine Submassif, the study of these occurrences by geochemical methods may help to interpret their geneses and to discover new deposits.

## ACKNOWLEDGMENTS

The authors thank ESAN for the permission to publish their data. Prof. Dr. Cemal Göncüoğlu is acknowledged for some petrographic-petrogenetic interpretations and valuable suggestions on a former version of the present paper. Mr. i. 0. Yılmaz kindly translated the manuscript. Thanks are also to the anonymous reviewers that helped to improve the manuscript.

## REFERENCES

Benedusi, S., and Bornioli, R., 1997, Maffei in Sardinia. A feldspar producer halfway between the ceramic districts of Italy and Spain: Euromin. 97, Ind. Minerals and Markets, Barcelona.

Bornioli, R.; Marini, C. and Mauro, G., 1995, The sodium feldspar deposit for unglazed stoneware at Ottana (Central Sardinia-Italy) Ceramics, 147-156.

Bozkurt, E.; Park, G.R. and Winchester, J.A., 1993, Evidence against the core/cover interpretation of the southern sector of the Menderes Massif, West Turkey, Terra Nova, 145-151.

Candan, O. and Dora, O.Ö., 1998, Menderes masifinde granülit, eklojit ve mavişist kalıntıları: Pan-Afrikan ve Tersiyer metamorfik evrimine bir yaklaşım: Türkiye Jeol. Kur. Bült., 41/1, 1/35.

Erdoğan, B., and Güngör, T., 1996, Menderes masifi güney kanadı boyunca çekirdek örtü ilişkisi: 49. Turkiye Jeoloji Kurultayı Bildiriler Kitabı, 78. Ankara.

Graciansky, P.de., 1965, Menderes masifinin güney kıyısı boyunca (Türkiye'nin SW'sı) görülen metamorfizma hakkında açıklamalar: MTA Bült., 64, 8-21.

Hetzel, R. and Reischmann, T., 1996, Intrusion age of Pan-African augen gneisses in the southern Menderes Massif and the age of cooling after Alpine ductile extensional deformation. Geological Magazin 133, 565-572.

Satır, M. and Friedrichsen, H., 1996, The origin and evolution of the Menderes Massif, W-Turkey: A Rb/Sr and Oxygen isotope study. Geol. Rundschau, 75/3. 703-714.

Şengör, A.M.C.; Satır, M. and Akkök, R., 1984, Timing of tectonic events in the Menderes Massif, Western Turkey. Implications for tectonic evolution and evidence for Pan-African basement in Turkey, Tectonics, 3/7, 693-707.

Tröger, W.E., 1969, Optische Bestimmung der gesteinsbildenden Minerale, E. Schweizerbartsche Verlagsbuchh., Stuttgart.

Mineral Res. Expl. Bul., 122, 41-50, 2000

# COPPER AND ZINC OCCURRENCES AT KILISE TEPE, MURGUL AREA, NE TURKEY

Radule POPOVIC*

ABSTRACT.- The copper occurrences in the Murgul area had been known in ancient times, but their systematic exploration and exploitation began at the end of nineteenth century, and later in twentieth century they had been continued and intensified. The Kilise Tepe showings argue, on the basis of slag material, show that there had been provided a primitive exploitation, judging from high copper (even 4%) contents. Otherwise, the Kilise Tepe district is built up mostly of volcanic and volcanic-sedimentary rocks units, chiefly of rhyolitic composition. These formations are injected along faults by minor quartzdiorite bodies, commonly in from of sills. In this field 12 copper and zinc-copper occurrences have been registered. The most important copper mineralizations occur in lower stratigraphic level, generally related to the argillized breccious zone with chalcopyrite fragments ("oreclasts"), dropping from the loose rock material with copper contents up to 20%. This situation is characteristical for the source part of the Kopitvan dere stream. On the other side, a stratiform ore body consisting around 2% copper takes place in the source part of Skutari Dere. It is supposed that these occurrences are continuation of the Anayatak - Çakmakkaya mineralization zone. In the same zone the mineralized rhyolite volcanic breccia appears as well, grading over 0,2% copper, where ore reserves of 10-20 million tons of the low grade copper ore are to be expected. The next occurrences are represented by mineralized quartzdiorite sills where zinc is predominant, grading from 1% to 10% and with copper as accompanying metal, showing contents from 0.1% to 0.5%. Finally, on the Kilise tepe - Kopuk zone, a belt of molybdenum geochemical anomalies is distinguished, with Mo contents ranging from 200 -1000 ppm. The potential of Kilise tepe area, taken as a whole, is considerable: 1- KiliseTepe mineralization could to be a continuation of the Anayatak - Çakmakkaya ore zone, and 2- in deeper levels quartz diorite sills, a mineralized quartz diorite could be expected maybe related to the porphyry type of the zinc and copper sulfide ore.

Key words: Copper, zinc, ore occurrences, volcanite, quartzdiorite, Kilise Tepe, Kopitvan Dere, Skutari Dere, Murgul, Turkey.

## INTRODUCTION

The copper ores at Minor Caucasus and so in the Murgul district are known in times before Christ (being known in ancient times), but the oldest systematic mining activity had dated from the medieval age. However, explorations and mass exploitation began near the end of nineteenth century and continuously (lesser breaks) have lasted till the present days. At the beginning of twentieth century as smelter was erected in Murgul, being operative till the middle of seventies.

If the Anayatak - Çakmakkaya localities are considered as two separete ore deposits (500 m apart from each other) it could be said that in the nearest surroundings of Murgul there are four copper deposits which have been subject of exploitation, (Fig. 1) and more than 30 occurrences with low level of research workings. Limited studies among these are 12 occurrences in a larger Kilise tepe area, or more exactly, in the space between Kurtumele önü and Yeşil Tepe. .

According to available information, indication for the first mineralizations were registered by Buser (1970) in the Kopitvan Dere valley and then Stern (1971), Popovic (1972) and Pejatovic (1979). Buser (1970) observed a very intensive silicification and pyritization in the source part of the Kopitvan Dere stream,

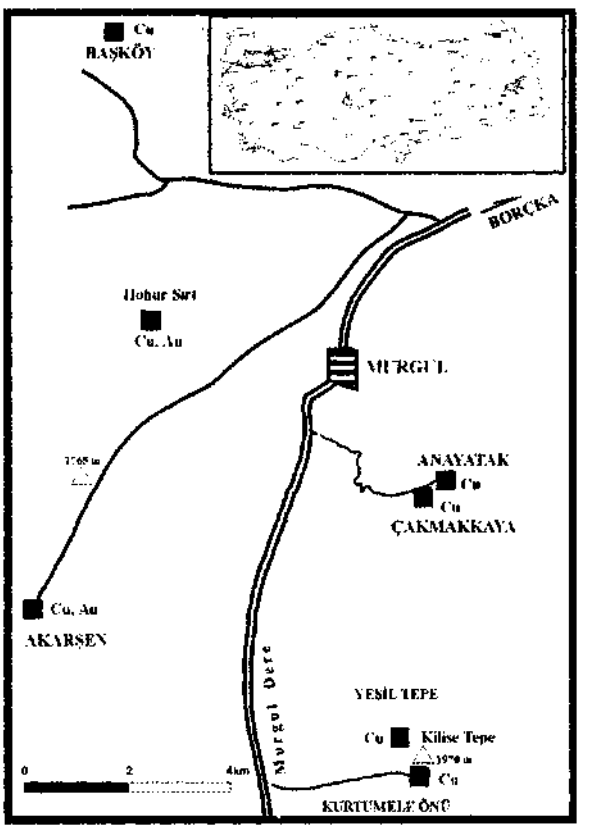


Fig. 1- Location map of the sulfid deposits in Murgul region (NE Turkey).

and in the torrential material of the stream itself they found numerous chalcopyrite fragments and pebbles with pyrite, later named as oreclasts. Although the terrain was covered by a detailed prospecting, including trenching (these workings were hindered by very steep slopes and practically impassable rhododendron vegetation without cutting), the search for the real source of chalcopyrite-pyrite fragments was not successful, except local augmentation of copper content and individual oreclasts in argilized zones. However, by prospecting and geochemical investigations, 10 copper and 2 zinc-copper occurrences as well as a zone with high molybdenum were discovered.

Descriptions about mineralizations mentioned above have not been published, except some basic informations, but taking into consideration a high potential of sulfide as a whole, it is of interest to attract attention of the broader public for further explorations.

Fig. 2- View to the southern slopes of Kilise tepe (dense intertwined rhododendron Trees with individual conifer trees are visible).

## PRINCIPAL GEOLOGICAL FEATURES

The Kilise Tepe surrounding is restricted to the spacious volcanic-sedimentary and volcanic complexes of the Murgul district. The oldest rocks are sandstones and tuffaceous sandstones, appearing in the southwestern sector, being, confined to a formation of the possible Upper Jurassic and Lower Cretaceous age, occurring in the Murgul Dere (Iskalka köprü) valley. Although they bear pyrite and weaker chalcopyrite mineralization, these are not of greater importance. Other formations are volcanic-sedimentary and volcanic in origin, whereas the intrusive rocks are quartzdiorites; the volcanites are mixed and difficult to be distinguished, especially in presence of submarine activity, followed at times by subaerial extrusions. These formations are of major importance, nevertheless if they are represented by rhyodacite, dacite and most commonly rhyolite flows, tuffs, agglomerates, breccias or redeposited, volcanic rocks, alternating with tuffaceous sandstones, conglomerates, quartzose sandstones and cherts (with Radiolaria - radiolarites and other microfossils). The mylonitization zones and tectonic breccias, as well as talus cones, covering large areas, appear as distinct geological bodies. Volcanites are generally Upper Cretaceous and Tertiary in age, and talus cones are practically contemporaneous. In the cones occur fragments and blocks of various sizes from the first size to blocks measuring twenty or more cubic meters. In the first moment one could have impression that, except talus cones, other rocks constitute an unique volcanic complex representing volcanic activity of variable intensity. These are, from one side, products of vigorous and explosive volcanism represented by flows, tuffs, breccias, alternating - from the other side with calm stages, producing deposition of sandstone and conglomerate beds and redeposited volcanic material. These stages are featured by radiolarites (cherts, Fig. 3).

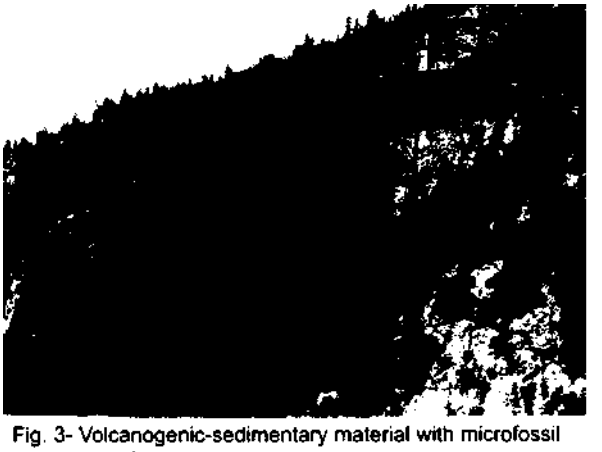

Fig. 3- Volcanogenic-sedimentary material with microfossil remains.

In later magmatic phases the volcanic and volcanic-sedimentary formations were faulted and cut by minor or major sills, dikes and other quartzdiorite bodies, generally of limited size, commonly injected along the fracturing structures. Above all, these intrusives represent only apical parts of a larger intrusive mass, directly related to the Tiryal Dağ - Tatos Dağları pluton

(batholith). It is of an importance to be noticed that among these rocks there is a younger differentiation product, determined as granite. Otherwise, all varieties, from diorites to granodiorites and quartzdiorites have been determined.

When the presence of individual formations is discussed, it should be stressed that in this terrain the both volcanic-sedimentary and sedimentary rocks are subordinated, compared with other volcanics. Rhyolitic rocks are the most abundant, followed by rhyodacites, and the least abundant are dacites and andesites.

It should be particularly stressed that te field as a whole had supported strong tectonical deformations, manifested as manifold fracturing of variable intensity, even accompanied by limited folding. Numerous ruptures are synchronous with volcanism, and some of them originated during relaxing stages of volcanism or after finishing that activity. The fact that in the redeposied (sedimentary) formations numerous folds are visible, testifies in favor of tectonics, probably having been occurred in Later Paleogene or in Neogene time.

It is necessary to notice that in a larger Kilise Tepe area the contact metamorphism is less well defined, although relatively numerous small quartzdiorite bodies are present. Only locally a weak cornitization and partial pyritization and silicification are observable, and some Cu-Zn mineralizations could be also restricted to the contact metamorphism, rapidly disappearing when drifted apart from the contact itself. Fractured structures often accompanied by intrusives, the size of intrusive bodies, degree of contact metamorphism, indicates a partly rather cooled magma, but the accompanied hydrothermal solutions could have an important role in formation of sulfide mineralizations. This has also been confirmed by the fact that volcanites were affected by repeated hydrothermal alterations, manifested by silicification and pyritisation as the most prominent ones, then by argillization, carbonatization (calcification), sericitization, epidotization and other. To those are to be added numerous Cu and Zn occurrences, following the mentioned alterations.

In frames of volcanic-sedimentary complexes the genuine cherts and quartzose sandstones, although are hard to be observed, have been still distinguished, representing - along with other rock types, an original petrogenic feature of this field. As an important charac-. teristic of this terrain, reflecting intensive disintegration of rocks, appear the erosional pyramids, rising up to 5 m and more above the botton covered by dense rhododendron forest, as visible in Figure 4.

Fig. 4- Erosional pyramid built up of silicified rhyolitic volcanites (source part of the Kopitvan Dere stream).

Observing the Kilise Tepe geological map (Fig. 5.) it is remarkable at the first sight that showings of copper and zinc mineralizations occur mostly along the faults, in higher parts of the relief. Some of these, however, appear as impregnation in rocks, but in such cases the fracturing structures generally control the mineralized areas. It should be mentioned too, as visible on the map as well (Fig. 5.), that a horizon - or better - a conglomerate formation composed of volcanite pebbles (being not agglomerate) has been distinguished, beneath it any occurrence of copper and zinc sulfides having not been registered to date. By that feature in a certain case the relative age of the Cu and Zn mineralization has been determined in the larger Kilise Tepe tract of land, including corresponding magmatism.

All copper and zinc ore occurrences could generally be divided into two groups: copper and zinc-copper mineralizations. It should be noted that all these occurrences are numbered, because in this area there are very little toponyms (these are Kurtumele önü, Kopuk, Kilise Tepe, Yeşil Tepe, Kopitvan Dere, Skutari Dere).

Going from the southeast to the northwest, i.e. from the Kurtumele önü peak, across the Kilise tepe - Kopuk ridge to Yeşil Tepe there are 12 Cu and Zn mineralizations, as well as three molybdenum geochemical anomalies. Some of them are grouped under the same number, so that all together they bear numbers from 1-9.

According to knowledge to date, as it has already been mentioned in part, all these showings are restricted to tectonic zones and porous rocks, such as pyroclastic material or volcanic flows, but also to the intrusive rocks, such as quartzdiorites. It is interesting that in samples from dacites copper and zinc concentrations have not been registered.

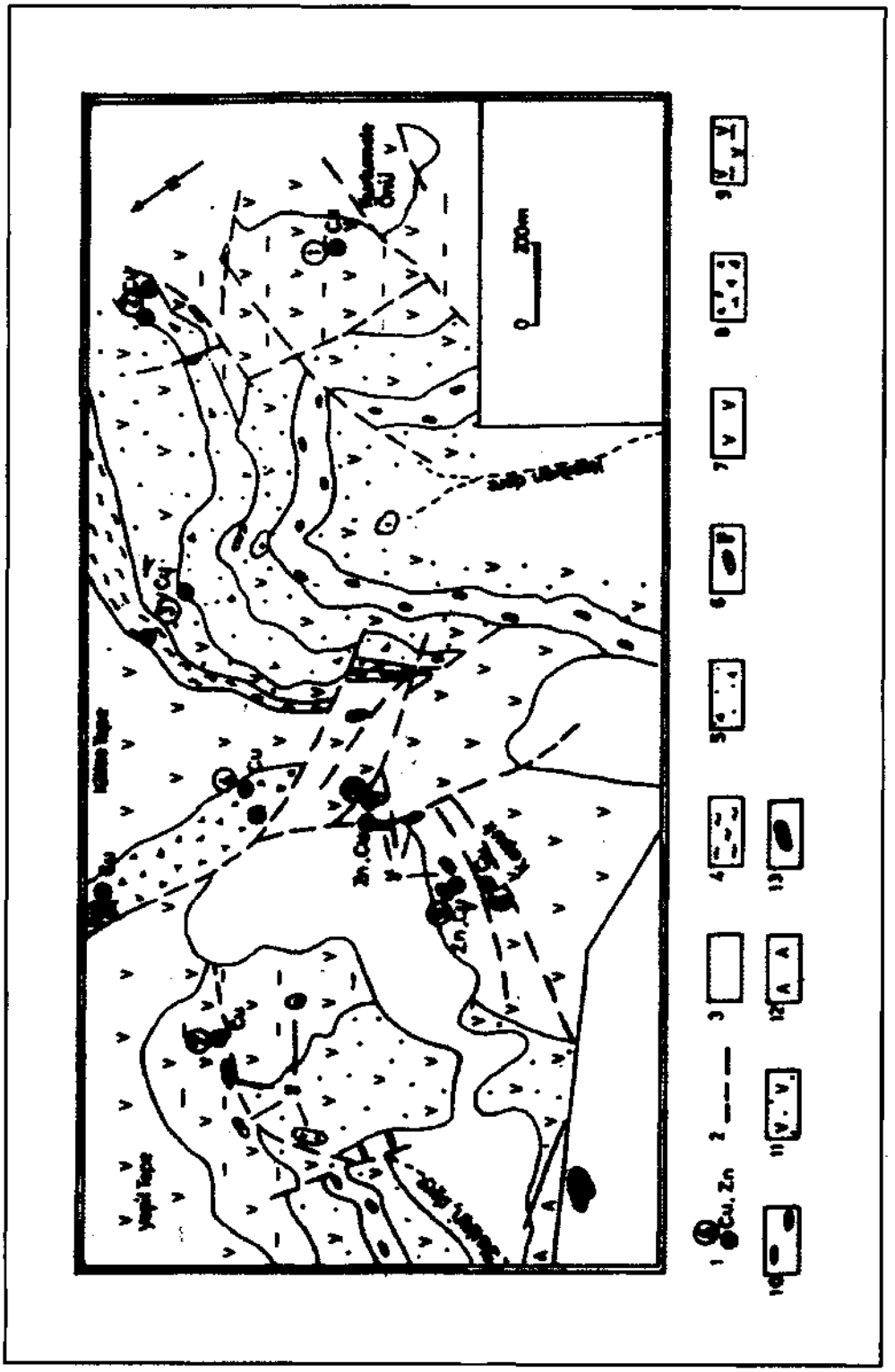


Fig. 5- Geological map of Kilise tepe. 1- Cu, Zn - ore occurrence, 2- fault, 3- rubble, 4- mylonitic zone kaolinized and pyritized, 5.- strongly alterated tectonic brccia, 6- quartzdiorite, 7- rhyolite and rhyolitic breccia, 8- strongly silicified and mineralized rhyolite volcanic breccia, 9- rhyodacite, rhyodacitic tuff, breccia and tuffaceous sandstone with chert and fossil remains, 10- tuffaceous sandstone and conglomerate, 11- rhyodacite, rhyodacitic tuffs, breccia and tuffaceous sandstone, 12- epidotized sandstone and tuffaceous sandstones, 13- sleg dump.

**Copper mineralizations**

*Occurrence No. 1.*- It is located on northwestern slopes of Kurtumele önü, at around 200 m from trigonometrical point, 1962 m of altitude. The minerali-zation occurs along a fault, observed at about 200 m, represented by pyrite and subordinated chalcopyrite, accompanied by limonite, mostly produced by pyrite oxidation. This is a vein 5 cm thick, visible along the mentioned fault for about 100 m. Chalcopyrite is irregu-larly distributed, judging from high variability of copper contents from 0,07% to 2%. In contrast to chalcopyrite, the pyritization is spread over the country rocks at 20 m in both fault sides. This is a nearly N - S trending fault, cutting the rhyolitic tuff.

At around 250 m easterly of this occurrence there is an outcrop of altered rhyolite with Cu-mineralization, showing grades of 0,3% Cu and 0,05% Zn.

*Occurrence No. 2.*- To the north-northeast from the occurence No. 1 extend rhyolitic coarse grained tuffs, with local appearences of cherts with Radiolaria (determined by D. Pesic, in Popovic, 1972). These tuffs are more or less silicified and pyritized. The occurrence No. 2 is at 400 - 500 m from the occurrence No. 1. These are actually two mineralized localities at a distance of around 80 m, being of similar features, thus being marked under a common number. This segment of the field is strongly technically fractured, and in a relatively limited area the six faults with various directions, cutting an old brecciated zone (probably tectonic in origin), highly silicified, kaolinized and pyritized, have been observed. Both outcrops of the Cu-mineralization are linked with this zone. At the northern contact of this zone is quartzose sandstone. From the other side, in the tectonic zone itself the appearences of contact metamorphism is visible, produced by quartzdiorite intrusions found in the surrounding of these mineralizations. For that reason mineralizations seem to be in direct genetic relation with mentioned minor quartzdiorite bodies. It is interesting to stress that the main ore mineral is chalcopyrite, whereas pyrite is subordinate and in that occasion chalcopyrite replaces pyrite, being younger of it. Beside these two minerals the paragenesis includes hematite (specularite) too, as well as rare sphalerite grains. Among secondary minerals chalcocite and rare malachite have been detected.Pyrite grains are commonly fractured, indicating their relative time of origin, compared with chalcopyrite, but the tectonic events as well, producig these breccia zones.

The Cu-mineralization is exposed over an area of about 10 $m^2$. Two channel samples both 0,2 m in length exhibited copper grades from 0,28% to 1% and zinc contents from 0,02% to 0,12%. With regard to general (vein-impregnation) feature, environment (tectonical breccia), geochemical limit (primary dispersion halo was investigated), this occurrence would not be interesting in particular, but being found in the same breccia zone as the occurrence. No. 3, it is considered that the zone as a whole should be systematically studied, cosidering the large dimensions of tectonic zone and that it includes quartzdiorite bodies, to which these mineralizations are generally related.

*Occurrence No. 3.*- Resembling to the previous one, three mineralizations are present here as well, one being represented only by chalcopyrite fragments as ore clasts. All of three mineralizations are located in the source part of the Kopitvan Dere stream. This is actually a highly silicified and pyritized zone, affected by intensive oxidation, related to the same tectonic zone as the occurrence No. 2. It should be stressed in particular, as visible on the map as well (Fig. 5), that at southern and southeastern slopes of Kilise Tepe two tectonic zones have been distinguished: one represented by mylonite and the other by silicified breccia. These arbitrarily estimated two zones are separated by the Rhyolite Volcanic-Sedimentary Formation, being reduced in southeastern parts by joining of both zones into a single zone. On the basis of such a statement it has been adopted opinion that this is the same single zone of considerable dimensions in all directions. In its upper part have been registered one and in the lower part two copper mineralizations. However, the geochemical anomalies of primary dispersion haloes are to be focussed, in which the copper grade is over 500 ppm; in such a way five to six or probably more Cu-mineralizations could be considered.

At 300 m to the southeast of Kilise Tepe an occurrence of Cu - mineralization was found in mylonite. The sampling was done by partial trenching and in a 1 m long channel sample a copper grade 0,43% was registered; in another sample at about 15 m to the south from the trench the copper content in a 0,5 m long sample was 0,23%. In both samples the zinc contents were less then 100 ppm. Otherwise, in this mineralization pyrite is principal and almost unique mineral, beside some subordinate chalcopyrite. The lower part of the tectonic zone, accompanied by strong silicification, pyritization and oxidation, was also trenched, but only individual fragments of the chalcopyrite ore were

found, showing 17,90% Cu. These are fragments of chalcopyrite-pyrite mineralization with zinc and lead grades less than 100 ppm. Unfortunately, we could not find the source of these fragments (oreclasts), thus cosidering that in the tectonic zone a larger orebody was fractured, and by motions along the zone the fragments (oreclasts) were brought into the contemporaneous erosional level. This assumption could further envisioned the Volcanic-sedimentary formation as well, taking place in the footwall part of tectonic zone, considering that it has existed a stratiform orebody, which is tectonically cut, providing the mentioned ore fragments. But this is only an assumption. It should be also added that at 300 m to the west a weak copper mineralization grading 0,08% Cu, and about 100 ppm or lesser zinc and lead, had been detected. It is of an importance to be noticed that this tract of land (easterly from the Kilise Tepe - Kopuk ridge) is depleted in zinc, and copper is practically the only metal (excluding iron) showing increased contents. Investigation of mineral composition of Cu - mineralizations in the source part of the Kopitvan Dere stream have indicated that chalcopyrite and pyrite are the most abundant ore minerals, concerning chalcopyrite as dominating in oreclasts, and in all other cases pyrite is leading ore mineral. It is interesting to be noticed that in cases when pyrite is chief mineral, chalcopyrite occurs in it along fissures and in some cases hematite is observable as well. Covelite and limonite as secondary minerals are constantly present. The size of pyrite grains are very variable, ranging from microscopic dimensions to 0,5 cm in diameter, exhibiting octahedron and pentagonal dodekahedron as the most common forms.

*Occurrences Nos. 4 and 5.*- Both of these occurrences are related to the same silicified rhyolitic volcanic breccia, gray-violet in color, occurring on western slopes of Kilise Tepe. This mineralized breccia zone of northern trending is more than 600 m long and around 140 m wide (real thickness is not known). From the western side it is bound by a fault zone and it grades easterly into Formation of rhyolite and rhyolitic breccia.

In view of exceptionally inaccessible and impassable terrain, in the breccia only three outcrops of Cu mineralizations have been registered (two exposures in the southern part are assigned as occurrence No. 4 and the No. 5 is located in the northern part). This breccia is subdivided as an individual geological body or formation, with regard to the strong silicification, pyritization and Cu - mineralization, compared with the other part of Formation of rhyolites and rhyolitic breccia.

Estimation of metal contents had been done at place assigned as occurrence No. 4 by spot sampling (samples are 0.2 m in length), being not possible to make a systematic sampling of such a large mass of the mineralized rhyolitic volcanic breccia. The eastern mineralization exhibited 0.2% Cu and the western one, situated at 150 m far from the first one 0.1% Cu. It is interesting to be emphasized the molybdenum anomaly for 500 ppm Mo, discovered by geochemical investigations, which could be characterized as Mo - mineralization, but molybdenite has not been detected by explorations to date. In-that way, molybdenum would not be taken into consideration, nevertheless that such anomalies even of higher metal contents had been registered in other parts of western slopes of the Kilise Tepe - Kopuk ridge.

The Cu - mineralization itself is situated along a fault zone, occurring near the contact of this rhyolitic breccia with the principal Formation (Fig. 5). The dominating ore mineral is pyrite, accompanied by rather subordinated chalcopyrite!. The most abundant nonmetallic mineral is quartz, which is younger tham pyrite and chalcopyrite.

On the northern slopes of Kilise Tepe an exposure denoted as occurrence No. 5 is located at 500 m north of outcrops marked under No. 4. This is, however, the same silicified rhyolitic volcanic breccia where the showing No. 4 has been registered. This zone continues to the north, but unfortunately it was impossible to follow it to its very end because of rough topography and missing of corresponding topographic maps. The mineralized exposure 5 x 3 m in size was sampled by trenching, forming a 0.5 m deep and 3 m long cut by blasting, where an 1.5 m channel sample (supposing the homogenity of mineralization) was taken, exhibiting copper content 0.21% and zinc 0.1%, with only traces of lead (70 ppm).

The ore paragenesis constitute pyrite (the most abundant), then chalcopyrite, sphalerite and sporadic galena. The crystallographic form of pyrite is here also cube and pentagonal dodekahedron as in the Anayatak orebody.

If taken into consideration the lithological environment appearence figure of Cu - mineralization (stockwork-impregnational), ore paragenesis, crystallographic form of pyrite, it could be concluded that there is a cosiderable similarity between Cu - occurrences in this volcanic breccia and roof parts of the Anayatak deposit.

From the other side one has impression that these mineralizations and silicified (rhyolitic) breccia are related to the same zone in which the Anayatak and Çakmakkaya deposits are present.

As far as concerned dimensions of these volcanic breccias (more than 600 m in length and 150 m in width), despite the relatively low copper grades (from 0.1% to 0.21%), they still represent a certain potential, confirmed by the fact that beneath this ore zone occurs a massive Cu - orebody, marked as Occurrence No. 7.

*Occurrence No. 6.*- Is situated at northern flanks of the Kopuk hill (the peak altitude 1795 m). One part of it is linked with the fault zone, and the other occurs as impregnations in the space between this zone and another fault parallel to the first one, at a distance of about 60 m. (Fig. 6).

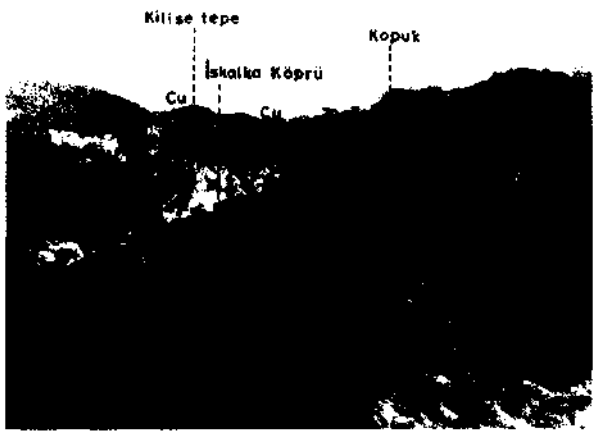


Fig. 6- Cu - Zn ore occurrences on the Kilise tepe - Kopuk ridge.

The mineralized fault zone is 1 m thick, whereas the ore vein, embedded in. it is 0.5 m in thickness, including pyrite and chalcopyrite as chief minerals, in some parts with traces of sphalerite and galena. The ore vein has been traced at only 10m, because of very steep slopes in the relief. In a 0.5 m long sample the contents of 0.3% Cu, 24 ppm Zn and 100 ppm Pb were found.

*Occurrence No. 7.*- Is located in the source part of the Skutari Dere stream, at about 700 - 800 m to the west of Kilise Tepe (altitude 1970 m). It occurs in "the. Volcanic-sedimentary Formation, composed of coarse grained rhyolitic and rhyodacitic tuffs, breccias and tuffaceous sandstones with radiolarian cherts. This is one of the most widespread formation, locally with higher pyrite impregnations (especially near the fault zones).

Here discussed occurrence of Cu-mineralization, occupies approximately the space between two nearly parallel faults. This is an evidently stratiform orebody showing thickness 2 m and length 5 m. The Cu-mineralization, appearing as impregnation grading into country rock, occurs within coarse-grained rhyolite, which is silicified, sericitized, chloritized and weakly argillized.

Two samples exhibited copper contents 1.8% and 2%, wheres zinc and lead grades were extremely low (less than 150 ppm Zn and 10 ppm Pb). The most abundant ore mineral is pyrite, accompanied by chalopyrite, covellite and limonite, these two of them as secondary minerals.

**Zinc and copper mineralizations**

*Occurrence No. 8.*- Is situated on western flanks of the Kilise Tepe - Kopuk ridge, forming with the occurrence No. 9 an unique zone, embedded in quartzdiorite, but they are distinguished as two localities being distanced at more than 200 m.

Volcanites of rhyolitic composition (rhyolite and corresponding breccia) are the main formation in this segment of the field, beside minor intrusions of mineralized quartzdiorites injecting rhyolites.

The mineralized zone trends parallel with the Kilise Tepe - Kopuk ridge, including the richer or weaker zinc mineralizations. The increased zinc contents occur not only in quartzdiorite, but also in volcanites. Taking into cosideration the zinc mineralization with Zn contents over 500 ppm, it constitutes a zone more than 400 m in length; the highest content in volcanites are to 0.1% Zn, whereas in quartzdiorite intrusions they range from 1% to 10%, usually accompanied by increased copper content, varying from 500 ppm to 0.5%. The occurrence No. 8 is characterized by mineralization of yellow sphalerite occurring chiefly in a sill, exhibiting thickness 0.5 - 2 m (Fig. 7) observed at 20 m in length. The zinc content is 1% and copper 0.5%; here are also remarkable secondary copper minerals, such as malachite, covellite and chalcopyrite. At about 40 m farther to the east occurs another quartzdiorite sill, also injected into a volcanite of rhyolitic composition, with an intensive pyrite-chalcopyrite mineralization, exhibiting grades of 1% Cu and 0.025% Zn (in a 0.2 m long sample). This mineralization is situated at the contact of quartzdiorite and rhyolite, represented by pyrite and chalcopyrite, with malachite and covellite as secondary minerals.

Fig. 7- Mineralized quartzdioritic sill (Y) in rhyolitic volcanites.

*Occurrence No. 9.-* Is located on the northern flanks of the Kopuk hill at 140 m from the peak or about 100 m northerly from the copper occurrence No. 6. This is also a mineralized quartzdiorite body, observed at about 4 m in length and 1 m in thickness. The quartzdiorite, being injected into rhyolite, as the previous ore occurrence, is simply soaked by sphalerite. This is metasomatic coarse grained sphalerite (grains are 3 mm in size) with little chalcopyrite of finer grains, replacing sphalerite. Only one sample was gathered from this locality, exhibiting 10% Zn, 0.05% Cu and 0.03% Pb.

This rock is microscopically determined as biotite microdiorite, affected by vigorous chloritization, calcification, sericitization, argillization and weaker silicification.

Observed as a whole, the space or zone respectively between occurrences Nos. 8 and 9 is focussed as an interesting zinc mineralization, accompanied by copper, being in direct association with quartzdiorite or with fracturing structures injected by small quartzdiorite bodies, probably forming channelways for posterior hydrothermal solutions bringing the described mineralization. These structures are generally of north - south to east - west trending.

All presented data may suggest an assumption on existence of a larger diorite to granodiorite mass as a possible bearer of the porphyry type copper and zinc mineralization.

## THE POTENTIAL ESTIMATION

According to available data, it could be considered that the tract of land between Kopuk to the southeast and Yeşil tepe to the northwest represents an area composed chiefly of volcanic and volcanic-sedimentary complexes, with subordinated minor quartzdioritic intrusive bodies, observed as:,exposures. On the basis of the appearance figure of quartzdiorite, lithological environment and mode occurrence of mineralization, four types of ore occurrences are to be distinguished (Fig. 8).

The first is vein type of Cu-mineralization with minor zinc and lead. These veins in all cases coincide with fault zones, exhibiting relatively high copper contents (to 2%).

The second type is represented by rich copper mineralization in from of "oreclasts" registered in the Kopitvan dere stream, as well as the occurrence No. 9, which could be supposed, according to preliminary information, to be stratiform mineralization. The both occurrences are embedded in volcanic-sedimentary complex, and from that reason it is logical the discovery of a stratiform copper mineralization to be expected.

The third type, considered as volcanogenic in origin, is placed in large masses of rhyolitic volcanic breccia. Two outcrops exhibited relatively low copper contents, but in deeper parts the more favorable contents, as for example over 0.5% Cu, could be expected, forming ore reserves at least 10 -20 million tons of arbitrary poor copper ore. Here it should be added that chalcopyrite-pyrite oreclasts in Kopitvan dere probably derive from the same zone in which the Anayatak - Çakmakkaya ore deposits are situated.

The fourth type is represented by zinc mineralizations accompanied by copper, occurring in minor quartzdiorite masses, injected along fault zones, bearing relatively high zinc grades (to 10% Zn). On the basis of such statement, as well as of copper and zinc contents in quartzdiorites (diorites/granodiorites) in other localities (for instance, on the Borçka - Artvin road, in granodiorites the contents of 0.25 Zn, 0.1% pb and 0.02% Cu have been found; on the road to Melo in the same rock the chalcopyrite and malachite have been observed) it could be supposed that in the deeper parts of Kilise tepe area exist larger granodiorite masses, the more so that to the south from this terrain occurs the large Tiryal Dağ - Tatos Dağları granodioritic pluton. In such a geologic situation the existence of the porphyry type of zinc and copper mineralization could be further supposed. In such a case the mineralized quartzdiorite bodies would represent only apical parts of a larger mineralized granodiorite mass.

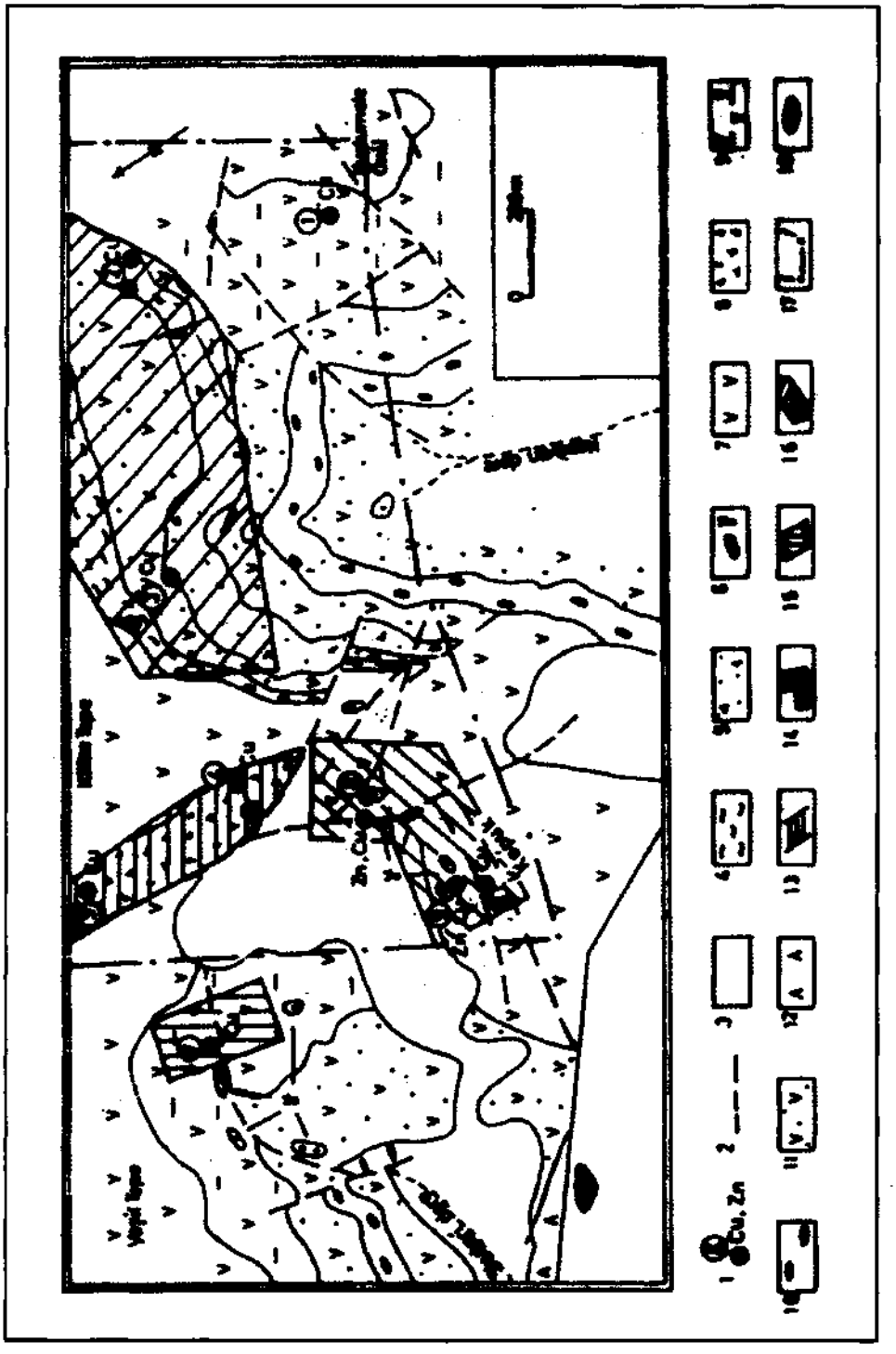

Fig. 8- Geological map of Kilise tepe and surrounding area showing potential mineralizations. 1- Cu, Zn - ore occurrence, 2- fault, 3- rubble, 4- mylonitic zone, 5- strongly alterated tectonic breccia, 6- quartzdiorite, 7- rhyolite and rhyolitic breccia, 8- strongly silicified and mineralized rhyolite volcanic breccia, 9- rhyodacite, rhyodacitic tuffs, breccia, and tuffaceous sandstone with chert and fossil remains, 10- tuffaceous sandstone and conglomerate, 11- rhyodacitic tuff, breccia and tuffaceous sandstone, 12- epidotized sandstone and tuffaceous sandstone, 13- volcanogenic type of Cu-mineralization, 14- vein type of Zn-Cu-Mo - mineralization, 15- stratiform type of Cu mineralization, 16- chalcopyrite oreclasts in tectonic zone, 17- area where is expected porphyryc type of Cu, Zn sulfide mineralizations, 18- sleg dump.

This (Zn-Cu) type mineralization is younger than Cu - minaralizations in the Kopitvan Dere stream and in the source part of the Skutari Dere stream, which are linked with older volcanic activity.

Beside the aforementioned, it should be noticed that along the western part of the Kilise Tepe - Kopuk ridge a prominent zone of molybdenum geochemical anomaly has been distinguished, reflecting primary dispersion haloes, exhibiting molybdenum contents to 1000 ppm. This zone is running along with zinc and copper occurrences, thus it could be related to the quartzdiorite bodies. However, if molybdenite or any other molybdenum mineral has not been detected so far, it cannot be more seriously discussed as a Mo-mineralization, although content of 1000 ppm are of economical importance.

Finally, in favor of considerable Cu and Zn potential of this district a slag dump has been found at 600 - 800 m to the west of Kopuk, covering an area of about 200 $m^2$, with visible thickness more than 1 m the slag fragments are stained with malachite and covellite. The chemical analysis of this slag exhibited following contents: 4% Cu, 0.6% Zn and 0.04% Pb. According to these records, first of all the high copper grades, as well as the visible secondary copper minerals, it is evident that the very rich ore was treated by primitive method, leaving much copper in the slag. It is not known the origin of ore and who exploited it, but discovery of rhyolite fragments in the slag points out the same lithological medium as in source part of the Skutari Dere stream. Beside these facts, it is evident that the ore was not transported uphill from the lower parts of the field even that there exists a deposit, neither from the tract of land easterly of the Kilise Tepe - Kopuk mountain ridge. It is logical that the smelted ore derived from the field sector west of the Kilise Tepe - Kopuk ridge.

## CONCLUSION

From the aforementioned, it is evident that the source part of the Kopitvan Dere and the field sectors trending westerly of the Kilise Tepe - Kopuk mountain ridge are considerable promising for discovery higher copper and zinc concentrations. For that reason the continuance of systematic investigations and explorations is suggested, taking into account the fact that this district represents a continuation of the Anayatak - Çakmakkaya zone, even more so that between these two deposits from one side and Kilise tepe ore occurrences from the other side, occur mineralizations in the Lebiskur dere valley as well, actually cutting the Anayatak - Çakmakkaya - Kilise Tepe ore-bearing zone. The unique character of this zone is proved by numerous identity features of ore deposits and occurrences along it.

*Manuscript received September 30, 1999.*

## REFERENCES

Buser, S., 1970, Geologie der Umbegung des Kupfergwerke, Murgul. MTA Fond of Geological Documentation, Ankara.

Pejatovic, S., 1979, Metallogeny of the Pontide-type Massive Sulfide Deposits: MTA Special Ed, No 177, p 98, Ankara.

Popovic, R., 1972, Report on detailed Geological Mapping (1:2000), Geochemical Prospecting and Researching of the Ore Occurrences in the Kilise tepe (Murgul) locality: MTA Fond of Geological Documentation, Ankara.

Stern, I., 1971, Yugoslav Jeologlar ekibi tarafından Murgul-Akarşen-Başköy (Türkiye) bölgesinde 1970 yılında yapılan jeolojik çalışmalar hakkında Rap., MTA Fond of Geological Documentation, Ankara.

Vujanovic, V., 1972, Determination of polished section from Kilise tepe in Popovic's Report, 1972: MTA Fond of Geological Documentation, Ankara.

Mineral Res. Expl. Bul., 122, 31-39, 2000

# REGIONAL METAMORPHISM OF THE DETRITIC ROCKS IN ORTAKÖY (AKSARAY) AREA

Kerim KOÇAK*

ABSTRACT.- The detritic rocks of Ortaköy area were undergone a regional metamorphism which caused development of the paragenesis: sillimanite + plagioclase ($An_{0.43}$) + orthoclase + quartz + biotite ($Ann_{0.08}$, $Phl_{0.012}$) + garnet ($Alm_{0.80-0.83}$, $^{pr}P_{0.10-0.08}$ $Sp_{0.048-047}$ $Grs_{0.048-0.045}$). By geothermobarometers of garnet-biotite and garnet-aliiminosilicate-quartz-plagioclase, the regional metamorphism conditions were determined as P= 3.3±0,36 kb and T=~600°C. The garnet has inverse mineralogical zoning due to homogenisation or exchange reaction between garnet and matrix. Decreasing of grossulerite content in the garnet towards its rim, and occurence of andalusite, chlorite and sericite show that P-T conditions in Ortaköy area follows a clockwise path in P-T-t trajectory.

## INTRODUCTION

The assemblage of magmatic and metamorphic rocks situated in the triangular area, where is geologically bounded by the Tuzgölü fault to the west, the Ecemiş Fault to the east and the İzmir-Ankara-Erzincan Suture to the north, is called as the Central Anatolian Massif (CACC, Göncüoğlu et al., 1991). The study area is situated in Ortaköy area (Fig. 1), western CACC.

Metamorphites in the CACC were studied by Erkan (1975, 1976, 1977), Göncüoğlu (1977), Seymen (1981, 1984) and Tolluoğlu (1986, 1987). In the study area, Bayhan (1990) and Türeli (1991), also worked about geochemistry of the igneous rocks.

The lithostratigraphic units of the Ortaköy area show that the Tamadağ Formation of Silurian-Devonian age is the oldest formation and includes migmatitic gneiss, migmatitic granite, semipelitic-psammitic gneiss with interlayers of marble, quartzite, calcsilicate-gneiss and amphibolite (Koçak, 1993, Fig. 1). This is overlain by the Bozçaldağ Formation of Upper Paleozoic age, which is mainly made of marble with lesser quartzite, semipelitic-psammitic gneiss, rare amphibolite and tremolite bearing gneiss. Koçak (1993) has found out acritarch *Leiosphaeridia* and *Lophosphaeriduim* sp., together with possible graptolite fragments-questionably of *Retiolites* sp in the residue obtained from marble samples in Tamadağ Formation by treatment of acetic acid. The first certain macro fossil, Heliolitinae (Heliolitida fam.) *Paeckelmannophora* sp., was discovered in the marble near the top of the Tamadağ Formation. The acritarchs give a *broad* a Cambrian to Devonian range, while coral gives a range of Lower Silurian to Upper Devonian.

The metasediments, undergone metamorphism in upper amphibolite fades (second sillimanite degree) conditions, intruded by Upper Cretaceous-Paleocene aged Ortaköy pluton including hornblendite, hornblend-diorite, biotite-hornblende granitoid, microgranite and quartz-alkali syenite (Ataman, 1972; Erkan and Ataman, 1981; Güleç, 1993; Koçak, 1993; Koçak and Leake, 1994).

In order to determine the P-T conditions in the area, sampling were carried out from detritic rocks of the Tamadağ Formation where cropped out in small area, surrounded by marbles of Bozçaldağ Formation. Mineral assemblage of sillimanite, plagioclase (An>15), orthoclase, quartz, biotite and garnet, that allows to geothermobarometer studies on, determined in the semipelitic gneiss in Sırayalardağı area. Chemical composition of the minerals, in which the rim was preferred, were analysed at Geology Department (Glasgow University, UK) by microprobe (Table 1).

## PETROGRAPHY

The paragenes developed by regional metamorphism in the detritic rocks are as follows: (between paranthesis are in minor amounts).

Bt+sil+qtz

Bt+pl+qtz(+zr)

Bt+plg+qtz+sil(+ap)

Pl+bt+or+qtz+mic+(+tur)

Qtz+sil+bt+pl(+zr)

Qtz+pl+bt+or

Sil+or+qtz+pl+bt+grt (+opq)

Sil+bt+plg+qtz (zr+sph+rt+mag+cas+hem)

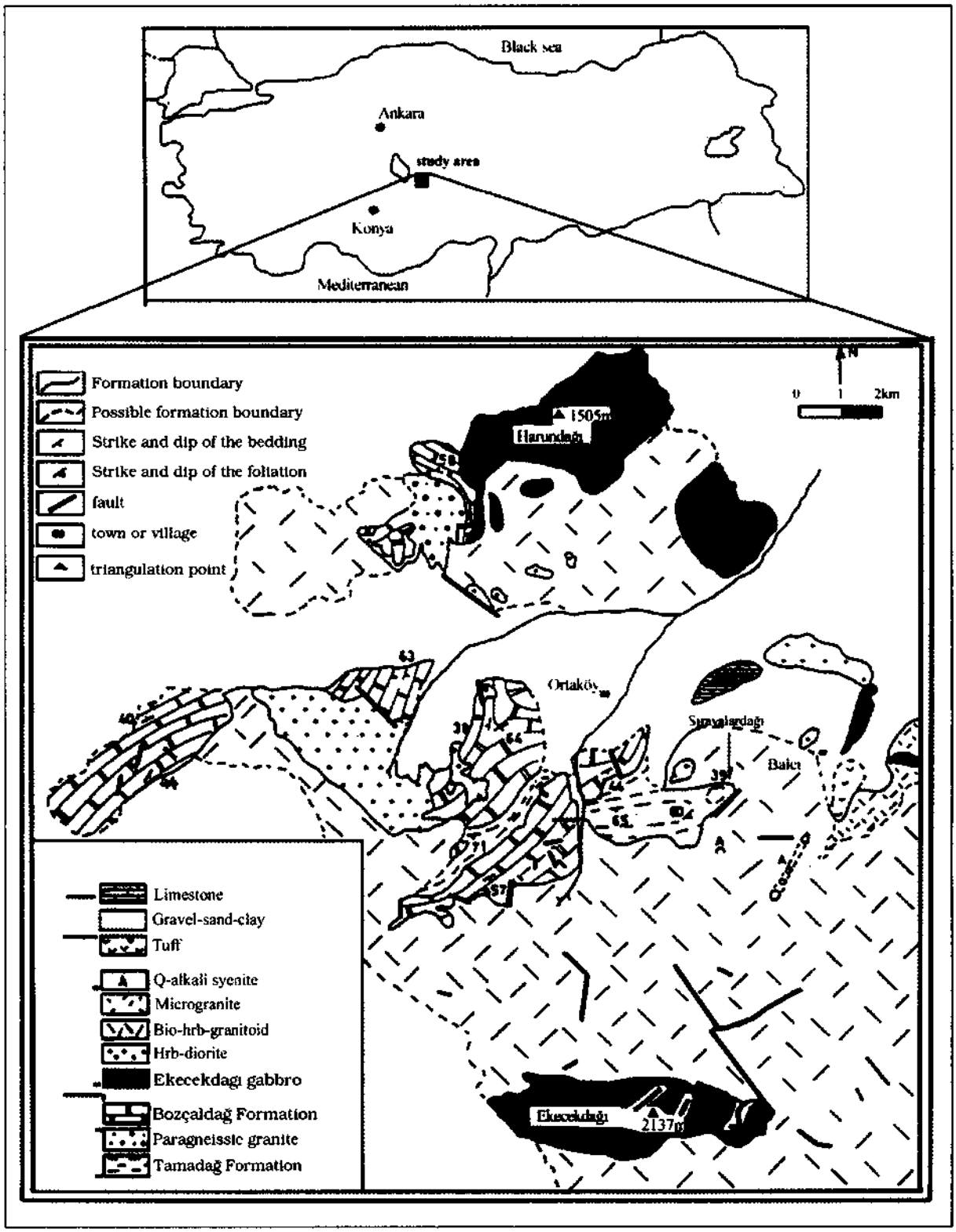


Fig. 1- Geological map of the studying area (Koçak, 1993).

**Table 1- Microprobe analyses of some minerals in the gneiss sample**

| | Garnet (core) | Garnet (edge) | Garnet[b] | Plg[b] | Bio[j] | Garnet[j] | Plg |
|---|---|---|---|---|---|---|---|
| $SiO_2$ | 36,77 | 36.38 | 37.49 | 57.45 | 34.73 | 36.89 | 55.80 |
| $TiO_2$ | 0,08 | 0,00 | 0,07 | 0,00 | 5,07 | 0,00 | 0,00 |
| $Al_2O_3$ | 21,08 | 20,90 | 21,32 | 26,69 | 18,98 | 21,10 | 28,35 |
| $Fe_2O_3$ | 0,00 | 0,74 | 0,00 | - | 2,71 | 0,12 | - |
| FeO^ | 36,48 | 35,88 | 36,49 | 0,14 | 19,88 | 36,95 | 0,06 |
| MnO | 1,94 | 2,11 | 2,132 | 0,03 | 0,08 | 2,07 | 0,00 |
| MgO | 2,39 | 2,67 | 2,60 | 0,00 | 5,87 | 2,02 | 0,16 |
| CaO | 1,56 | 1,51 | 1,71 | 8,76 | 0.01 | 1.58 | 10.55 |
| $Na_2O$ | | | | 6,36 | 0,41 | | 5,35 |
| $K_2O$ | | | | 0,19 | 9,64 | | 0,15 |
| $Cr_2O_3$ | 0,02 | 0,00 | 0,07 | | | 0,02 | |
| (Total) | 100,32 | 100,19 | 101,88 | 99,62 | 97,38 | 100,75 | 100,42 |
| Formula based on 24 oxygens for garnet, 32 oxygens for plagioclase and 22 oxygens for biotite | | | | | | | |
| Si | 5,93 | 5,89 | 5,96 | 10,32 | 5,60 | 5,95 | 9,98 |
| Ti | 0,01 | 0,00 | 0,00 | 0,00 | 0,61 | 0,00 | 0,00 |
| Al | 4,01 | 3,99 | 3,99 | 5,65 | 2,71 | 4,01 | 5,98 |
| $Fe^{3+}$ | 0,00 | 0,09 | | | 0,37 | 0,01 | |
| $Fe^{2+}$ | 4,92 | 4,86 | 4,85 | 0,02 | 2,68 | 4,98 | 0,01 |
| Mn | 0,26 | 0,29 | 0,29 | 0,00 | 0,01 | 0,28 | 0,00 |
| Mg | 0,58 | 0,65 | 0,61 | 0,00 | 1,41 | 0,48 | 0,04 |
| Ca | 0,27 | 0,26 | 0,29 | 1,69 | 0,00 | 0,27 | 2,02 |
| Na | | | | 2,22 | 0,13 | | 1,86 |
| K | | | | 0,04 | 1,98 | | 0,03 |
| Cr | 0,002 | 0,00 | 0,00 | | | 0,00 | |
| An% | | | | 42,7 | | | 51,67 |
| Ab% | | | | 56,2 | | | 47,4 |
| Or% | | | | 1,1 | | | 0,89 |

[b] used for geobarometer calculations,

j used for geothermometer calculations,

[A] Fe/Fe2+F3+ in garnet is calculated according to Drop (1987)/ and Fe/Fe2+F3+=0.12 assumed for the biotite (Guidotti and Dyar, 1991; Holdaway and Mukhopadhyay, 1993).

The sample analysed mainly contains sillimanite (% 35, <0.4 mm), plagioclase+orthoclase (%30, <0.4 mm), quartz (%20, <0.4 mm), biotite (%5,~1 mm), garnet (%5, <0.8 mm), and andalusite+ chlorite+sericite+opaque iron ore (5%) in a lepidonematoblastic texture (Fig. 2). The sillimanites, in which sericite developed around, usually have needless and sometimes fibrous shape. The plagioclase crystals often show polysynthetic and albite-carlsbad twinnings. The garnet containing plagioclase, biotite and quartz inclusions, is retrograted to biotite along its edge. The biotite, displayed light-dark brown colour and pleochroism, is altered to chlorite and opaque iron ore. The andalusite formed as small crystals within sillimanites (Fig. 3).


a)

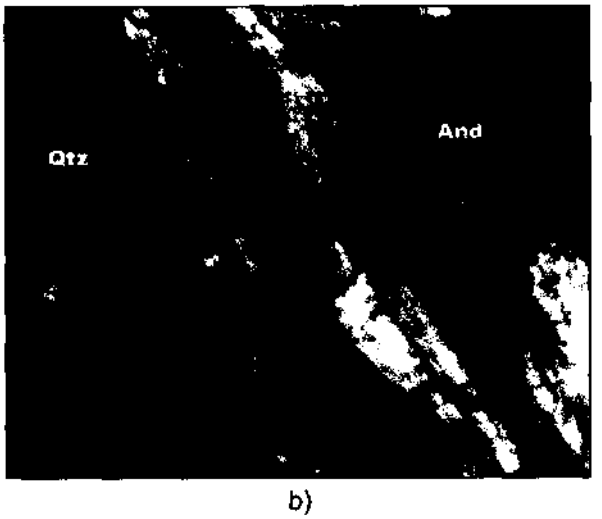


b)

Fig. 2- Andalusite within the sillimanite a) Single polar *40 b) Cross polars *40 N.(S: sillimanite, Qtz: quartz, A: andausite).

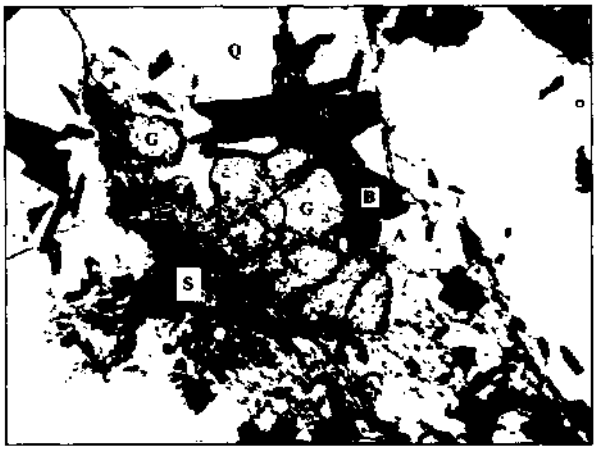


Fig. 3- Mineral relations in the samples analysed (G: garnet, S: sillimanite, B: biotite, Q: quartz, A: plagioclase (anorthite) single polar* 20.

The existence of biotite, plagioclase and quartz inclusions in the garnet indicates that a reaction took place between the inclusion and their host. The garnet has contact with biotite,plagioclase and quartz due to that the reaction possibly went back:

An > gros + 2/3sil + 1/3qtz
(Kretz, 1959; 1964) (1)

Fe-garnet + Mg-biotite > Mg-garnet + Fe-biotite
(Kretz, 1959; 1964). (2)

Co - existence of orthoclase and sillimanite show brekdown of muscovite.

Mus+qtz > sil+or+$H_2O$ (Ewans and Guidotti, 1966; Thompson, 1976, 1982; Vielzeuf and Boivin 1984). (3)

Conversion of biotite to chlorite, sillimanite to sericite and andalusite can take place owing to retrograde metamorphism

3sil+3qtz+2K++3$H_2O$ > 2mus+2$H^+$
(Chinner, 1961; Carmichael, 1969) (4)

sil > and (Holdaway, 1971; Richardson et al., 1969; Kerrick, 1987). (5)

## MINERAL CHEMISTRY

The garnet shows inverse chemical and mineralogical zoning; spessartine (0,03 mole) and pyrobe (0,07 mole) increase while almandine (0,06 mole) and grossularite (0,01 mole) decrease towards rim (Fig. 4). The inverse zoning, common in high grade rocks, may be explained by exchange reaction between garnet and matrix (Loomis, 1975), resorbtion of garnet (Grant and Weiblen, 1971), or homogenisation of zoned garnet (Blackburn, 1969). Minimum crystallisation temperature of the garnet-biotite pair (600°C) is high enough to

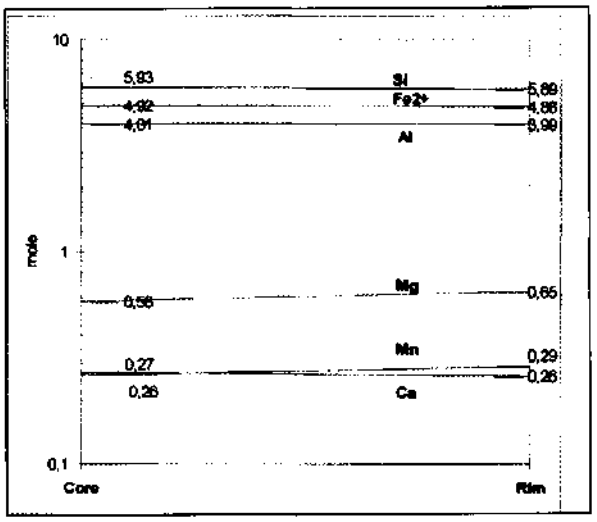


Fig. 4- Mineralogical zonation in the garnet.

allow homogenisation of the zoned garnet. As no resorbtion observed in the sample, either the exchange reaction and/or homogenization of the zoned garnet could be responsible for the zoning.

Decreasing grossularite content towards rim of the garnet, as well as crystallisation of the andalusite, chlorite and sericite indicates that pressure-temperature-time (P-T-t) path follows a clockwise pattern in the area (Fig. 5).

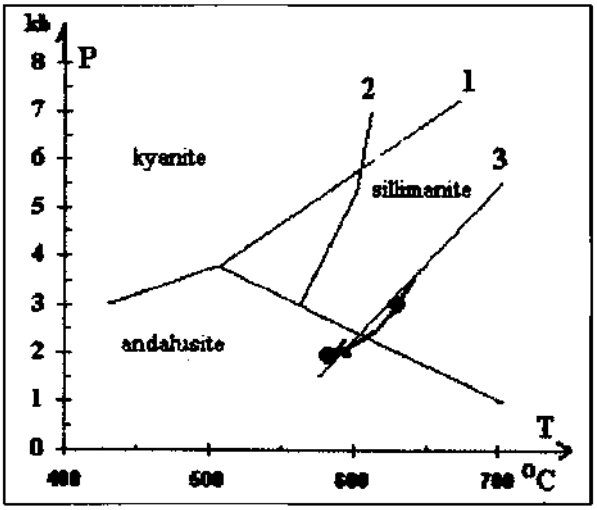


Fig. 5 - Conditions of,the regional metamorphism in the Ortaköy area and P-T-t path (error in the geothermobarometer calculations is taken account plotting of the P-T values in the diagram). 1- $Al_2 SiO_5$ diagram of Holdaway and Mukhopadhway (1993a) 2- Chl + Mus - And + Bio + Qtz + $H_2O$ (Bird and Fawcett, 1973) 3- Mus+Qtz > Kfs+ Als+$H_2O$ reaction is calculated for a $H_20$ =0.8 (Reinhardt,l992).

In the sample, free garnet is poorer in Ca (0.03 mole) than the garnets in contact with plagioclase while it is poorer in $Fe^{2+}$ (0.12 mole) and richer in $Mg^{2+}$ (0.17 mole) with respect to the garnet in contact with biotite. Similarly, the plagioclase in contact with the garnet is poorer in An (8.97 mol) than free plagioclase.

## GARNET-ALUMINOSILICATE-QUARTZ GEOTHERMOBAROMETER

Pelitic schist and gneisses are secure qualitative indicator for metamorphic grade over wide P-T conditions. Gamet-aluminosilicate quartz-plagioclase (GASP) geobarometer is used widely in conditions ranging from greenschist to granulite fades (Ghent, 1976; Aranovich and Podlesskii, 1980; Newton and Haselton, 1981; Hodges and Crowley, 1985; Koziol and Newton, 1988). In reaction, mass-balance equation is as follows:

$$CaAl_2Si_20_8 \quad CaAl_{0.67}SiO_4 + 2/3\ Al_2SiO_5 + 1/3\ Si0_2 \quad (1)$$

An component in plagioclase — grossuler component in garnet — sillimanite — quartz

Volume change in the reaction is considerably high and hence increasing pressure moves equation towards right, increases activity ratio (agrs/ aan) and Ca content of the garnet relative to plagioclase. GASP applied to the sample and 3.35 kb is obtained as minimum crystallisation pressure (Table 2). GASP geobarometer of Powell and Holland (1988) also applied to the sample and 3.27 kb is found for 600°C. The results obtained are almost identical for two geobarometer. Taken into consideration of the uncertainty of calculation (0,36 kb, Powell and Holland, 1988) minimum crystallisation pressure would be 3-3.5 kb for the semipelite.

## GARNET-BIOTITE GEOTHERMOMETER

A range of geological thermometer has been developed in pelitic systems, however best calibrated one is garnet-biotite exchange geothermometer (Hodges and Crowley, 1985; Holdaway and Mukhopadhyay, 1993b).

$$Fe_3Al_2Si_3O_{12}+KMg_3Al_2Si_3O_{10}(OH)_2 \quad Mg_3Al_2Si_3O_{12}+KFe_3AlSi_3O_{10}(OH)_2 \quad (2)$$

Fe-garnet + Mg-biotite — Mg-garnet + Fe-biotite

As volume change in the reaction is quite small, to increase the temperature makes biotite rich in Fe and garnet rich in Mg. Several garnet-biotite geothermometers have been applied to the semipelite:

**Table 2- GASP geobarometer.**

| **Garnet** | **Almandine** | **Spessartine** | **Pyrobe** | **Grossularite** |
|---|---|---|---|---|
| | 0,803 | 0,048 | 0,101 | 0,048 |
| **Plagioclase** | **An** | **Ab** | **Or** | |
| | 0,428 | 0,562 | 0,01 | |
| **Barometer calibrations** | | | | |
| **Temperature used °C** | | 600 | | |
| | ln K | log K | | **P(kbar)** |
| Grs + 2Sil + Qtz = 3 An | 7,873 | 3,419 | | **3,35** |

**Table 3- Calculations of the geothermometer.**

| **Mg/(Mg+Fe) Garnet end member** | | | | | | | **Biotite** | |
|---|---|---|---|---|---|---|---|---|
| Grt | Bt | Kp | Alm | Sps | Prp | Grs | X(Ti) | X(Alvı) |
| 0,088 | 0,344 | 5,45 | 82,9% | 4,7% | 8,0% | 4,5% | 0,122 | 0,062 |
| **RESULTS** | | | **TEMPERATURE (deg °C)** | | | | | |
| P kbar | HS82 | T76 | HL77 | FS78 | PL83 | Dasg91 | B92-HW | B92-GS |
| **3** | **600** | **590** | **580** | **582** | **584** | **476** | **581** | **572** |

Thompson (1976) geothermometer was calibrated by correlation of KD values of natural garnet-biotite association against estimated temperatures based on experimental phase equilibrium. Ferry and Spear (1978), and Perchuk and Lavrent'eva (1983) experimentally calibrated thermometers in a system with Fe/Fe+Mg ~0,9 and Fe/Fe+Mg ~0,6 respectively. Bhattacharya et al., (1992) and Hodges and Spear (1982) considered unideal conditions in geothermometer calibrations. An empirical thermometer was developed by Dasgupta et al., (1991) via statistical regression of Ferry and Spear's (1978) experimental data.

Minimum crystallisation temperature of the garnet and biotite, determined by using the geothermometers, was given in Table 3 with same data used in calculation. The results (581, 572, 600°C) obtained from geothermometers (except Dasgupta et al., 1991), based on unideal solid solution assumption between garnet-biotite are nearly same with the ones determined by using geothermometer based on ideal solid solution between garnet and biotite (582, 590 and 584). That is, equilibrium constant (K) is nearly equal to the equilibrium distribution constant (KD). This can be explained by (1) small deviation of biotite-garnet from ideal solid solution, (2) tendency to equilibria, and (3) application of the geothermometer to the sample containing similar Fe/Mg in experiment. As calculation error taken into account (e.g. ± 25°C of Ferry and Spear, 1978), minumum crystallisation temperature of garnet and biotite in the semipelite would be about 600°C.

## DISCUSSION AND CONCLUSIONS

Paragenes of plagioclase ($An_{0,43}$), biotite ($Ann_{0.08,}$ $Phl_{0,012}$), garnet ($Alm_{0.08\text{-}0.83}$ $Prp_{0,10\text{-}0,08}$ $Sp_{0,048\text{-}047}$ $Grs_{0,048\text{-}0,045}$) and sillimanite were determined in the semipelites metamorphosed under upper amphibolite fades conditions.

The garnet shows inverse mineralogical and chemical zoning: spessartine and pyrobe increase while almandine and grossularite decrease towards rim. It can be explained by exchange reaction between garnet and matrix and/or homogenisation of the zoned garnet.

By using various garnet-biotite and garnet-aluminosilicate-quartz-plagioclase geothermobarometers, minimum crystallisation pressure and temperature in Ortaköy area were succesfully determined as 3.3±0.36 kb ve ~600±25 (Table 2, 3). Erkan (1976) determined

three different isograds which corresponds to > 500 ˚C, -600 ˚C and ~700 ˚C temperature (< 5 kb) in northeast of the city of Kırşehir while Seymen (1984) estimated P-T conditions of 400-700 ˚C at - 1.5-2 kb pressure, on the basis of index minerals in northwest of Kırşehir. The P-T values obtained in Ortaköy area therefore correspond to Erkan (1976) and Seymen's (1984) data However, the Ortaköy values, determined by stoichiometric calculations based on mineral chemistry obtained via microprobe analyses, are much more sensitive and definitive than the others based on investigations of polarizan microscope.

Whitney and Dilek (1997-1998) were suggested that the Niğde metasedimentary protoliths were buried to 16-20 km (5-6 km) depth at >700 ˚C temperature in relation with the closure of Tethyan seaways in Early Cenozoic and were later, following cooling and rifting, undergone second heating (<10 km and <600˚C) event during Miocene magmatism. The sillimanites were tightly folded during first metamorphism and then scarn zone including andalusite and cordierite were developed by intrusion of the granitoids into the metadetritic rocks. Development of andalusite was followed by asecond, prograde episode of sillimanite growth during low-pressure-high-temperature metamorphism in the central part of the massif, where magmatism was most extensive. In Ortaköy area, decreasing grossuler content of the garnet towards its rim indfcates that the garnet was grown >3.3± 0,36 kb pressure. Crystallisation of the andalusites, situated within the sillimanites as small crystals, as well as chlorite and sericite indicates decreasing pressure. Therefore, Ortaköy metasedimantery protoliths were buried >10-13 km depth during crustal thickening in relation with closure of the Neo-Tethyce (Göncüoğlu et al., 1991) and then the massif were uplifted, inducing crystallisation of andalusite, sericite and chlorite. Alternatively, P-T in Ortaköy area follows a clockwise pattern in P-T-t projectory (Fig. 5). As no occurence of secondary sillimanite observed in the Ortaköy area, it is possible to say that Miocene magmatism, suggested by Whitney and Dilek (1997, 1998), has not taken place in the study area.

There is no substantial difference between the results obtained by, geothermometer based on ideal and unideal solid solution. This can be explained by deviation of garnet-biotite from ideal solid-solution, and/or tendency of the garnet-biotite pairs-towards equilibrium or application of the geobarometer tq the sample containing similar Fe/Mg in the experiment

## REFERENCES


Aranovich, L.Y.A. and Podlesskii, K.K., 1980, The garnet-plagioclase barometer: Doklady, Earth Science Sections, 251, 101-103.

Ataman, G., 1972, A study on the radiometric age of Cefalikdağ, one of the granite-granadiorite bodies outcropping on the south-east Ankara, Hacettepe Science and Engineering Journal, 2, 44-49 (in Turkish).

Bayhan, H., 1990, Mineralogical, petrographic and geochemical study of the Ortaköy granitoid (east of Salt Lake) located within the 1st Turkish National Geotraverse, TÜBİTAK Project No, TBAG-841, 68pp (unpublished-in Turkish).

Bhattacharya, A.; Mohanty, L.; Maji, A.; Sen, S.K., and Raith, M., 1992, Non-ideal mixing in the phlogopite-annite binary; constraints from experimental data on Mg-Fe partitioning and a reformulation of the biotite-garnet geothermometer: Contr. Min. Pet., 111,87-93.

Bird. G.W. and Fawcett. J.J., 1973, Stability relations of Mg-chlorite-muscovite and quartz between 5 and 10 kb water pressure: J.Pet., 14. 415-425.

Blackburn, W.H., 1969, Zoned and unzoned garnets from the Grenville gneiss around Gananoque, Ontario: Can. Min., 9, 691-698.

Carmichael, D.M., 1969, On the mechanism of prograde metamorphic reactions in quartz-bearing pelitic rocks; Con.Min.Pet., 20, 244-267.

Chinner. G.A., 1961, The origian of sillimanite in Glen Clova: Angus. J. Pet., 2. 213-23.

Dasgupta, S.; Sengupta, P.; Guha, D. and Fukuoka, M., 1991, A refined garnet-biotite Fe-Mg exchange geothermometer and its application in amphibolites and granulites: Contr. Min. Pet., 109, 130-137.

Drop, G.T.R., 1987, A general equation for estimating Fe3+ concentrations in ferromagnesian silicates and oxides from microprobe analyses, using stoichiometric criteria: Min.Mag., 51, 431-450.

Erkan, Y, 1975, Orta Anadolu Masifinin güneybatısında (Kırşehir bölgesinde) etkili rejyonal metamorfizmanın petrolojik incelenmesi: HÜ. Yer Bilimleri Enst., Doçentlik Tezi. Ankara, 147 s., (unpublished).

_____,1976, Kırşehir çevresindeki rejyonal metamorfik bölgede saptanan izogradlar ve bunların petrolojik yorumlanmaları:Yer bilimleri, 2, 23-54.

_____,1977, Orta Anadolu masifinin güneybatısında (Kırşehir bölgesinde) etkili rejyonal metamorfizma ile amfibol minerallerinin bileşimi arasındaki ilişkiler: Yer bilimleri, 3/1,41-46.

Erkan, Y. and Ataman, G., 1981, Orta Anadolu masifinin (Kırşehir yöresi) metamorfizma yaşı üzerine K/Ar yöntemi ile bir inceleme: T.J.K. 35. Bilimsel ve Teknik Kurultayı bildiri özetleri, 33.

Evans, B.W. and Guidotti, 1966, The sillimanite-potash feldspar isograd in western Maine: USA, Cont. Min.Pet., 12, 25-62.

Ferry, J.M. and Spear, F.S., 1978, Experimental calibration of the partition of Fe and Mg between biotite and garnet: Contr. Min. Pet., 66: 113-117.

Ghent, E.D., 1976, Plagioclase - garnet - $Al_2SiO_5$ - quartz: a potential geothermometer - geobarometer: Am.Min.,61, 710-714.

Göncüoğlu, N.C., 1977, Geologie des weslichen Niğde-Massivs, PhD thesis, Rheinischen Friedrich-Wilhelms-Uni., Bon, 180.

_____; Toprak, G.M.K.; Kuşçu, I.; Erler, A. and Olgun E., 1991, Geology of the western part of the Central Anatolian Massif, Part 1: southern part, Middle Eeastern Technical University (METU) Turkish Petroleum Corporation (TPAO) project Report, 140 pp, (unpublished-in Turkish).

Grant, J. and Weiblen, P.W., 1971, Retrograde zoning in garnet near the second sillimanite isograd: Am.J.Sci., 270, 281-296.

Guidotti, C.V. and Dyar, M.D., 1991, Ferric iron in metamorphic biotite and its petrologic and crystallochemical implications: Am.Min., 76, 161-175.

Güleç, N., 1993, Ağaçören granitoyidinden jeokronolojik bulgular: Hacettepe Üniversitesinde yer bilimlerinin 25. Yıl sempozyumu, s. 49-50.

Hodges K.V. and Spear, F.S., 1982, Geothermometry, geobarometry and the $Al_2SiO_5$ triple point at Mt. Moosilauke, New Hampshire: Am.Min., 67, 1118-34.

_____and Crowley, P.D., 1985, Error estimation and empirical geothermobarometry for pelitic systems: Am. Min., 70, 702-709.

Holdaway, M.J., 1971, Stability of andalusite and the aluminum silicate phase diagram, Am. J. Sci., 271, 97-131.

_____and Mukhopadhway. B., 1993 a, A reevaluation of the stability relations of andalusite: Thermochemical data and phase diagram for the aluminium silicates. Am.Min., 78, 298-315.

_____and_____, 1993 *b,* Geothermobarometry in pelitic schists: A rapidly evolving field: Am.Min., 78, 681-693.

Kerrick, D.M., 1987, Fibrolite in contact aureoles of Donegal, Ireland, Am.Min., 72, 240-254.

Koçak, K., 1993, The petrology and geochemistry of the Ortaköy area, Central Turkey, PhD thesis, Glasgow Uni., Scotland, 280 (unpublished).

_____and Leake, B.E., 1994, The petrology of the Ortaköy district and its ophiolite at the western edge of the Middle Anatolian Massif, Turkey, Jour. A. Earth Sciences, 18/2, 163-174.

Kozial, A.M. and Newton, R.C., 1988, Redetermination of the garnet breakdown reaction and improvement of the plagioclase-garnet-$Al_2SiO_5$-quartz geobarometer: Am.Min., 73, 216-23.

Kertz, R., 1959, Chemical study of garnet, biotite and hornblende from gneisses of Soutwestern Quebec, with emphasis on the distribution of elements in coexisting minerals, Journal of Geo., 67, 371-402.

_____, 1964, Analysis of equilibrium in garnet-biotite-sillimanite gneisses from Quebec, Journal of Pet., 5, 1-20.

Loomis, T.P., 1975, Reaction zoning of garnet: Contr. Min. Pet., 52, 285-305.

Newton, R.C. and Haselton, H.T., 1981, Thermodynamic calibration of the garnet-plagioclase-$Al_2SiO_5$-quartz geobarometer: Newton, R.C., Navrotsky, A. and Wood, B.J. (Ed), Thermodynamics of Minerals and melts, Springer-Varlag de, New York, 131-147.

Perchuk, L.L. and Lavrent'eva, I.V., 1983, Experimental investigation of exchange equilibria in the system cordierite-garnet-biotite: Saxena, S.K. (Ed), Kinetics and equilibrium in mineral reactions: Advances in Physical Geochemistry, New York, Springer-Verlag de, 3, 199-239.

Powell, R. and Holland, T.J.B., 1988, An internally consistent dataset with uncertainties and correlations: 3. Applications to geobarometry, worked examples and a computer program: J.Met.Geo., 6, 173-204.

Reinhardt, J., 1992, Low pressure, high temperature metamorphism in a compressional tectonic setting: Mary Kathleen Fold Belt, northeastern Australia, Geo.Mag., 129,41-57.

Richardson, S.W.; Gillbert, M.C. and Bell, P.M., 1969, Experimental determination of kyanite-andalusite and andalusite-sillimanite equilibria: The aluminium silicate triple point, Am.J.Sci., 267, 259-272.

Seymen, i., 1981, Kaman (Kırşehir) dolayında Kırşehir masifinin stratigrafisi ve metamorfizmasi: TJK Bült., 24/2, 7-14.

_____, 1984, Kırşehir masifi metamorfitlerinin jeolojik evrimi: T.J.K. Ketin Sempozyumu, 133-148.

Thompson, A.B., 1976, Mineral reactions in pelitic rocks: I Prediction of P-T-X (Fe, Mg) phase relations, II Calculation of some P-T-X (Fe, Mg) phase relations, Am.J.Sci., 276: 401-454.

Tolluoğlu, A.Ü., 1986, Orta Anadolu masifinin güneybatısında (Kırşehir yöresinde) Petrografik ve petrotektonik incelemeler: H.Ü. Fen Bilimleri Enstitüsü, Doktora Tezi, Ankara, 237 s., 8 Ek. (unpublished).

_____, 1987, Orta Anadolu masifi metamorfitlerinin (Kırşehir kuzeybatısı) petroğrafik özellikleri: Doğa Bilim, Derg., Müh. ve Çevre, 11/3, 344-361.

Türeli, T.K., 1991, Geology, petrography and geochemistry of Ekecikdağ plutonic rocks (Aksaray region-Central Anatolia), PhD., Thesis, Middle Eastern Technical University, Ankara, 194p.

Vielzeuf, D. and Bovine. P., 1984; An algorithm for the construction of petrogenetic grids-Application to some equilibria in granulitic paragneisses, Am.J.Sci., 284,760-791.

Whitney, D.L. and Dilek, Y., 1997, Core complex development in central Anatolia: Geology 25, 1023-1026.

_____and_____, 1998, Metamorphism during crustal thickening and extension in central Anatolia: the Niğde metamorphic core complex. Journal of Petrology 39, 1385-1403.

# LITHOSTRATIGRAPHY AND SEDIMENTOLOGY OF THE MIOCENE BASIN BETWEEN MUT-KARAMAN, (CENTRAL TAURIDS)

Eşref ATABEY*; Nevbahar ATABEY*; Aynur HAKYEMEZ*; Yeşim İSLAMOĞLU*; Şinasi SÖZERi**; N. Nimet ÖZÇELiK***; Gerçek SARAÇ*; Engin ÜNAY**** and Sedef BABAYİĞİT*

ABSTRACT.- The study area includes Mut-Karaman part of the Mut Miocene Basin. Lowermost lithostratigraphic unit of Miocene is Göcekler formation which is represented by mudstone and conglomerate of Aquatian age. This formation is unconforably overlies the late Cretaceous basement. The Göcekler formation gradually pass both laterally and vertically into the Aquatian-alt Burdigalian The Fakırca formation which is characterized by clayey limestone/sandstone and coal bearing shale. Clayey limestone part of the Fakirca formation is recognized as the Kestelkapızı member. Marine rock units in the region can be grouped into five formation: The Mut formation, the Köselerli formation, the Dağpazarı formation, the Tirtar formation and the Ballı formation. The Mut formation, the Köselerli formation and the Dağpazarı formation is form the lower part of the sequence. At the upper part of sequence there are the Tirtar formation and the Ballı formations. The Mut formation and the Köselerli formation are represented by limestones, clayey limestone and marl, whereas the Dağpazarı formation consist of calcarenite, limestone, claystone, mudstone. Mut formation and Köselerli formation are laterally transitional and are of Upper Burdigalian-Langian-Serravalian (?Lower Serravalian) age. The Dağpazarı formation was deposited in Langian-Serravalian (?Lower Serravalian) time interval. The Tirtar formation is represented by limestone and unconformably overlies the Dağpazarın formation. The Tirtar formation is represented by limestones. The age of the Tirtar formation is Serravalian (?Upper Serravalian)- Tortonian. The lateral equivalent unit of the Tirtar formation is the Ballı formation and is composed of clayey limestone and marl. At the top, Pliocene continental elastics and lacustrine limestones unconformably overlies the Miocene sequence.

# GEODYNAMIC PHASES OF THE ARAÇ MASSIF, WESTERN PONTIDS, KASTAMONU, TURKEY

Doğan AYDAL*****

ABSTRACT- This paper is concerned with the geological, mineralogical and geochemical properties of Araç massif. The Araç massif is mainly composed of ophiolites and metamorphic rocks. The age of the metamorphic rocks, which are dominant rock group in the study area, are ranging from Pre-Malm to Upper Cretaceous. K-Ar age determination were performed in hornblendes derived from amphibolites, which are previously thought to be Precambriam age in the study area. According to the K-Ar age results, which gives 130-146 ma, suggests that the amphibolites were affected by retrograde metamorphism, which took place in Berriasian (Lower Cretaceous). These ages are believed to represent the metamorphism age, not the occurence age of the formation. Because of this, the occurence of the Bekirçay formation should have taken place before this retrograde metamorphism. Some very intensely altered metaophiolitic bloks were found as xenolits in Bekirçay metamorphic units. Therefore the age of the metaophiolites shoud have been older than the Bekirçay formation. Mercimekdere metaophiolites were overlain, not only by Bekirçay formation, but also by Kavacık formation, which is represented by graphite-garnet micaschist in the study area. The Bekirçay formation and the other above mentioned formation is overlayed discordantly by Palaeozoic metasediments, namely the Dumantepe formation, which consists of various low grade schists and phyllites. The Mesozoic is represented by Yongalıdağ formation, Pelitveren ophiolitic melange and serpentinized, carbonatized and sillicified rocks, so called listwaenites of the Gemiköy formation. Finally, this Mesozoic formations were transgresively superseded by biosparite and biomicrite units of the Araç formation. The area and surroundings were then affected by post Eocene faulting. According to the geochemical investigations, it can easily be said that ultramafic rocks occured as mantle fractionates and all mafic rocks were originated from subalcaline tholeiitic magma. Amphibolites are found as metaluminous, while garnet-micaschist are peraluminous and epidote-amphibolites show both character in different places. Carbonaceous rocks in the study area are found to be rich in calcite rather than dolomite and other minerals.

# MINERALOGY-PETROGRAPHY AND GEOCHEMISTRY OF KONYA MIOCENE VOLCANIC UNITS AND GENERAL DETERMINATION OF NEOFORMED CLAY MINERALS

Selahattin KADİR* and Zehra KARAKAŞ**

ABSTRACT.-Volcanic, sedimentary and volcano-sedimentary units are wide spreaded in south and southwest of Konya. Mineralogy and micromorphology of ignimbrite and nuee ardentes as well as domes exhibit characteristic of rhiyolite, dacite, andesite, basalt and tuff. Tuffs are classified as vitric, lithic and crystal tuffs, based on the volcanic glass, rock fragments and crystal properties while Argillisation and limonitisation are common in tuff, these alteration products are less or not present in the other volcanic rocks. Generally, argillisation and limonitisation are dominant in the fracture of volcanic glasses, which is the main component of tuffaceous units. In addition, argillisation is observed in feldspar and opacitazat and chloritisation in biotite and hornblende. As a result of XRD studies in the tuffaceous units Halloysite, kaolinite, smectite, palygorskite and illite type clay minerals and opal-CT, feldspar, quartz, amphibole, serpentine, minamiite and jarosite type non-clay minerals are determined SEM studies indicate that halloysite, kaolinite and smectite are generally developed in the dissolution voids and fractures of volcanic glasses. Chemical analyses reveal that halloysite, kaolinite and smectite units and adjacent volcanic rocks are similar. Formation of clay minerals in the study area are controlled by the movement of water as well as the mobility of the ions of volcanic glass and feldspar. The field observation, mineralogical, chemical, and micromorphological determinations indicate that halloysite, kaolinite and smectite could be formed diagenetically following the period of depositions of tuffaceous materials by the effect of ground and meteoric water.

# GEOCHEMiCAL PROPERTIES THOSE IDENTIFYING THE ENVIRONENT OF MANGANESE OXIDE MINERALIZATION OF KASIMAĞA (KESKİN - KIRIKKALE)

Şükrü KOÇ**, Öner ÖZMEN*** and Nursel ÖKSÜZ****

ABSTRACT- Kasımağa Mn- oxide ore deposit is found in basalt, radiolarite and marl of pelagic deposits of ophiolitic series of Kırşehir massif in the form of scattered, banded or bedded structures of varying thinckness. Paragenesis of ore mineralization is formed by braunite, pyrolusite, ramsdellite, geothite, hematite, and magnetite. Based upon the findings from the analysis of samples such as low-and variable Fe/Mn ratios; low trace ele ment contents and negative anomaly of Ce (a rare earth element) suggest that ore mineralization took place under submarine hydrothermal condition. Two major different clusters determined from the major and trace elements were attributed to the rigorous fractionation developed mainly from the same solution.